



Diffusion of chloride-36 and carbon-14 in a backfill barrier composed of 75% basalt and 25% bentonite by Craig G Rieger

A thesis submitted in partial fulfillment of requirements for the degree of Master of Science in Chemical Engineering
Montana State University
© Copyright by Craig G Rieger (1985)

Abstract:

Effective diffusion coefficients were measured for chloride-36 at ambient temperature ($\sim 20^{\circ}\text{C}$), 60°C , and 90°C in a water-saturated 75%/25% basalt-bentonite mixture. Three separate tests for each of the given temperatures were run at two bulk densities of the medium, i.e., 1.6g/cm^3 and 1.8g/cm^3 . The same tests were run for carbon-14, but the data could not be analyzed to find diffusion coefficients.

The diffusion of chloride was found to increase with increasing temperature.

Increasing the bulk density of the diffusion medium inhibited the movement of chloride and reduced the diffusion coefficient.

A one-dimensional model that was solved using the assumption of linear sorption of the tracer described the diffusion of chloride well.

The effective diffusion coefficient of chloride is larger for experimental systems in which the tracer is initially present in the diffusive medium compared with when it is initially present in a solution adjacent to the medium.

The diffusion coefficients of carbon-14 were not measurable because it formed a precipitate or sorbing complex with calcium and/or magnesium.

DIFFUSION OF CHLORIDE-36 AND CARBON-14 IN A
BACKFILL BARRIER COMPOSED OF 75% BASALT AND
25% BENTONITE

by
Craig G Rieger

A thesis submitted in partial fulfillment of
requirements for the degree

of
Master of Science
in
Chemical Engineering

MONTANA STATE UNIVERSITY
Bozeman, Montana

June 1985

MAIN LIB
N378
R436
C.2

APPROVAL

of a thesis submitted by
Craig Garland Rieger

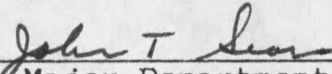
This thesis has been read by each member of the thesis committee (ex. John F. Relyea) and has been found to be satisfactory regarding content, English usage, format, citation, biographical style, and consistency, and is ready for submission to the College of Graduate Studies.

6/17/85
Date


Chairperson, Graduate Committee

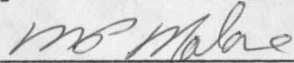
Approved for the Major Department

6/17/85
Date


Head, Major Department

Approved for the College of Graduate Studies

6-19-85
Date


Graduate Dean

STATEMENT OF PERMISSION TO USE

In presenting this thesis in partial fulfillment of the requirements for a master's degree at Montana State University, I agree that the Library shall make it available to borrowers under rules of the Library. Brief quotations from this thesis are allowable without special permission, provided that accurate acknowledgement of source is made.

Permission for extensive quotation from or reproduction of thesis may be granted by my major professor, or in his absence, by the Director of Libraries when, in opinion of either, the proposed use of the material is for scholarly purposes. Any copying or use of the material in this thesis for financial gain shall not be allowed without my written permission.

Signature Craig S. Riegel
Date 6/15/85

ACKNOWLEDGEMENTS

The author would like to thank the faculty and staff of the Chemical Engineering Department at Montana State University for their help and support during his six years of attendance. The insights given by my two major advisors, Dr. Douglas Smith presently at the University of New Mexico and John F. Relyea at Rockwell Hanford Operations is much appreciated.

Special thanks goes out to my parents, Darwin and Donna Rieger for their continual encouragement while I was attending school, and finally to Professor H. A. Saner, whose concern and help for me and others motivated me early on in the chemical engineering curriculum at this university.

TABLE OF CONTENTS

	Page
1. LIST OF TABLES.....	vii
2. LIST OF FIGURES.....	viii
3. ABSTRACT.....	x
4. INTRODUCTION.....	1
The Backfill.....	4
Related Work.....	5
Clay Minerology.....	8
Chloride-36.....	12
Carbon-14.....	13
Research Objective.....	15
5. EXPERIMENTAL.....	16
Materials.....	16
Experimental Procedure.....	18
6. MATHEMATICAL MODELLING AND STATISTICAL ANALYSIS...	28
Procedure.....	31
7. RESULTS AND DISCUSSION.....	34
Diffusion of Chloride-36:	
Temperature Effects.....	34
Bulk Density Effects.....	36
Correlation of Data to Theoretical Model.....	38
Multiple Linear Regression of Data.....	43
Comparison of Results With Other Investigations.	44
Diffusion of Carbon-14.....	47
Difficulties With Carbon-14.....	51
8. SUMMARY.....	54
9. RECOMMENDATIONS FOR FUTURE RESEARCH.....	56

TABLE OF CONTENTS--Continued

	Page
10. REFERENCES CITED.....	58
APPENDICES.....	64
Appendix A-Computer Programs.....	65
Appendix B-Raw Data For Tests Displayed In Figures.....	76
Appendix C-Specified Concentration of Ions in Synthetic Groundwater.....	111
Appendix D-Nomenclature.....	113

LIST OF TABLES

	Page
1. Relative Amounts of Sized Basalt Used.....	16
2. Chloride-36 Diffusion Coefficients and Error Terms.....	39
3. Coefficients of Correlation (r) and Determination (r^2), and Percent Error in Slope.....	40
4. Diffusion Coefficients For Tritium.....	45
5. Effective Diffusion Coefficients For Chloride....	45
6. Solubilities and Ion Amount Present in Synthetic Groundwater.....	47
7. Fortran Program To Calculate Least-Squares Best Fit For a Set of Data Points.....	66
8. Fortran Program To Determine The Effect of Data Errors on The Effective Diffusion Coefficient....	70
9. Program To Calculate a Multiple Linear Regression Coefficients, Basic.....	75
10. Specified Concentration of Ions in Synthetic Groundwater.....	112

LIST OF FIGURES

	Page
1. Engineered Barriers.....	2
2. A Proposed Structure For Montmorillonite, (Edelman and Favejee).....	9
3. A Second Proposed Structure For Montmorillonite, (Hofmann, et al.).....	10
4. Diffusion Cell Parts.....	20
5. Extruder.....	24
6. Core Slicer.....	26
7. Temperature Dependence of Chloride Diffusion.....	35
8. Dependence on Bulk Density of Chloride Diffusion.....	37
9. Diffusion Test, Carbon-14 (D-C14-020-002).....	48
10. Diffusion Test, Carbon-14 (D-C14-020-011).....	50
11. Diffusion Test, Carbon-14 (D-C14-060-004).....	52
12. Diffusion Test, Carbon-14 (D-C14-060-016).....	53
13. Chloride-36 Diffusion Test: D-C136-020-002.....	78
14. Chloride-36 Diffusion Test: D-C136-020-003.....	79
15. Chloride-36 Diffusion Test: D-C136-060-004.....	80
16. Chloride-36 Diffusion Test: D-C136-060-005.....	81
17. Chloride-36 Diffusion Test: D-C136-060-006.....	82
18. Chloride-36 Diffusion Test: D-C136-090-007.....	83
19. Chloride-36 Diffusion Test: D-C136-090-008.....	84
20. Chloride-36 Diffusion Test: D-C136-090-009.....	85
21. Chloride-36 Diffusion Test: D-C136-020-010.....	86
22. Chloride-36 Diffusion Test: D-C136-060-011.....	87
23. Chloride-36 Diffusion Test: D-C136-020-013.....	88
24. Chloride-36 Diffusion Test: D-C136-090-015.....	89
25. Chloride-36 Diffusion Test: D-C136-020-016.....	90
26. Chloride-36 Diffusion Test: D-C136-060-017.....	91
27. Chloride-36 Diffusion Test: D-C136-090-018.....	92
28. Chloride-36 Diffusion Test: D-C136-020-019.....	93
29. Chloride-36 Diffusion Test: D-C136-020-020.....	94
30. Chloride-36 Diffusion Test: D-C136-090-021.....	95
31. Chloride-36 Diffusion Test: D-C136-060-022.....	96
32. Carbon-14 Diffusion Test: D-C14-020-002.....	97
33. Carbon-14 Diffusion Test: D-C14-060-003.....	98
34. Carbon-14 Diffusion Test: D-C14-060-004.....	99
35. Carbon-14 Diffusion Test: D-C14-090-005.....	100
36. Carbon-14 Diffusion Test: D-C14-090-006.....	101
37. Carbon-14 Diffusion Test: D-C14-020-007.....	102
38. Carbon-14 Diffusion Test: D-C14-020-008.....	103
39. Carbon-14 Diffusion Test: D-C14-060-009.....	104

LIST OF FIGURES--Continued

	Page
40. Carbon-14 Diffusion Test: D-C14-020-011.....	105
41. Carbon-14 Diffusion Test: D-C14-090-012.....	106
42. Carbon-14 Diffusion Test: D-C14-020-014.....	107
43. Carbon-14 Diffusion Test: D-C14-060-016.....	108
44. Carbon-14 Diffusion Test: D-C14-020-020.....	109
45. Carbon-14 Diffusion Test: D-C14-020-021.....	110

ABSTRACT

Effective diffusion coefficients were measured for chloride-36 at ambient temperature ($\sim 20^{\circ}\text{C}$), 60°C , and 90°C in a water-saturated 75%/25% basalt-bentonite mixture. Three separate tests for each of the given temperatures were run at two bulk densities of the medium, i.e., $1.6\text{g}/\text{cm}^3 \pm .1\text{g}/\text{cm}^3$ and $1.8\text{g}/\text{cm}^3 \pm .1\text{g}/\text{cm}^3$. The same tests were run for carbon-14, but the data could not be analyzed to find diffusion coefficients.

The diffusion of chloride was found to increase with increasing temperature.

Increasing the bulk density of the diffusion medium inhibited the movement of chloride and reduced the diffusion coefficient.

A one-dimensional model that was solved using the assumption of linear sorption of the tracer described the diffusion of chloride well.

The effective diffusion coefficient of chloride is larger for experimental systems in which the tracer is initially present in the diffusive medium compared with when it is initially present in a solution adjacent to the medium.

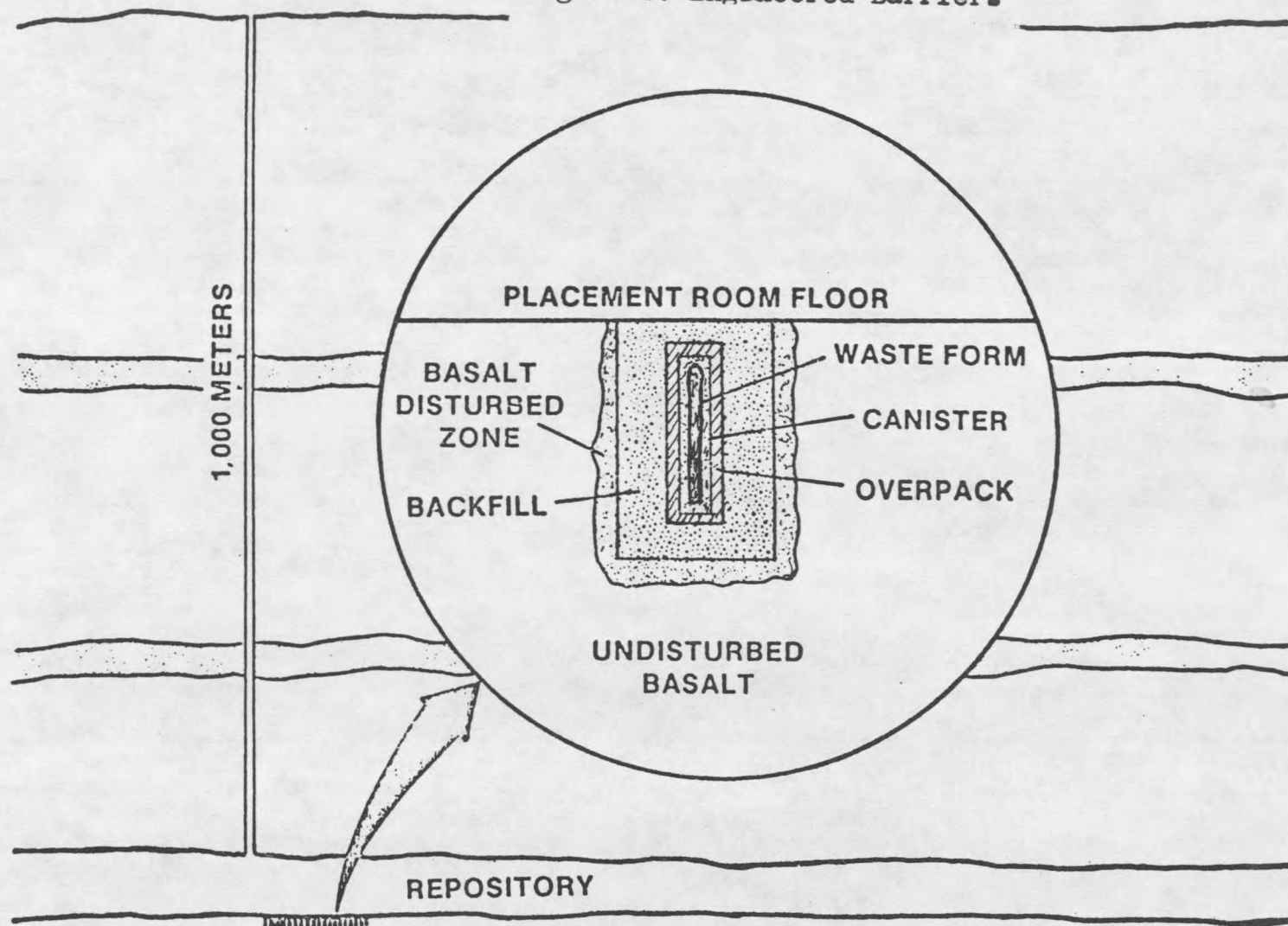
The diffusion coefficients of carbon-14 were not measurable because it formed a precipitate or sorbing complex with calcium and/or magnesium.

INTRODUCTION

In 1951, electricity was first generated using nuclear fuel in the United States (1). Since then, nuclear power has become an important alternate source of energy in this country. Consequently, the safe disposal of radioactive waste produced from atomic reactors and defense work is an important national problem (2). One of the most attractive disposal alternatives is to deposit the wastes in deep, stable geologic formations, i.e., salt, tuff, basalt (2). Basalt and tuff are both volcanic formations, the latter being derived from ash and is consequently more porous. Both natural and engineered barriers will be used to impede the movement of radionuclides into the biosphere from these repositories (3). This generalized concept is diagramed in Figure 1 for engineered barriers in basalt (3). Each barrier is designed in accordance with the specific waste form chosen to be buried and also with respect to the geologic environment that controls the stability of the repository (3).

In this investigation the backfill barrier will be the medium of interest. The backfill barrier is a continuous layer that surrounds the waste container, filling all the void between the overpack and the host rock

Figure 1. Engineered Barriers



(4). To be an effective backfill barrier, a substance must have the capacity to sorb radionuclides diffusing from the waste material (4). Just as important, the backfill material should have a low permeability, adequate thermal conductivity for heat transfer, and be resistant to fracture (4). In this way, the backfill can act as an inhibitor of radionuclide migration in the event of canister leaks, etc. In this work the barrier will be composed of 75% crushed basalt and 25% sodium bentonite clay. This mixture is a candidate for use in the basalt repositories proposed for the Hanford nuclear waste disposal area (5).

Certain standards of repository performance have been set by the Environmental Protection Agency (EPA) and the Nuclear Regulatory Commission (NRC) (6). The repository must be shown to satisfy these requirements before it can be licensed (6). Therefore, a study must be undertaken to obtain data on the performance of the repository. One of the first steps in this study is the measurement of effective diffusion coefficients for the various radionuclides through the proposed backfill barrier (5). A range of experimental conditions which effect reaction conditions and chemical transport properties in the area of the repository must be included in the study (6). In this

work, temperature and bulk density have been chosen as the main variables, because of the significant effects they have on the diffusion of the radionuclides. The tracers will be chloride-36 and carbon-14, diffusing through a water-saturated backfill. Although both radionuclides are used in anion form, each may exhibit different types of behavior in the clay (7,8). Therefore, the properties of the backfill are an important factor in how the tracers diffuse.

THE BACKFILL

The starting raw bentonite used in the testing was mainly a sodium bentonite clay, as mentioned earlier. The remaining portions included components such as quartz, feldspars, and smaller amounts of other impurities (5).

Basalt is a low-permeable, magmatic rock that is prevalent in the geologic formations of the proposed repositories on the Hanford area. Its permeability is on the same order of magnitude as bentonite, i.e., 10^{-9} - 10^{-15} m/s (9,10). This material will be used in the barrier in the form of small, granular particles (less than 16 mesh), facilitating compaction of the mixture. Therefore, because of the small size and low permeability of the basalt particles in the backfill, it is not considered to be a

medium through which diffusion occurs. The bentonite acts as a continuous medium for diffusion, and reduces the pore volume throughout the compacted backfill(6). It does this by adsorbing water and swelling to fill the voids in the crushed basalt(7).

RELATED WORK

Several factors, besides those already mentioned, also influence the diffusion of radionuclides through a porous solid. Temperature is one such factor that was varied in this work. A general trend of how temperature affects the diffusion coefficient is known. Relyea(11) states that diffusion increases with temperature, due to the increase in the kinetic energy of the particles.

Eriksen et al. have run diffusion tests on bentonite, using chloride-36 and iodide-131 as tracers, in both breakthrough and concentration profile tests (12). In these experiments two temperatures were used (25°C,70°C), and air-dry bentonite was compacted before water uptake (and saturation) occurred. They found considerable resistance to the diffusion of chloride-36 and iodide-131, most likely caused by interactions with the clay-water system. The smaller interparticle and intralamellar voids seemed to inhibit the diffusion of water through the bentonite. The

larger intralamellar and interparticle voids were therefore assumed to be the main passages of the anions.

In Kissel's et al. (13) investigation of chloride movement through Houston Black swelling clay, they too found that the larger (connected) soil pores are often important pathways for Cl^- movement. Even though Cl^- can move quickly through these pores, there was some resistance to the Cl^- movement due to interactions of the clay structure and the negative charge of the anions. Movement of anions in this system may also be different than in compacted clays, where there will be reductions in the size and differences in the shape of the voids and pores(14). Therefore, the interactions between the radioactive anions and the clay/water system may be different for compacted and uncompact clay. For example, Lai et al. (15), like Kissel et al. (13) found that the negative charge of the clay seemed to have been a factor in anion diffusion. Repulsive forces that are created were found to reduce the mobility of the anion. Compaction of the clay further reduces the cross-sectional area available for diffusion and by doing this creates a larger repulsive force of the clay on the anion.

Dutt and Low(16) postulated that not only are anions repulsed by the negative clay layers, but they also have

difficulty entering the clay from an adjacent solution. Eriksen et al. (12) used a test where the initial concentration of the tracer was present in the fluid adjacent to the clay. The radionuclide would then diffuse into the clay as well as through it. Comparing with Hamid's (17) results, Eriksen et al.'s values for the diffusion coefficient of iodide were one to two orders of magnitude smaller. In Hamid's work (17), he measured the diffusion coefficient within clay soil for iodide. Therefore, the postulate of Dutt and Low must have some validity.

In Dutt and Low's (16) work they also compared the diffusion of alkali chlorides with that of heavy water (D_2O). They found very little difference between the size of the values except that the diffusion coefficient for the heavy water was larger. This is because the electrical interactions of the clay with the ions reduced the mobilities of the ions (16).

The retention of iodine in various substances was studied by B. Allard et al. (19). A significant amount of iodine was found to be sorbed by montmorillonite, especially in the presence of chloride. Hamid (17) also found iodide to be sorbed onto clay soil. Consequently, Hamid (17) found the diffusion coefficient for I-ions to be lower than that for Cl-ions. This implies that Cl^- ,

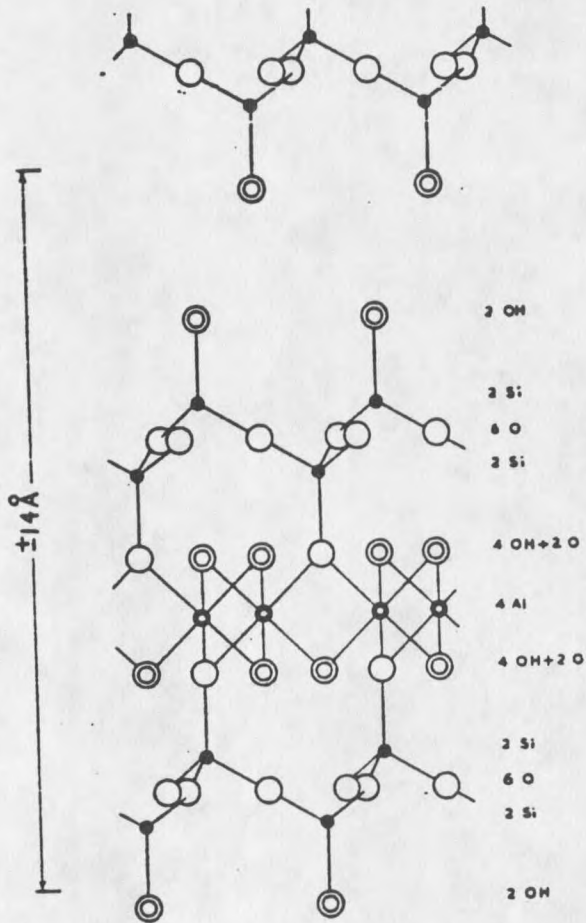
although also an anion, is less likely to be sorbed by a clay than I^- . Because they are both halogens, the properties of the ions should be similar (19). The iodide ion is much larger though, and the electrostatic interactions of the clay layers with the ion may be greater and consequently a difference in sorption properties results.

Other studies have been performed on the movement of radionuclides in compacted bentonite (12,15,20). Many radionuclides, which exist as cations under repository conditions are sorbed by the clay due to cation-exchange processes. Movement of the cations can be assumed to be through the interlamellar as well as the intralamellar space, unlike anions (12).

CLAY MINEROLOGY

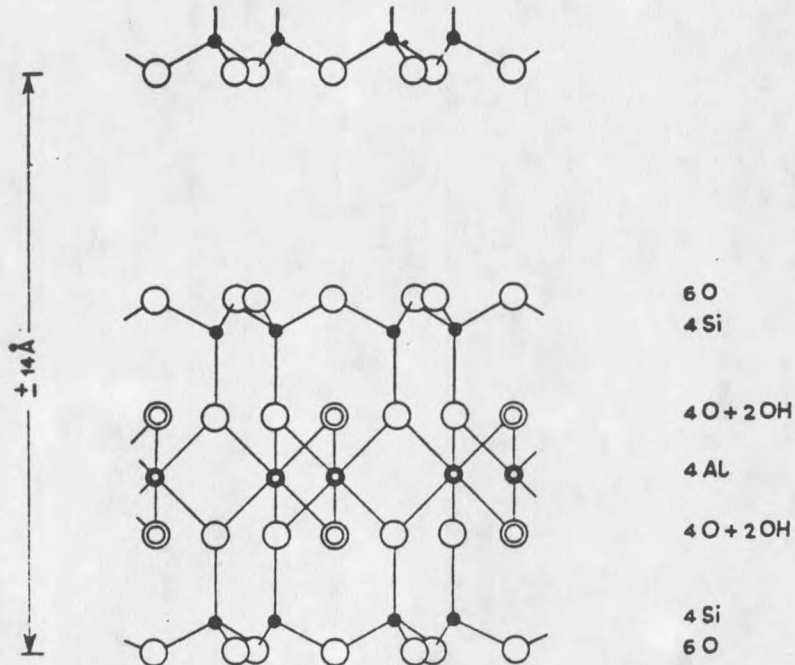
Two idealized lattice structures for montmorillonite, the major component of bentonite rock are depicted in Figures 2 and 3 (8). These structures depict the clay as neutral, although montmorillonite is known to have a negative charge (7). This charge is created because the composition of the clay platelet can vary due to isomorphous substitution of the trivalent Al with Mg, Fe, Cr, Zn and other atoms (7). That is, aluminum, with its

Figure 2. A Proposed Structure For Montmorillonite



THE PROPOSED STRUCTURES FOR MONTMORILLONITE (IDEALISED)

Figure 3. A Second Proposed Structure For Montmorillonite



THE PROPOSED STRUCTURES FOR MONTMORILLONITE (IDEALISED)

higher positive valence is replaced by elements of a lower valence. The tetravalent Si itself will occasionally be replaced by Al in the structure (7).

The layer structures are weakly bonded to each other with van der Waals forces (7). The water will penetrate these layers and form hydrogen bonds with the oxygen-containing clay platelet surfaces (7). The resulting interlamellar swelling can add up to four monomolecular layers of water between the layers of clay (7). Depending on how little the pressure is that is put on the clay, repulsion of like-charged clay layers can cause the uptake of more water (7). If the water causes the plates to separate by more than 10\AA , which is more than three times the size of the tracers used in this investigation, a second stage of swelling occurs (7). This type of swelling will cause the bentonite clay to expand to much larger volumes and disperse into a finely divided suspension (7).

Because the crystal layers carry a net negative charge, this charge is compensated for by cations adhering to the surface of the layers (7). When water is present, these cations will tend to diffuse away from the surface due to a lower concentration in the bulk solution (7). The resulting double layer thickness then contains cations that are readily exchangeable (7). Diffusing cations therefore

may have movement hindered due to sorption on the clay (7). Anions, on the other hand, will be repelled by the negative clay layers and remain in the bulk water of the intralamellar space (7).

The double layer can be varied in size by the amount of electrolyte present (21). In this way, electrolyte concentration can cause swelling of the clay and a reduction of its porosity (21). Consequently, the resulting double layer will be decreased in width and the pores will become more clogged with increasing ion concentration (7,21). For monovalent counter-ion concentrations varying from 0.01-100mmol/dm³, the approximate double layer thickness varies from 1000 down to 10 \AA (7). For divalent counter-ions in the same concentration range, the thickness varies from 500-5 \AA (7). The pH of the clay solution is also known to affect the double layer, especially at the edges where aluminum ions are exposed (7). The edge has a tendency to become positive at low pH (7). This will give the clay an ability to sorb anions, albeit small amounts compared to the net negative charge of the clay (7,22).

CHLORIDE-36

Radiotracers have found increasing importance in the study of water movement through porous media (23). In this

investigation, chloride-36 has been chosen as a tracer of water diffusion through the backfill. This tracer was chosen due to the tendency of the chloride to diffuse through the pore water with little chance of being sorbed onto the clay (24).

There are some differences between the movement of water and chloride through a clay because of the influences of the negative potential in the pore volume (7). Rolfe and Aylmore (25) reported that diffusion can at least partially compensate for these differences, which would be more noticeable at higher flow rates through the clay. This suggests that chloride movement in the clay is much like that of water at low pressures. Therefore, the chloride-36 tracer should describe the transport of water through the bentonite with some accuracy. Tritium, in the form of heavy water, should even be better at describing the water transport in the clay, but the differences between it and Cl^- should also be small (16).

CARBON-14

Carbon-14 (half-life: 5730 yrs.) in radioactive waste is a potential long-term biological hazard (26). In the form of carbonate, which is the tracer used in this work, it can react with Ca^{++} or Mg^{++} in the groundwater to form a

weak complex or precipitate (27). Consequently, sorption of the complex or precipitate on the bentonite can occur (26). The formation of the magnesium or calcium complexes and precipitates depend on the temperature, pH, Eh, and concentrations of the ionic species in the groundwater (26,28). Carbon-14 may react with hydrogen and form other species as well, such as carbonic acid and HCO_3^- ion (26). There is also a chance that the carbonic acid will react to form CO_2 and water, depending on where the equilibrium lies (28).

Allard et al. (26) investigated the possibility of carbon-14 sorption using various geologic media, including sodium montmorillonite and also a bentonite/quartz (10/90) mix. Using several contact times (3days-6mos.), they found that while there was no sorption on sodium montmorillonite, there was some on the bentonite/quartz mix. They explained this by pointing out that the bentonite used contained calcium, which gave a higher concentration of calcium ion in the liquid. It is therefore possible that there is no carbonate sorption on the bentonite if it is a sodium clay. However, to determine the actual importance of carbonate sorption, the effects of other variables will have to be established ,e.g., calcium concentration.

Besides the information already given, ^{14}C -carbonate tracer is expected to have the same anion interactions with the clay as chloride-36, possibly more pronounced because of the larger negative charge of the carbonate. However, the actual role that the different size and shape may have on the diffusion of the two radionuclides is uncertain. Carbonate is expected to have a smaller diffusivity than chloride because of its larger size (11), i.e., about 2.81\AA and 1.81\AA , respectively (29,30). Also, it is known that calcium carbonate can cause variations in the swelling behavior of clay (31), which may affect its diffusion properties.

RESEARCH OBJECTIVE

The objective of this research was to measure effective diffusion coefficients for chloride-36 and carbon-14 through a compacted 75/25 basalt/Na-bentonite mixture. The tests will be performed at three different temperatures, i.e., 20, 60, and 90°C , and two bulk densities, i.e., 1.6 and 1.8g/cm^3 . From the data, a relationship between the effective diffusion coefficient and the two variables is to be determined. The experimental results should also develop a better understanding of the mechanism of anion movement through swelling clays.

EXPERIMENTAL

MATERIALS

The basalt used was taken from the Columbia Basin area in the state of Washington. The rock was originally picked from outcroppings near the Hanford area. This specific basalt was chosen due to its availability in the underlying formations of the proposed radioactive waste repository on the Hanford site. Only those samples that did not appear to be weathered, i.e., yellowed or eroded, had been chosen. The rock was then crushed to smaller sizes before it was available for use in this investigation.

The rock was further crushed in a shadow box. The relative amounts of each appropriate mesh size are given in Table 1.

Table 1. *Relative Amounts of Sized Basalt Used

**Mesh	-16+60	-60+120	-120+230	-230+325	-325+400	-400
Amount(g)	1558	120	174	58	30	60
Total of All Mesh=2000g						

*- These amounts are relative because 4000g were prepared and then this amount was split in half with a riffle splitter

**- - means that it passes through this mesh size
+ means that it will not pass through this mesh size

A technician determined the grain density of the basalt mixture to be 2.89g/cm^3 using a air equilibration pycnometer. The procedure involves putting a known amount of sample in a vial with water (32). The necessary parameters such as water density are known.

The sodium bentonite used was mined in Wyoming. The specific location is unknown. The bentonite came in a fine powdered form and contained small amounts of impurities such as quartz and feldspars (5). The bentonite was chosen due to its ability to swell and fill voids in rock, but also due to its low permeability and retardation properties (7). The grain density of the bentonite was determined to be 2.69g/cm^3 by R.A. Carlson, a fellow worker (33).

A 666.7g portion of bentonite was stirred in with the basalt mixture to form a 75/25 mix of basalt to bentonite. The resulting blend was split four times with a riffle splitter for mixing purposes, and then split into eight portions, archived, and stored.

To obtain portions small enough for the individual tests, the larger containers were mixed as before and then split down into 8-18g individual portions. During this procedure, the portion that was to be split was mixed thoroughly before each splitting. It was found that this method would appear to give a more accurate splitting of

the material. Once enough small portions were made, e.g., there were two for each test, the samples were archived and stored.

The moisture content of the basalt/bentonite mixture was determined to be 1.5% in March of 1984. The moisture content was redetermined in July of 1984 and was found to be 2.7%. The procedure for determining the moisture contents was ASTM D2216-80. The method involved the drying of a backfill sample for approximately 1 day in a GCA/Precision Scientific heated vacuum dessicator set at $110^{\circ}\text{C} \pm 5^{\circ}\text{C}$. The first moisture content measurement on the backfill used a drying oven, as called for in the procedure, instead of a heated vacuum dessicator. The other measurement of the moisture content of the backfill used the dessicator because it kept the atmosphere thoroughly dry around the drying sample. For other moisture content readings of the test cores, the samples (1-2.5g slices of the core) were possibly contaminated with a tracer. To safely contain the radioactivity, the heated vacuum dessicator could conveniently be put in a hood whereas an oven could not.

EXPERIMENTAL PROCEDURE

A piece of equipment called a diffusion cell was fabricated by craftsmen for this investigation. The cell contains two half cells, depicted in Figure 4b. There is a surrounding cylinder with screw caps on the outside. The total cell as it appears on the outside is pictured in Figure 4a.

The half cells were to be packed similarly in most respects for each cell, i.e., backfill composition, bulk density, except that one half cell contained a tracer while the other did not. For diffusion to occur, one of the half cells containing the tracer was put in contact with the other half cell containing only the saturated backfill mixture.

Two bulk densities, 1.6g/cm^3 and 1.8g/cm^3 were used in this investigation, although for the carbon-14 tests only 1.6g/cm^3 was used. To produce test cores that were of the right bulk density, a certain amount of a synthetic groundwater was put with the air-dry backfill samples and mixed. The amount of water to be used was given by the following equations (34):

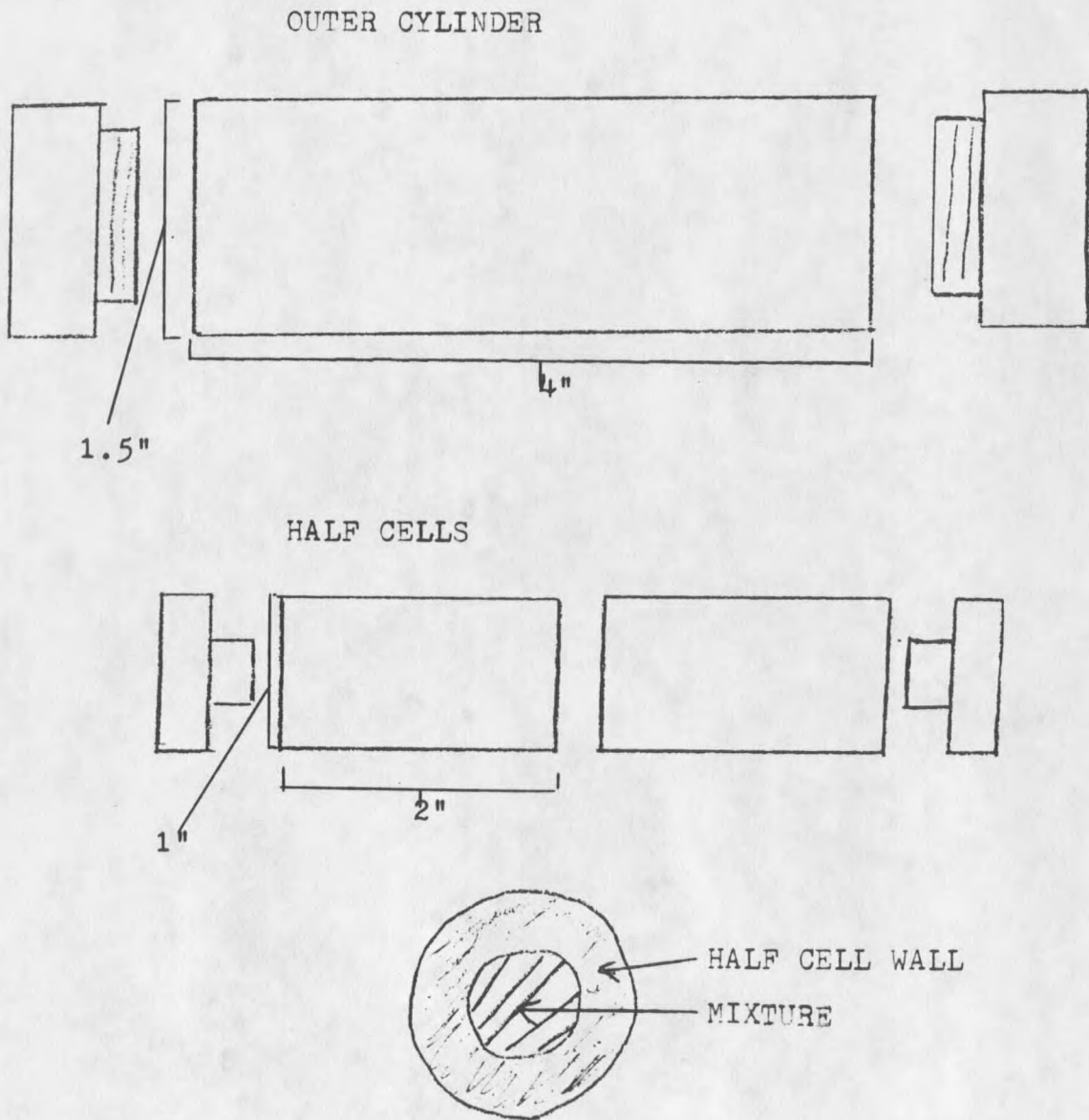
Amount of Air-dried Backfill:

$$X = (BD)(V_h)(1+W)$$

Total Porosity of Backfill-water Mixture:

$$P_t = 1 - [X] \left[\frac{F_1}{PD_1} + \frac{F_2}{PD_2} \right] / [V_h(1+W)]$$

Figure 4. Diffusion Cell Parts



Amount of Water To Be Added To Dry Backfill:

$$Y_w = (P_t)(PW)(V_h) - (W)(X)$$

X=amount of air-dried backfill (g)

BD=specified bulk density (g/cm^3)

V_h =volume of half cell ($\sim 5.3\text{cm}^3$)

W=moisture content of backfill

P_t =total porosity of the resulting backfill-water mixture

F_i =weight fraction of the i th component in the backfill
(75% basalt/25% bentonite)

PD_i =grain density of the i th component in the backfill

PW=density of water ($1\text{g}/\text{cm}^3$)

Y_w =amount of water (g) needed to be added to air-dry backfill sample to get specified bulk density

Since two mixtures were prepared for each test cell, each water amount was measured separately. For the untagged mixture, i.e., without the tracer, the synthetic groundwater was measured out on a scale ($\pm 0.001\text{g}$) and set aside. For the tagged mixture, a $20\mu\text{l}$ spike was added to the measured water amount for the chloride-36 tests and a $40\mu\text{l}$ for the carbon-14 tests. Two $20\mu\text{l}$ samples were then taken from the tagged mixture to be counted for an initial concentration determination. Also, 15ml of instagel (containing a phosphor) were added to each sample for purposes of counting on the Packard (Tri-carb 4000 series) scintillation machine.

The water samples, tagged and untagged, were added to the two backfill samples and stirred thoroughly. (Note: The mixtures were stirred again after an hour.) The sample

containers containing the mixtures were then put in a humidity chamber (dessicator filled with water) for equilibration overnight. The teflon parts of the diffusion cell were put under water overnight to insure total saturation of the parts. The next day the total weight of the parts ($\pm 0.01g$) was determined.

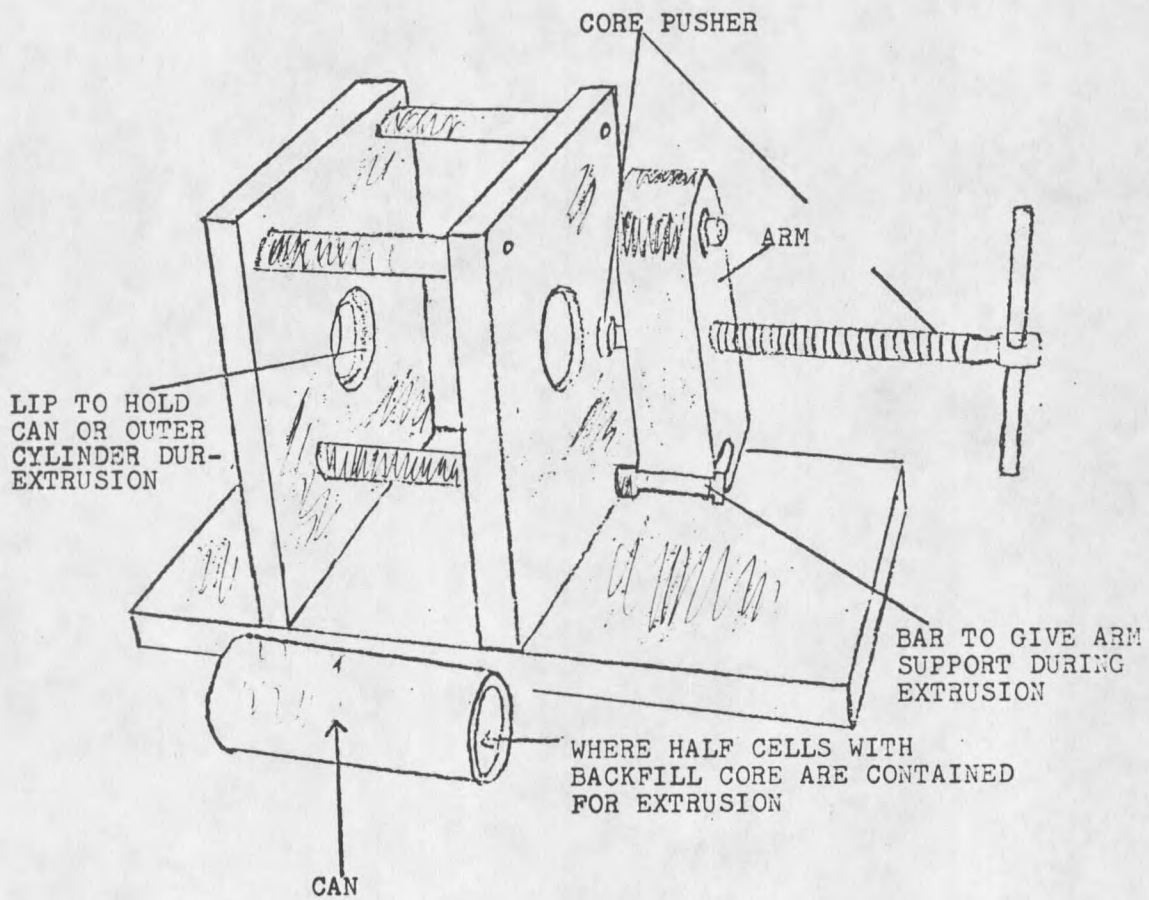
The half cells were packed starting with the untagged mixture. First, small amounts of the mixture were spooned into the half cell. Second, the mixture was packed down with a stainless steel rod until saturation was reached, or rather until the material glistened. This process was continued until the half cell was filled to about 1/16" above the top. The packed material was then levelled with a straight-edged blade. This procedure was repeated for the tagged mixture.

Once both half cells were packed, a teflon disk was placed between the half cells as they were brought together. This unit was then loaded into the surrounding cylinder. The diffusion cell was then reweighed in order to determine the amount of material packed in the cell. The cell was equilibrated after weighing for as long as deemed necessary to reach uniformity of concentration in the tagged half cell. For chloride-36 this period was only one day because it is a fast moving tracer.

After the time for equilibration had passed, the teflon disk was removed from between the half cells to allow diffusion of the tracer. During this period, the diffusion cell was placed in a humidity chamber controlled at one of the three temperatures (ambient~20,60,90°C). For the 60°C environment a New Brunswick Controlled Environment Incubator Shaker was used. For the 90°C environment a Blue M Stabil-therm oven was used. The diffusion was allowed to continue until the tracer went a sufficient amount into the untagged portion of the diffusion cell but not to the end. In order to determine a correct amount of time, some extra trials had to be used.

After the diffusion time had expired, the diffusion cell was removed from the given humidity chamber. Approximate diffusion times were as follows: 1) They were about five hours for the ambient tests; 2) about 3 hours for the 60°C tests, and 3) about 2 hours for the 90°C tests. For the 60°C and 90°C tests the cells were put in an ice bath for five minutes first, and then the cells would be frozen in liquid nitrogen for five minutes (35). The inner clay core was extruded using the machine depicted in Figure 5. First, the outer shell was removed. Then, using the can pictured on the left of Figure 5, the inner (backfill) core was extruded.

Figure 5- Extruder



The core was sliced using the machine in Figure 6. Starting with the untagged end, 0.5cm was pushed under the blade by the core pusher and sliced off. (Note: The threaded bolt connected to the core pusher has 10 threads per cm.) The sample was caught in a metal can and dried in the heated vacuum dessicator to determine its moisture content. The procedure used was ASTM D2216-80, as mentioned before. The bulk density was then determined using the equation (34):

$$\text{BULK DENSITY} = 1 / [(1 / 2.84) + \text{MOISTURE CONTENT}]$$

where

$$\text{BULK DENSITY} = M_s / V$$

and

$$V_w + V_s = V$$

$$V_w = M_w / P_w$$

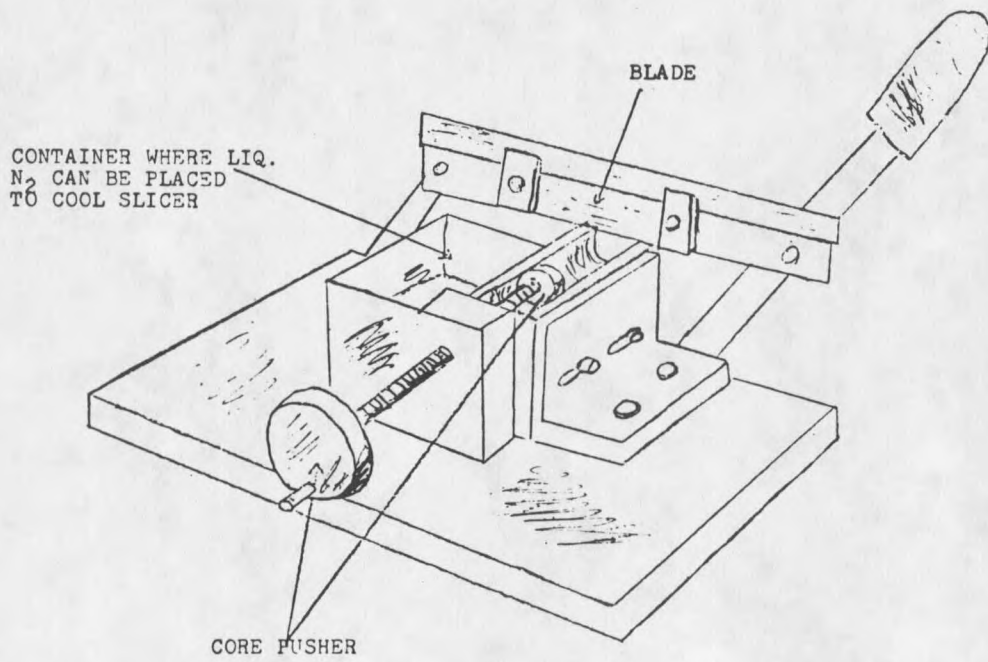
$$V_s = F_1 (M_s) / PD_1 + F_2 (M_s) / PD_2$$

$$M_w / M_s = W$$

M_w = water mass
 M_s = solid mass
 P_w = water density
 V_w = water volume
 V_s = solid volume
 V = total volume

W = moisture content
 F_1 = basalt fraction
 F_2 = bentonite fraction
 PD_1 = basalt grain density
 PD_2 = bentonite grain density

Figure 6. Core Slicer



In this manner, the final bulk density can be checked with that originally calculated. The process was continued with 0.1cm slices being sliced off the core and put into scintillation vials until the core was gone. The vial containing the interface was marked. The actual vial containing the interface may have been off by one or two vials. This was because of the difficulty in finding the interface due to the uniformity in appearance of the core.

For scintillation counting of the slices, 10ml of deionized water and 10ml of instagel were added. Upon shaking of the vials, a suspension of the solid would form. Chemically quenched standards were prepared by adding a known amount of spike into three vials containing 15ml of instagel. Optically quenched standards were made from a range of slices from 0.15-0.6g from an untagged core made especially for the purpose. Only five standards were used to cover the same range that was expected with slices from testing. The vials were made into a suspension for scintillating, just as with other sample slices, and to each vial a given amount of tracer spike was added. For any other details or procedures of the beta liquid scintillation analysis used in this investigation, refer to ASTM D3648-78.

MATHEMATICAL MODELLING AND
STATISTICAL ANALYSIS

For diffusion of anions in soil the transport equation is given by (36):

$$D\frac{\partial^2 C}{\partial x^2} = \frac{\partial C}{\partial t} + (\rho_b / Q_v) \frac{\partial S}{\partial t} \quad [1]$$

where:

D=diffusion coefficient

C=concentration of anion in soil

S=amount of anion sorbed by soil

ρ_b =soil bulk density

Q_v =volumetric moisture content of the saturated soil paste

A linear relationship in terms of the anion concentration is assumed for sorption onto the clay. If the surface and solution phases are in local equilibrium, then:

$$S = K_d C \quad [2]$$

where K_d is a constant called the distribution coefficient.

Combining equations 1 and 2 gives the following:

$$D\frac{\partial^2 C}{\partial x^2} = (1 + K_d (\rho_b / Q_v)) \frac{\partial C}{\partial t} \quad [3]$$

Defining the retardation factor, R_o , as $K_d \rho_b / Q_v$, equation 1 may be written:

$$(D/(1+R_o)) \partial^2 C / \partial x^2 = \partial C / \partial t \quad [4]$$

where $D/(1+R_o) = D' =$ Effective diffusion coefficient,

and for the final form of equation 1:

$$D' \partial^2 C / \partial x^2 = \partial C / \partial t \quad [5]$$

For the system in this work (see Figures 13-31, App. B), the initial and boundary conditions are:

$$C(x < 0, 0) = \text{initial concentration} = C_o \quad [6]$$

$$C(x > 0, 0) = 0$$

$$C(-\infty, t) = C_o$$

$$C(\infty, t) = 0$$

The solution of this model then is (37):

$$C = 0.5 C_o \operatorname{erfc}(x / (2\sqrt{D't})) \quad [7]$$

where: $\operatorname{erfc}(z) = (2/\sqrt{\pi}) \int_{x/(2\sqrt{D't}}^{\infty} \exp(-n^2) dn$

Equation 7 may be rearranged to yield:

$$C/C_0 = \frac{1}{\sqrt{2\pi}} \int_{-\infty}^{-x/(\sqrt{2D't})} \exp(-z^2/2) dz \quad [8]$$

The above equation is similar to the formula for the cumulative probability of a standard normal distribution (38):

$$P = \frac{1}{\sqrt{2\pi}} \int_{-\infty}^z \exp[-t^2/2] dt \quad [9]$$

The definition of a probit or probability unit is given as (39):

$$P = \frac{1}{\sqrt{2\pi}} \int_{-\infty}^{Y-5} \exp(-u^2/2) du \quad [10]$$

The C/C_0 values can be converted to percentages and probit values found for these percentages from tables in Finney (39). A regression of the probit values (Y) versus the axial distance (x) will then give an equation of the form:

$$Y = -bx + a \quad [11]$$

For a perfect match by the least-squares estimators, $a=5$ and $b=1/(\sqrt{2D't})$, and the effective diffusion coefficient can be found from:

$$D' = 1/(2b^2t) \quad [12]$$

PROCEDURE

An IBM PC and LOTUS 123 software were used to perform all calculations of the regression analysis and error analysis involving the slope and diffusion coefficient. The following are the equations for the standard deviation of x and y (38):

$$\text{SDEV}(x) = [(\sum x^2 - (\sum x)^2 / N) / (N-1)]^{1/2} \quad [13]$$

$$\text{SDEV}(y) = [(\sum y^2 - (\sum y)^2 / N) / (N-1)]^{1/2} \quad [14]$$

where N=the number of data points

x=independent variable

y=dependent variable

The equations for the slope and y-intercept are given as (38):

$$b = [\sum xy - (\sum x \sum y) / N] / [\sum x^2 - (\sum x)^2 / N] \quad [15]$$

$$a = (\sum y - b \sum x) / N \quad [16]$$

The following equation is that for the sampling correlation coefficient, r (38). [r=1 for a perfect linear relationship]

$$r = b * \text{SDEV}(x) / \text{SDEV}(y) = \text{SDEV}(xy) / [\text{SDEV}(x) \text{SDEV}(y)]^{1/2} \quad [17]$$

The error in the slope (and standard deviation), and consequently the error in the diffusion coefficient, are given as follows (40). The errors are given in terms of two standard deviations of the slope.

$$\text{SDEV}(b) = [(\Sigma(y - a - bx)) / [(N-2)(\Sigma x^2 - (\Sigma x)^2 / N)]]^{1/2} \quad [18]$$

$$\text{Percent Error in Slope} = 2(\text{SDEV}(b))(100)/b \quad [19]$$

Error Term For

$$\text{Diffusion Coeff.} = 2(\text{SDEV}(b))(D')/b \quad [20]$$

Multiple linear regression analysis was done on the chloride-36 data, where the \log_{10} of the diffusion coefficient is the dependent variable (y) and the bulk density and inverse of the temperature are the two independent variables (x_1, x_2). In this way, the effective diffusion coefficient can be found for other conditions within the range tested. The equations are based on methods utilized in Steel and Torre (41).

$$y = B_0 + B_1 x_1 + B_2 x_2 \quad [21]$$

where

$$B_2 = (A_1 * A_3 / (A_2 - A_4)) / (A_1^2 / (A_2 - A_5))$$

$$B_1 = (A_3 - A_1 * B_2) / A_2$$

$$B_0 = (S_y - B_1 * S_{x1} - B_2 * S_{x2}) / N$$

and

$$A_1 = \frac{\sum x_1 x_2 - \sum x_1 \sum x_2}{N}$$

$$A_2 = \frac{\sum x_1^2 - (\sum x_1)^2}{N}$$

$$A_3 = \frac{\sum x_1 y - \sum x_1 \sum y}{N}$$

$$A_4 = \frac{\sum x_2 y - \sum x_2 \sum y}{N}$$

$$A_5 = \frac{\sum x_2^2 - (\sum x_2)^2}{N}$$

$$S_{x1} = \sum x_1$$

$$S_{x2} = \sum x_2$$

$$S_y = \sum y$$

The average activation energies were determined from the diffusion coefficients found for chloride-36. The activation energy, E_a , is given by (42):

$$E_a = -RT \ln D' + RT \ln A \quad [22]$$

where

A=Arrhenius frequency factor

R=gas constant

RESULTS AND DISCUSSION

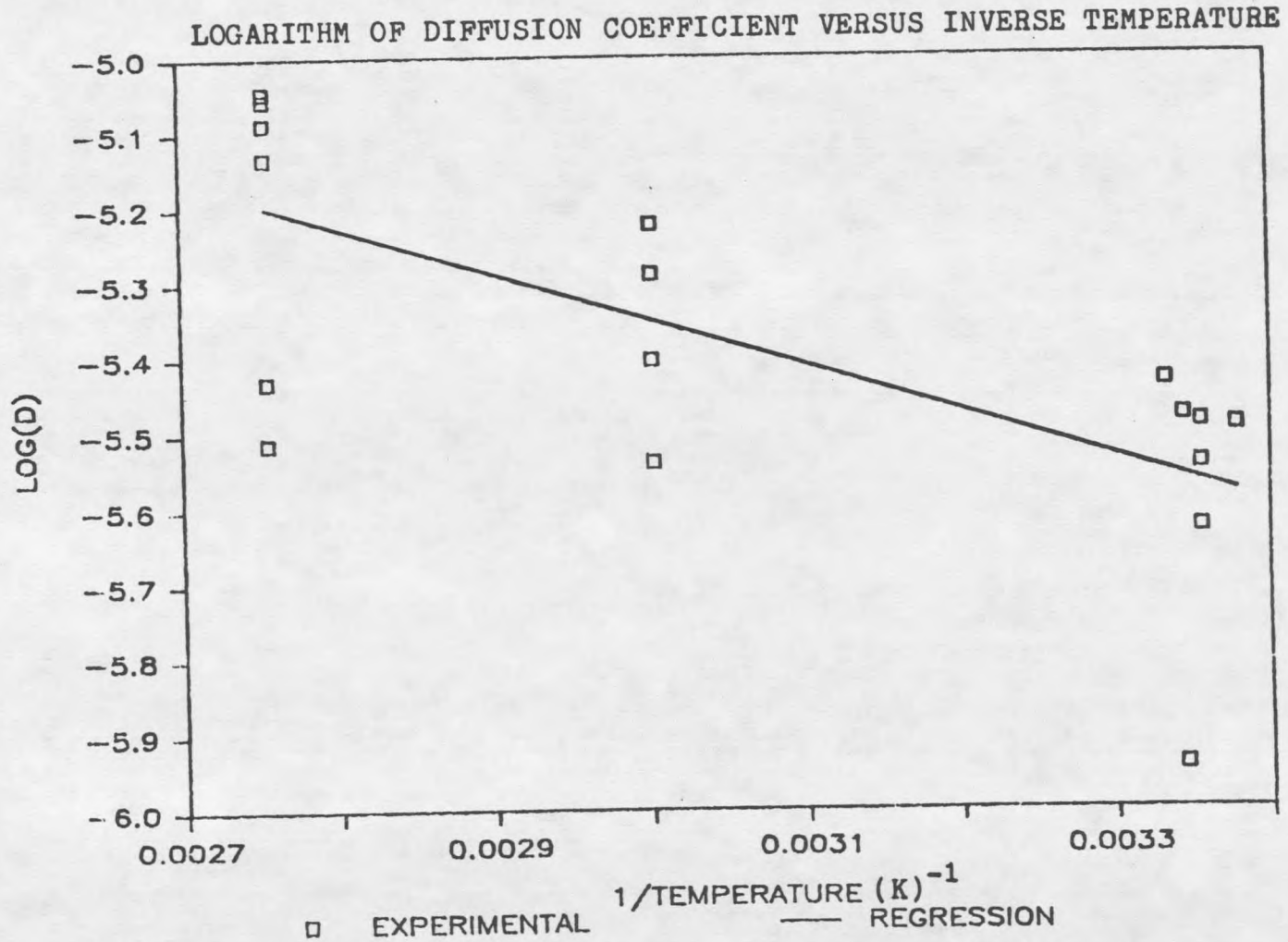
A concise edition of the data and results discussed in this thesis is presented in Appendix B. The raw data for the individual tests are displayed in plot form. The corresponding regression curve for the data is presented in each of the figures.

DIFFUSION OF CHLORIDE-36:

TEMPERATURE EFFECTS

The diffusion coefficient is expected to vary as a function of temperature. The Arrhenius expression generally describes this behavior. The data for the effective diffusion coefficients at the two bulk densities ($\pm 0.1 \text{ g/cm}^3$) were fitted to the natural logarithm form of the Arrhenius equation to determine the activation energies. The program used to fit the data, called BEFIT, is listed in Appendix A. The resulting activation energies (E_a), presented as general information, for 1.6 g/cm^3 and 1.8 g/cm^3 are 14000 J/mole and 10000 J/mole, respectively. In Figure 7, the general tendency of the diffusion coefficient to decrease with increasing inverse temperature, i.e., to increase with increasing temperature,

Figure 7. Temperature Dependence of Chloride Diffusion



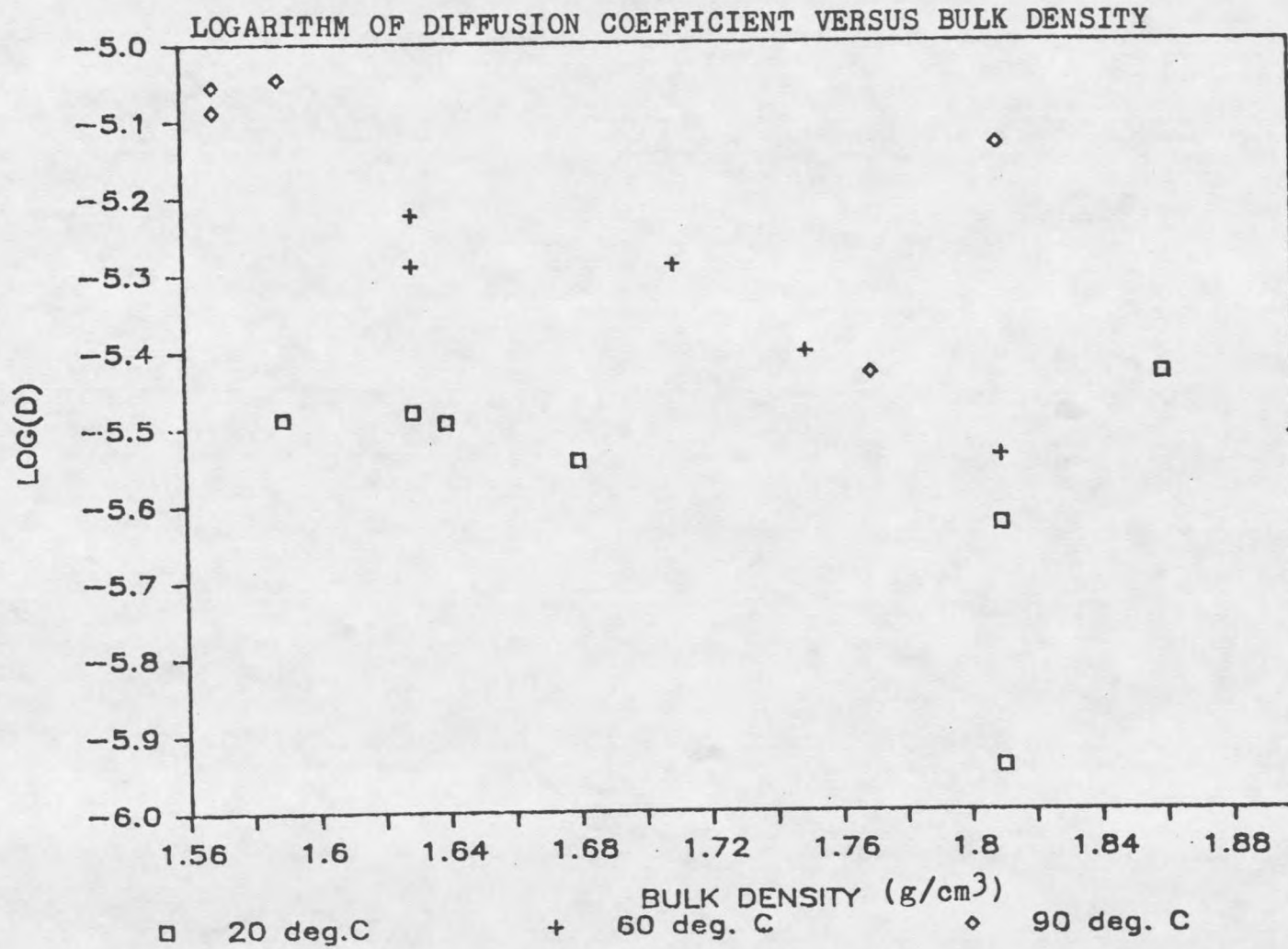
is displayed. The figure is presented in logarithmic form and a regression line of the entire set of data is shown. Note that the variation in bulk density is not taken into account, and the data scatters around a temperature. In fact, as the temperature increases, the scatter in the data becomes larger. These effects will be discussed in more depth later.

BULK DENSITY EFFECTS

In Figure 8, the logarithms of the chloride diffusion coefficients are plotted versus bulk density. For the data at each temperature, there is a tendency for the diffusion coefficient to decrease with increasing bulk density. This stands to reason, since there are smaller pore water pathways in which the anion can diffuse. The circumference of the pathways should also decrease, causing the electrostatic interactions between the clay layers and the anion to increase. Consequently, the diffusion of chloride is further hindered at higher bulk densities, which agrees with what was found experimentally.

The reduction of the chloride diffusion coefficients due to bulk density, i.e., porosity and tortuosity effects, is also noticed when comparing them to those in bulk water. The diffusion coefficient of chloride in bulk

Figure 8. Dependence on Bulk Density of Chloride Diffusion



water at 25°C is $2.03 \times 10^{-5} \text{ cm}^2/\text{s}$ (42), or roughly one order of magnitude greater than the coefficient in the clay basalt mixture. Comparing this value to the effective diffusion coefficients at 1.6 and 1.8g/cm³ bulk density (and 25°C) assuming sorption is negligible, the tortuosity factors of the backfill are determined to be 2.46 and 3.38, respectively. The porosity of the backfill decreases 16% as the bulk density increases from 1.6 to 1.8g/cm³, while the tortuosity increases 37%. Therefore, the effects of bending the pore water pathways appears to become more important in hindering diffusion of chloride at higher bulk densities. As you would expect, long straight pathways are apparently the most conducive to diffusion of the anion.

CORRELATION OF DATA TO THEORETICAL MODEL

The C/C_0 data for each test was fitted to the 1-dimensional model previously presented. The resulting effective diffusion coefficients and error terms are given in Table 2.

The error term data presented in Table 2 gives an indication of the deviations of the individual diffusion coefficients and scatter in the data. The scatter was determined using two standard deviations of the slope, which for normal statistics covers a 95% confidence region.

Table 2. Chloride-36 Diffusion Coefficients (cm^2/s) and Error Terms

Test	Conditions ($^{\circ}\text{C}$, g/cm^3)	Diffusion Coeff.	Error Term
20-002	26, 1.63	3.32E-06	3.61E-07
20-003	23, 1.64	3.22E-06	2.53E-07
60-004	60, 1.63	5.99E-06	7.29E-07
60-005	60, 1.63	5.99E-06	2.72E-07
60-006	60, 1.63	5.14E-06	5.29E-07
90-007	90, 1.57	8.17E-06	5.26E-07
90-008	90, 1.59	9.01E-06	9.66E-07
90-009	90, 1.57	8.80E-06	1.13E-06
20-010	27, 1.86	3.70E-06	1.83E-07
60-011	60, 1.81	2.89E-06	5.18E-07
20-013	26, 1.81	1.14E-06	2.12E-07
90-015	90, 1.90	3.07E-06	9.83E-07
20-016	25, 1.81	2.36E-06	1.36E-07
60-017	60, 1.71	5.14E-06	6.56E-07
90-018	90, 1.77	3.71E-06	6.99E-07
20-019	25, 1.68	2.86E-06	3.11E-07
20-020	25, 1.59	3.25E-06	1.64E-07
90-021	90, 1.81	7.35E-06	7.88E-07
60-022	60, 1.75	3.95E-06	3.78E-07

Although the error term is useful, the deviation of the diffusion coefficients from the theoretical model can best be detected by referring to the linear correlation of the data to the model. In Table 3 the correlation coefficient for each test and the resulting coefficient of determination are presented. In addition, the percent variation of the slope (2 standard deviations) is also presented to indicate how much the error in the slope varies with the correlation.

Table 3. Coefficients of Correlation (r) and Determination (r^2), and Percent Error in Slope

Test	Correlation Coeff.	Coeff. of Deter.	% Err in Slope
20-002	-.9883	.9767	10.89
20-003	-.9931	.9862	7.86
60-004	-.9768	.9541	12.16
60-005	-.9977	.9954	4.54
60-006	-.9870	.9742	10.28
90-007	-.9949	.9898	6.43
90-008	-.9859	.9720	10.72
90-009	-.9801	.9606	12.80
20-010	-.9970	.9940	4.95
60-011	-.9768	.9541	17.91
20-013	-.9751	.9508	18.58
90-015	-.9415	.8864	32.01
20-016	-.9971	.9942	5.76
60-017	-.9841	.9685	12.75
90-018	-.9785	.9575	18.86
20-019	-.9884	.9769	10.86
20-020	-.9975	.9950	5.05
90-021	-.9887	.9775	10.73
60-022	-.9921	.9843	9.56

For all but one data point, there is only 0.5-5% of the data variation not accounted for by the linear relationship between the probit values (of C/C_0 percentages) and axial distance. The error in the slope gets larger as the correlation gets smaller, as you would expect. For test 20-013 the correlation is -0.9751 and the percent error in the slope is 18.58%. For test 90-018, where the correlation is -0.9415, the error in the slope almost doubles to 32.01%. Although the correlation of the

test data with the theoretical is generally good, the y-intercepts still vary from 5, the value for an exact fit. This, in fact happens with all the tests. The majority of the y-intercepts from the tests range between 4.00 and 4.75. The relationship between correlation and proximity to the exact value of the y-intercept is not straightforward. Even if the correlation of one test is better than another, the deviation of the y-intercept from 5 for the test may be larger. To trace the causes of this fluctuation in the y-intercept, a program was written which would test the change in the diffusion coefficient due to errors in the raw data. The listing of the program can be found in Appendix A.

In the program, a set of C/C_0 ratios was produced from the theoretical model using a typical diffusion coefficient and time. A random error generated to fit a normal curve was then added to the C/C_0 values at a set standard deviation of the normal curve. Diffusion coefficients were then produced using the same mathematical (probit) analysis as used for experimental data. For a standard deviation of only 0.001, the new diffusion coefficient deviated from the original by 35%. The respective correlation was only 0.896. For increasing standard deviations of the error, the new diffusion

coefficients deviated further and the correlation became worse. The y-intercept values started at values larger than 5 (sdev=0.001) and then gradually decreased below 5 for increasing standard deviation. The greatest changes were noticed for the initial standard deviation of 0.001, even though the standard deviation was increased by increments of 0.05. It appears that the value of the diffusion coefficient is sensitive to the values of the experimental data using the probit analysis method. The variation in the y-intercept values produced with this method from that expected was therefore probably caused by data fluctuations. Since the correlation coefficients of the tests were so good, it is reasonable to assume that any sources of fluctuation affected all the data in a similar way. One possible cause may have been due to packing inconsistencies along the outer radius of the core, in other words, small gaps or nonuniformities in radius. Since the initial concentration for each test was taken as an average of several slices, the average values may have been too large. This effect would cause concentration values smaller than expected and the resulting y-intercept to also be reduced.

A better method of analysis could be used to determine the diffusion coefficients from the theoretical

solution, i.e., one that is less sensitive to errors in the data. One method would be to determine the area under the C/C_0 plot (versus axial distance), and compare it with areas predicted from a Gaussian distribution for various values of the diffusion coefficient.

Although better methods could have been used for the mathematical analysis of the diffusion coefficient, one thing can be concluded about the actual model used to describe the results. Because the data correlated well to the line determined in the probit analysis (excluding any errors in the intercept), the theoretical solution with the linear sorption assumption was valid in describing the data.

MULTIPLE LINEAR REGRESSION OF DATA

An equation for the logarithm of the effective diffusion coefficient (D) versus inverse temperature (1/T) and bulk density (BD) was determined to be:

$$\log D = -1.786442 - 577.6931/T - 1.074521(BD)$$

This equation may not best describe the relationship of the diffusion coefficient to the variables, but does take the Arrhenius behavior into account. The program used to

perform the regression is presented in Appendix A. The correlation coefficient was 0.855 and the resulting coefficient of determination was 0.732. Therefore, 26.8% of the variation was due to variables besides temperature and bulk density. Referring to Figure 8, it can be seen that the diffusion coefficients tend to scatter more at higher bulk density. Some of this scatter is due to the "dryness" of the mixture when packing. During the time that the equilibration disk was removed from between the half cells, and especially at the 90°C tests, the interface would dry exceptionally fast. Therefore, at higher bulk densities the drying effects became more of a problem. In effect, the area around the interface would have to resaturate and the diffusion of chloride would slow down. The resulting diffusion coefficients would therefore be smaller than expected. The results in Figure 8 do depict some diffusion coefficient values that could correspond to these effects. With test 90-015 (Table 3) the correlation coefficient of this 90°C test is even noticeably worse than the others.

COMPARISON OF RESULTS WITH OTHER INVESTIGATIONS

Eriksen et al. (12) found diffusion coefficients for chloride in bentonite that are approximately 2 orders of magnitude smaller than those obtained in this

investigation. The reason that his values are smaller is found by looking at the experimental setup. While in this investigation the tracer is initially mixed in with the clay, in Eriksen's investigation the tracer was initially placed in a solution adjacent to the clay. Therefore, the anion must first diffuse through the interface between the solution and the clay. Since the clay is negatively charged, there will be an additional barrier to diffusion of the anion at the interface. The decrease in the diffusion coefficient is caused by diffusion resistances due to charge repulsions between the clay and the anion.

McIntyre (43) measured diffusion coefficients for tritium-labelled water under the same conditions and same diffusive medium as used in this work. Values of the diffusion coefficients for the different conditions are given in Table 4.

Table 4. *Effective Diffusion Coefficients For Tritium
(cm^2/s)

Temperature ($^{\circ}\text{C}$)	20@5 $^{\circ}\text{C}$	60 $^{\circ}\text{C}$	90 $^{\circ}\text{C}$	
Bulk D.	1.61	2.89E-06	7.15E-06	1.56E-05
(g/cm^3)	1.79	2.56E-06	6.85E-06	1.47E-05

*Average values of the coefficient at an average bulk density.

In Table 5 the effective diffusion coefficients for chloride are listed for bulk densities of $1.6\text{g}/\text{cm}^3$ and

1.8g/cm³ at the same three temperatures as listed above. These values are taken from the multiple linear regression equation.

Table 5. Effective Diffusion Coefficients For Chloride
(cm²/s)

Temperature (°C)	20±5°C	60°C	90°C	
Bulk D. (g/cm ³)	1.60	3.33E-06	5.75E-06	7.99E-06
	1.80	2.03E-06	3.50E-06	4.88E-06

The similarity of the chloride and tritium diffusion coefficients is evident, especially at the lower temperature and bulk density. Since tritiated water is a neutral tracer, its diffusion would be expected to be more rapid than with chloride. McIntyre found with a 95% confidence level and the Student-t test that there is some adsorption. Some process of tritium exchange with water may therefore be present. If sorption of chloride was also present, it should likewise have noticeably smaller diffusion coefficients, which it does not. This would imply that chloride is not significantly sorbed by the clay.

The ratio of the effective diffusion coefficients for tritium and chloride (Temp. ~20°C) compared to the ratio of their molecular diffusivities (42) are as follows: 1) At 1.6g/cm³ bulk density, the ratio is 0.868 (effective)

compared to 1.1, and 2) at 1.6g/cm^3 , the ratio is 1.26 (effective) compared to 1.1. The self-diffusion of water is larger than the diffusion of chloride in bulk water, but does not move faster in the clay where other variables are affecting the movement of tritium. Obviously at higher bulk density the effects of the negative charge of the clay affect chloride more than tritium, although the hindrances for tritium movement may still be there.

DIFFUSION OF CARBON-14

The movement of carbon-14 through clay was not as straightforward as that for chloride. Although ^{14}C -carbonate is also an anion, its chemistry is different from chloride in many ways. In the first few tests run with carbon-14 tracer, little movement was noticed. This type of behavior is depicted in Figure 9. The most likely explanation is the reaction of carbonate with calcium or magnesium to form a precipitate or cationic complexes that could be sorbed. The solubility of calcium carbonate in water is 0.0012 parts per 100 parts of water (44). For magnesium, it is 0.0106 parts per 100 parts of water (44). The solubilities of the individual ions present together, i.e., Ca^{2+} , Mg^{2+} , and CO_3^{2-} , are compared to the approximate amounts of these ions in the synthetic groundwater in Table 6.

Figure 9. Diffusion Test, Carbon-14

D-C14-020-002

CARBON-14 C/Co

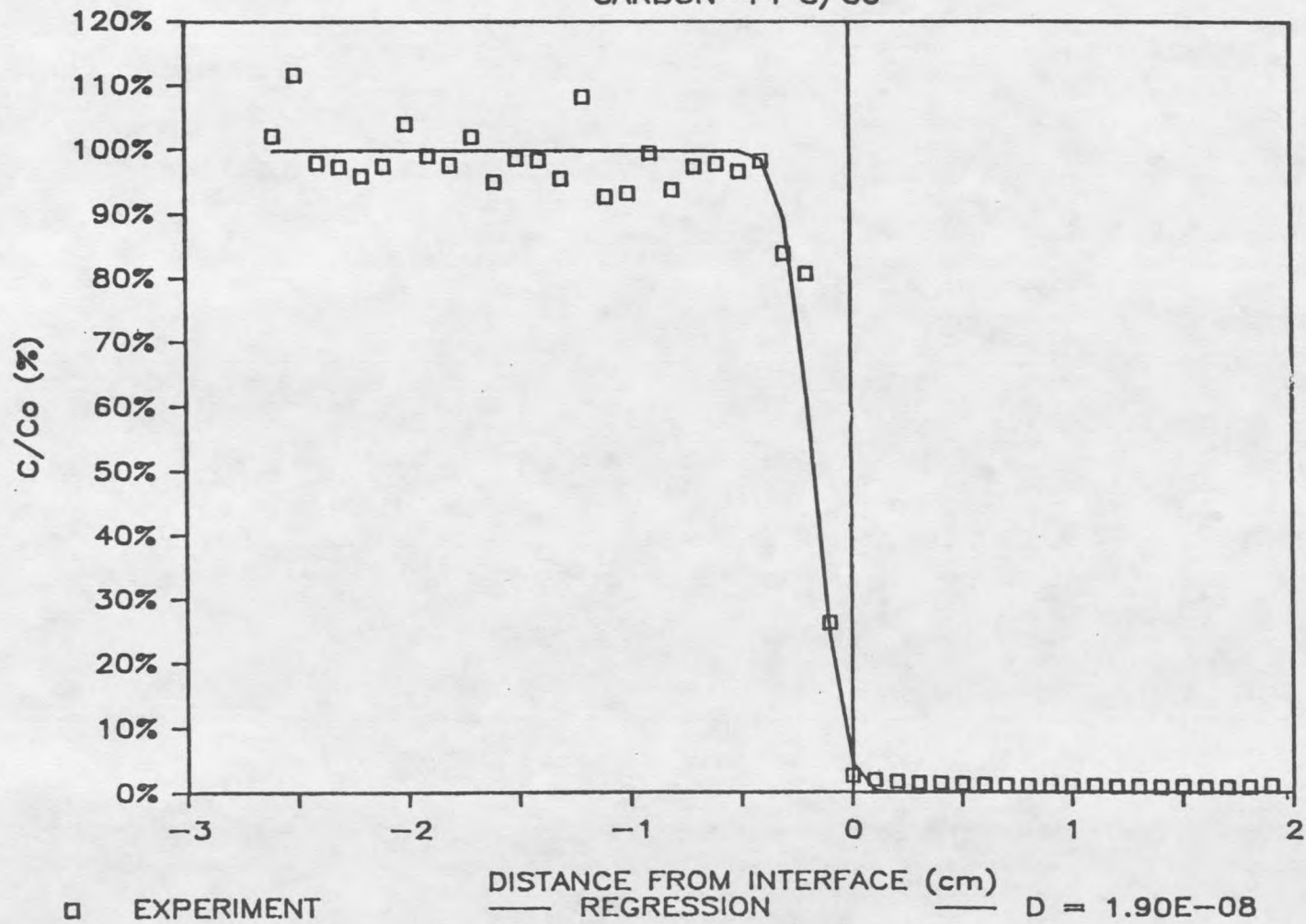


Table 6. *Solubilities and Ion Amount Present in Syn. Groundwater

Ion	Solubility (g)	**Ion Amount Present (g)
Ca ²⁺	.000024	.000014
Mg ²⁺	.000106	.0000002
CO ₃ ²⁻	.000036	.00027

* per 5g of solution

**see Appendix C

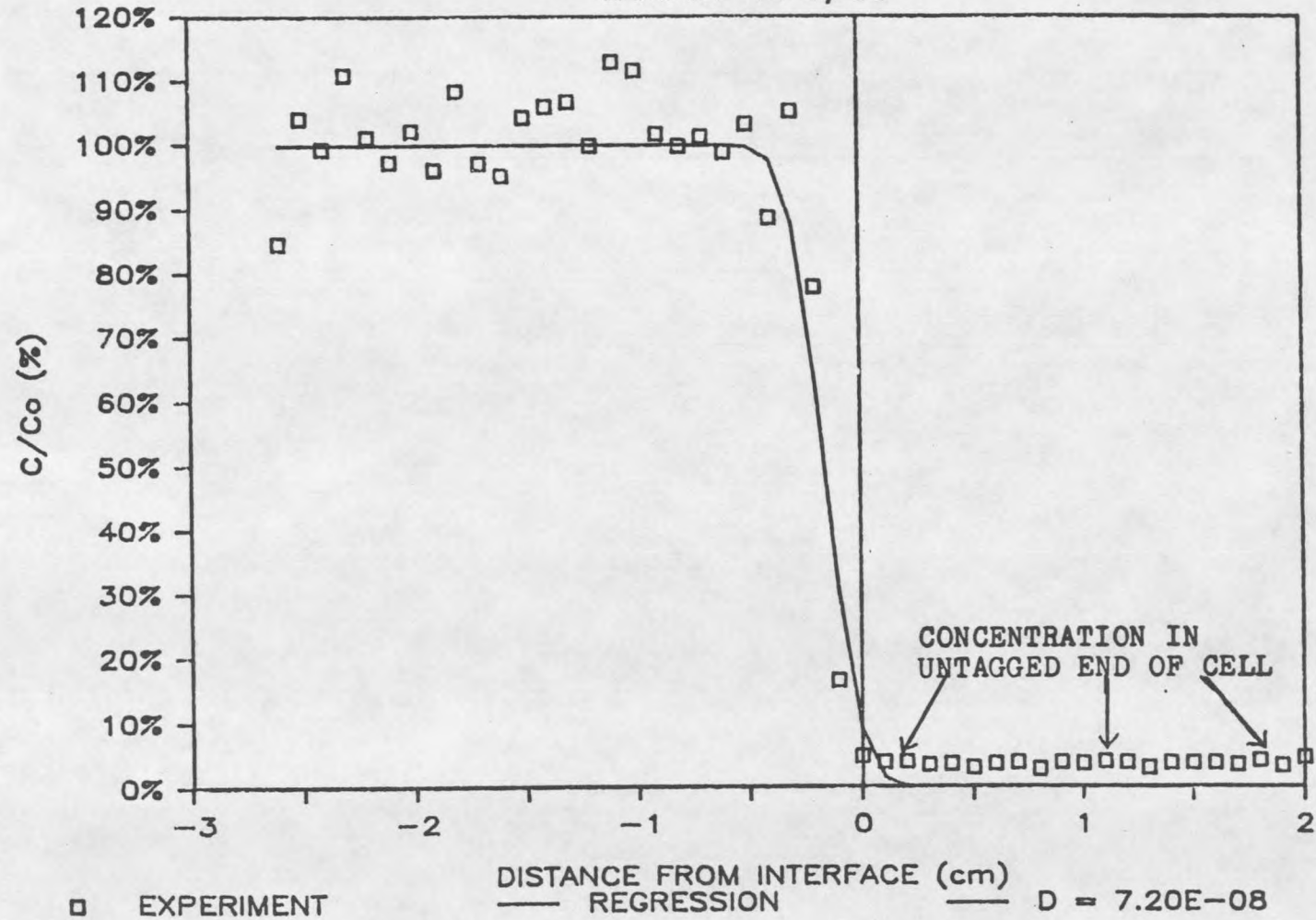
There is an excess of carbonate present in the solution, but the amount of calcium ion present is just under the solubility limit. Since the amounts of ion present in the water includes that which was originally added, any further addition of calcium from impurities on the clay could cause precipitation of CaCO₃. What is soluble will diffuse fast, as depicted in Figure 10. In this figure there is a small amount of tracer that has actually diffused through the untagged end of the core and leveled off at about 5-10%, while the remaining amount stayed in the tagged end.

While precipitation of calcium carbonate is a major concern with ¹⁴C-carbonate diffusion, complexation is also a possible cause of carbonate retention. With complexation, calcium (or magnesium) reacts with HCO₃⁻ formed in the solution to in turn form CaHCO₃⁺. The cation can then possibly be sorbed to the clay due to a cation exchange mechanism.

Figure 10. Diffusion Test, Carbon-14

D-C14-020-011

CARBON-14 C/Co



One factor influencing both precipitation and complexation of carbonate equilibria is pH (26). While pH was not a variable in this investigation, it is apparent that the basic pH of the synthetic groundwater (9.77) is suitable for forming a precipitate or complex. This is particularly interesting since CaCO_3 is originally slightly undersaturated in the groundwater.

DIFFICULTIES WITH CARBON-14

For the majority of the carbon-14 tests, there was a large degree of scatter in the concentration values measured for the tagged end of the core. Instead of finding a uniform horizontal concentration in the tagged region, a scattered display of values was found. In Figures 11 and 12 this behavior is shown. Some values of the concentration have even dropped to zero in Figure 12. The one reason that seems most probable for explaining this behavior is the formation and dispersion of $^{14}\text{CO}_2$. Whatever appears to be happening to the samples affects some more than others. There may be something wrong in the procedure that would cause evolution of $^{14}\text{CO}_2$ or scintillation counting problems with the tracer. The temperature of the test does not appear to affect the process.

Figure 11. Diffusion Test, Carbon-14
 D-C14-060-004
 CARBON-14 C/Co

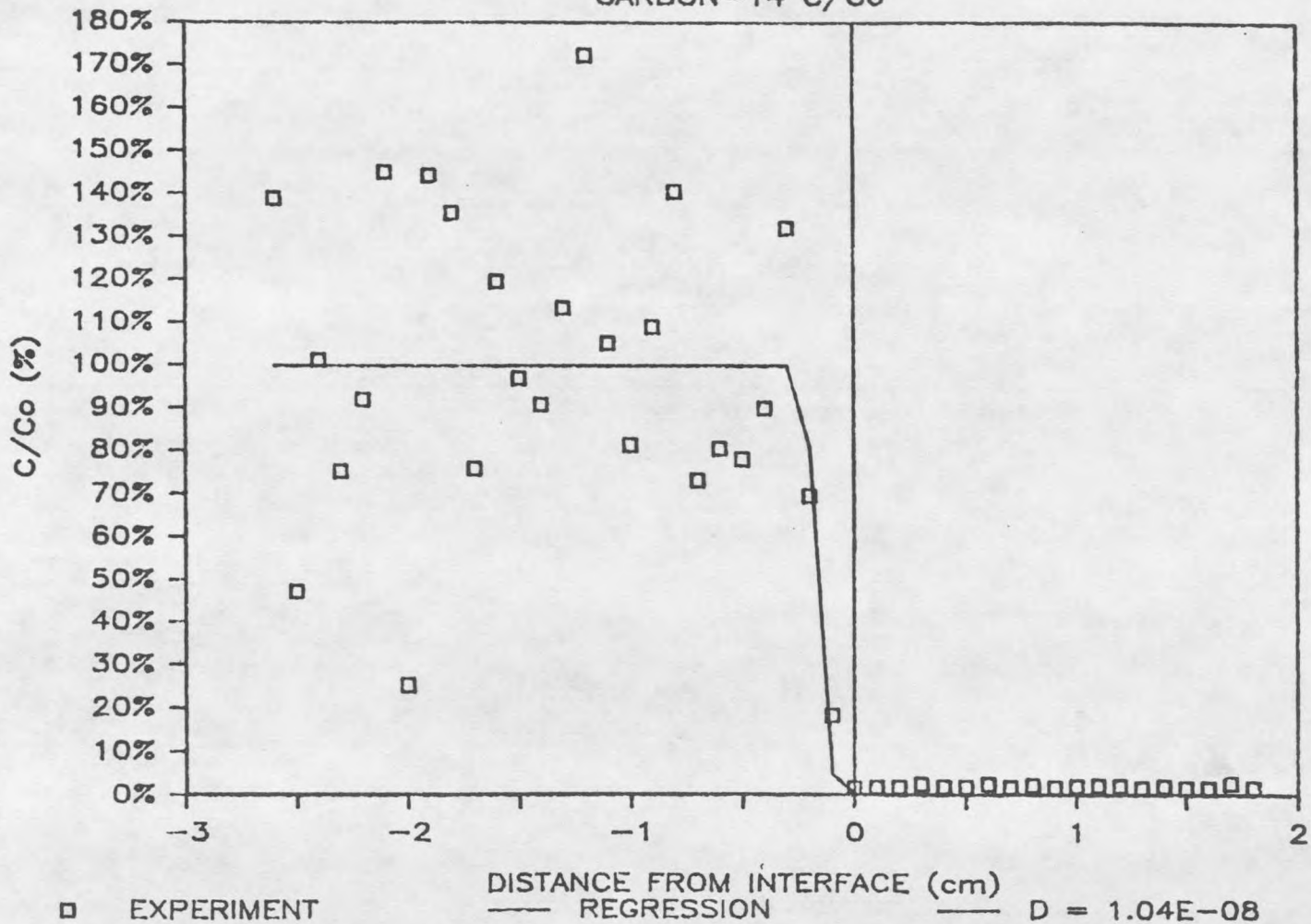
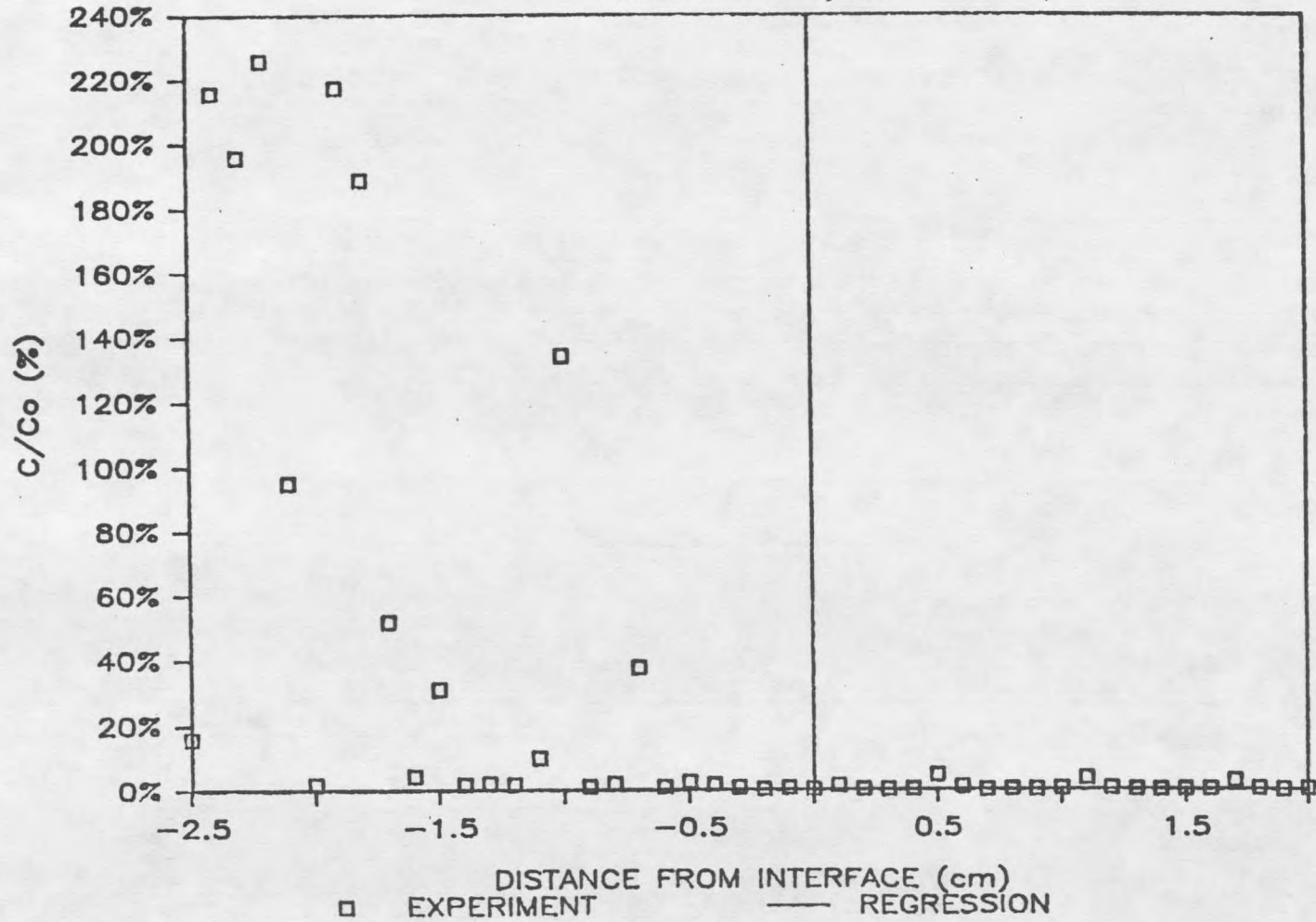


Figure 12. Diffusion Test, Carbon-14

D-C14-060-016

CARBON-14 C/Co



SUMMARY

1. The effective diffusion coefficients of chloride-36 increase with temperature.
2. As bulk density of the water-saturated basalt and bentonite mixture increases, the diffusion of chloride slows down. Relative to bulk water diffusion, this relationship was also found to be true due to tortuosity and porosity effects of the bentonite.
3. The data was well-described by a 1-dimensional model. The chloride appeared not to be significantly sorbed by the the clay, and a linear sorption isotherm adequately described its behavior.
4. A different method of fitting C/C_0 data to the theoretical solution to determine a diffusion coefficient should be used instead of using probits.
5. A 26.8% variation in the logarithm of the diffusion coefficient for chloride-36 was caused by variables other than bulk density and temperature.
6. The diffusion of chloride is faster if the tracer is initially present in the clay compared with when it is initially not in the clay but in an adjacent solution. With the latter setup, the chloride must still diffuse into the clay.

7. The majority of the ^{14}C -carbonate did not diffuse in the tests, but instead appears to have formed a precipitate or sorbable complex with calcium or magnesium.

RECOMMENDATIONS FOR FUTURE RESEARCH

1. In future research investigations a method of data fitting that uses the areas under the gaussian C/C_0 curve should prove to more accurate for calculating diffusion coefficients.
2. For investigations at higher temperatures, i.e., over 60°C , a diffusion cell or method should be used that does not require exposure of the half cell interfaces to the atmosphere. Thereby, the drying at the interface and its effects will be minimal.
3. Sorption experiments with ^{14}C -carbonate could be performed at varying pH values using the same type of synthetic groundwater as used in this investigation. An analysis of the calcium content of the raw material clay would also prove useful in predicting if the solubility limit of CaCO_3 has been reached.
4. A study of the effects of the experimental procedure, specifically the procedure surrounding the scintillation analysis, could prove helpful in determining if it affects the evolution of CO_2 from carbonate. The relationships between the chemistry of

carbonate and the effects it has on quenching
chemical or otherwise could also be studied.

REFERENCES CITED

REFERENCES CITED

1. Glasstone, Samuel, Sourcebook on Atomic Energy, 2nd ed., D. Van Nostrand Co., Inc., Princeton, 1958, p.462.
2. Roy, R., "Science Underlying Radioactive Waste Management: Status and Needs", Scientific Basis for Nuclear Waste Management, vol. I, Plenum Press, New York, pp.1-20, 1979.
3. Smith, M.J., Engineered Barrier Development for a Nuclear Waste Repository Located in Basalt: An Integration of Current Knowledge, RHO-BWI-ST-7, pp. 2:20-34,69, Rockwell Hanford Operations, Richland, Washington, 1980.
4. Nowak, E.J., "The Backfill as an Engineered Barrier For Nuclear Waste Management", Scientific Basis for Nuclear Waste Management, vol. 2, Plenum Press, New York, pp. 403-410, 1980.
5. Wood, M.I., J.F. Relyea, D.L. Lane, and R.A. Carlson, Chemical and Physical Properties of Waste Packing Materials, SD-BWI-TI-155, pp. 9,19,35, Rockwell Hanford Operations, Richland, Washington, 1983.
6. White, L.A., M.J. Bell, and D.M. Rohrer, "Regulation of Geologic Repositories for the Disposal of High-Level Radioactive Wastes", Scientific Basis for Nuclear Waste Management, vol. 2, Plenum Press, New York, pp. 5-19, 1980.
7. van Olphen, H., An Introduction to Clay Colloid Chemistry, 2nd ed., John Wiley and Sons, New York, 1977, pp. 30-157.
8. Searle, A.B. and R.W. Grimshaw, The Chemistry and Physics of Clays, 3rd ed., Interscience Publishers, Inc., New York, 1959, pp. 145,146.
9. Deju, R.A. and G.C. Evans, "Status Report on Studies to Assess the Feasibility of Storing Nuclear Waste in Columbia Plateau Basalts", Scientific Basis for Nuclear Waste Management, vol. 2, Plenum Press, New York, pp.69-76, 1980.

10. Pusch, R. and A. Bergstrom, "Highly-Compacted Bentonite - A Self-Healing Substance For Nuclear Waste Isolation", Scientific Basis for Nuclear Waste Management, vol. 3, Plenum Press, New York, pp. 553-560, 1981.
11. Relyea, J.F., "Diffusion Coefficients and Their Use", Nuclear Technology, vol. 51, pp. 156-161, 1980.
12. Eriksen, T., A. Jacobsson, and R. Pusch, "Ion Diffusion Through Highly Compacted Bentonite", SKBF/KBS, Teknisk Rapport 81-06, 1981.
13. Kissel, D.E., J.T. Ritchie, and E. Burnett, "Chloride Movement in Undisturbed Swelling Clay Soil", Soil Science of America Proceedings, vol. 37, pp. 21-24, 1973.
14. Westsik, J.H., Jr., L.A. Bray, F.N. Hodges and E.J. Wheelwright, "Permeability, Swelling and Radionuclide Retardation Properties of Candidate Backfill Materials", Scientific Basis for Nuclear Waste Management, Elsevier Science Publishing Co., Amsterdam, pp. 329-336, 1982.
15. Lai, T.M., and M.M. Mortland, "Diffusion of Ions in Bentonite and Vermiculite", Soil Science Society Proceedings, pp. 353-357, 1961.
16. Dutt, G.R. and P.F. Low, "Diffusion of Alkali Chlorides in Clay-Water Systems", Soil Science, vol.93, pp. 233-340, 1962.
17. Hamid, A., "Diffusion Coefficient of I-Ions in Saturated Clay Soil", Plant and Soil, vol. 36, pp. 709-711, 1971.
18. Allard, B., B. Torstenfelt, K. Andersson and J. Rydberg, "Possible Retention of Iodine in the Ground", Scientific Basis for Nuclear Waste Management, vol. 2, pp. 673-680, 1980.
19. Sienko, M.J. and R.A. Plane, Chemical Principles and Properties, 2nd ed., McGraw-Hill, New York, 1974, pp. 16-18.

20. Nowak, E.J., "Diffusion of Radionuclides in Brine-Saturated Backfill Barrier Materials", Mat. Res. Soc. Symp. Proc., vol. 15, Elsevier Science Publishing Co., Amsterdam, pp. 735-741, 1983.
21. Moore, D.E., C.A. Morrow, and J.D. Byerlee, "Use of Swelling Clays to Reduce Permeability and Its Potential Application to a Nuclear Waste Repository Sealing", Geophysical Research Letters, vol. 9, no. 9, pp. 1009-1012, 1982.
22. Anderson, M.A., and A.J. Rubin (editors), Adsorption of Inorganics at Solid-Liquid Interfaces, Ann Arbor Science Publishers, Ann Arbor, Michigan, 1981, p. 127.
23. Nelson, R.W., and A.E. Reisenauer, Application of Radioactive Tracers in Scientific Groundwater Hydrology, Hanford Atomic Products Operation, GE Co., Richland, Washington, 1963, p. 207.
24. Pusch, R., T. Eriksen, A. Jacobsson, "Ion/Water Migration Phenomena In Dense Bentonites", Scientific Basis for Radioactive Waste Management, vol. V, Elsevier Science Publishing Co., Amsterdam, pp. 649-658, 1982.
25. Rolfe, P.F. and L.A.G. Aylmore, "Water and Salt Flow Through Compacted Clays", Journal of Colloid and Interface Science, vol. 79, no. 2, pp. 301-307, 1981.
26. Allard, B., B. Torstenfelt, and K. Andersson, "Sorption Studies of H_2CO_3^- on Some Geologic Media and Concrete", Scientific Basis for Nuclear Waste Management, vol. 3, Plenum Press, New York, pp. 465-472, 1981.
27. Dixon, J.B., and S.B. Weed (editors), Minerals in Soil Environments, Soil Science of America, Madison, Wisconsin, 1977, p. 316.
28. Loewenthal, R.E., and G.V.R. Marais, Carbonate Chemistry of Aquatic Systems: Theory and Application, Ann Arbor Science Publishers, Ann Arbor, Michigan, 1976, p. 189.

29. Wells, A.F., Structural Inorganic Chemistry, 3rd ed., Oxford University Press, London, 1962, p. 707.
30. Sidgwick, N.V., The Chemical Elements and Their Compounds, vol. II, Oxford University Press, London, 1950, p. 1098.
31. Rimmer, D.L., and D.J. Greenland, "Effects of Calcium Carbonate on the Swelling Behavior of Soil Clay", Journal of Soil Science, vol. 27, pp. 129-139, 1976.
32. Schatz, A.L., RHO-BW-RN-15, pp.4,5.
33. Carlson, R.A., RHO-BW-NB-164, p.6.
34. Whitwell, J.C., and R.K. Toner, Conservation of Mass and Energy, McGraw-Hill, New York, 1973.
35. Brown, D.A., B.E. Fulton and R.E. Phillips, "Ion Exchange Diffusion: I. A Quick-Freeze Method For the Measurement of Ion Diffusion in Soil and Clay Systems", Soil Sci. Soc. Am. Proc., vol. 28, pp.628-632, 1964.
36. Lai, S.H., and J.J. Jurinak, "Cation Adsorption in One Dimensional Flow Through Soil: A Numerical Solution", Water Resour. Res., vol. 8, pp. 99-107, (1972).
37. Crank, J., The Mathematics of Diffusion, Oxford-Clarendon Press, Oxford, 1975, p.12.
38. Miller, I., and J.E. Freund, Probability and Statistics For Engineers, 2nd ed., Prentice-Hall, Englewood Cliffs, N.J., 1977, pp. 104-108, 289-327.
39. Finney, D.J., Probit Analysis, Cambridge University Press, 1952, p.23, 283-287.
40. Hald, A., Statistical Theory With Engineering Applications, John Wiley & Sons, New York, 1952, pp. 528-540.
41. Steel, R.G.D., and J.H. Torre, Principles and Procedures of Statistics, McGraw-Hill, New York, 1960.

42. Atkins, P.W., Physical Chemistry, Freeman & Co., San Francisco, 1978, p. 836.
43. McIntyre, C.V., Master's Thesis, University of Idaho, Moscow, 1985.
44. Perry, R.H., and C.H. Chilton, Chemical Engineers' Handbook, 5th ed., McGraw-Hill, New York, 1973, 3-10,15.

APPENDICES

APPENDIX A
COMPUTER PROGRAMS

Table 7. Fortran Program To Calculate Least Squares Best Fit

```

C*****
C   THIS PROGRAM COMPUTES THE LEAST SQUARES FIT
C   FOR A SET OF EXPERIMENTAL DATA POINTS (N<100)
C   WRITTEN BY DOUGLAS SMITH, UNIV. OF NEW MEXICO,
C   ALBUQUERQUE, NM, 87131
C*****
      DIMENSION A(10,10), X(10), B(10), C(10,10), S(10)
      DIMENSION W(100), U(100), XX(10), YY(6)
      DO 10 I=1,10
        XX(I)=0.0
10    CONTINUE
      DO 20 I=1,6
        YY(I)=0.0
20    CONTINUE
C*****
C                               INPUT DATA
C*****
      WRITE(6,*)
      WRITE(6,*) ' INPUT THE DESIRED ORDER '
      READ(5,*) N5
      WRITE(6,*)
      WRITE(6,*) ' INPUT THE # OF DATA PAIRS '
      READ(5,*) N
      WRITE(6,*)
      WRITE(6,*) ' INPUT THE DATA PAIRS-X,Y '
      N1=N5+1
      DO 30 I=1,N
        READ(5,*) X1,Y
        U(I) = X1
        W(I) = Y
        if(x1.eq.0.) goto 30
        DO 40 J=1,10
          XX(J)=XX(J) + X1**J
40    CONTINUE
        DO 50 J=1,6
          YY(J)=YY(J) + Y*X1**(J-1)
50    CONTINUE
30    CONTINUE
      WRITE(6,*)
C*****
C                               LEAST SQUARE
C*****
      A(1,1)=FLOAT(N)
      DO 60 I=1,5
        I1=I+1
        A(1,I1)=XX(I)
60    CONTINUE
      DO 70 J=2,6

```

Table 7--Continued

```

DO 70 I=1,6
  I1=J+(I-2)
  A(J,I)=XX(I1)
70 CONTINUE
DO 80 J=1,6
  B(J)= YY(J)
80 CONTINUE
900 DO 90 I=1,N1
    DO 100 J=1,N1
      C(I,J)=A(I,J)
100 CONTINUE
    C(I,N1+1)=B(I)
90 CONTINUE
N2=N1+1
N3=N1-1
DO 110 I=1 , N1
  S(I)=C(I,1)
  DO 120 J=2, N1
    IF(ABS(S(I)).LT. ABS(C(I,J))) S(I)= C(I,J)
120 CONTINUE
110 CONTINUE
DO 130 K=1, N3
  X(K)=C(K,K)/S(K)
  I1=K
  K1=K+1
  DO 140 I=K1,N1
    IF(ABS(X(K)).GE.ABS(C(I,K)/S(I))) GOTO 140
    X(K)=C(I,K)/S(I)
    I1=I
140 CONTINUE
  IF(I1.EQ.K) GOTO 690
  DO 150 J=K,N2
    D=C(K,J)
    C(K,J)=C(I1,J)
    C(I1,J)=D
150 CONTINUE
690 DO 160 I=K1,N1
    D=C(I,K)/C(K,K)
    DO 170 J=K,N2
      C(I,J)=C(I,J)-D*C(K,J)
170 CONTINUE
160 CONTINUE
130 CONTINUE
C(N1,N2)=C(N1,N2)/C(N1,N1)
DO 180 I2=1,N3
  I=N1-I2

```

Table 7--Continued

```

D=0.0
I1=I+1
DO 190 J=I1,N1
  D=D+C(I,J)*C(J,N2)
190 CONTINUE
  C(I,N2)=(C(I,N2)-D)/C(I,I)
180 CONTINUE
C*****
C          PRINT ROUTINE
C*****
  WRITE(6,*)
  WRITE(1,300)C(1,N2)
  WRITE(6,300)C(1,N2)
300  FORMAT(1X,'F(X)= ',E12.5)
  DO 200 I=2,N1
    WRITE(1,310) C(I,N2),I-1
    WRITE(6,310) C(I,N2),I-1
310  FORMAT(1X,'+ ',E12.5,'X^'I3)
200  CONTINUE
  WRITE(6,*)
  WRITE(1,*)
  WRITE(6,*) 'INPUT 1.0 FOR COMPARISON OF EXPERIMENTAL
*AND'
  WRITE(6,*) 'PREDICTED Y VALUES'
  READ(5,*)J9
  WRITE(6,*)
  IF(J9.EQ.1.0) GOTO 500
350  WRITE(6,*)
  WRITE(6,*) 'INPUT NEW ORDER, INPUT 0 IF DONE'
  READ(5,*) N5
  IF(N5.EQ.0) GOTO 1000
  N1=N5+1
  GOTO 900
500  WRITE(1,510)
  WRITE(6,510)
510  FORMAT(10X,'X',10X,'Y-EXP',10X,'Y-CALC'//)
  DO 210 I=1,N
    Z=0.0
    DO 220 J=1,N1
      IF(U(I).EQ.0.) GOTO 220
      Z=Z+C(J,N2)*U(I)**(J-1)
220  CONTINUE
  WRITE(6,520)U(I),W(I),Z
  WRITE(1,520)U(I),W(I),Z
520  FORMAT(7X,E12.5,5X,E12.5,5X,E12.5)
210  CONTINUE

```

Table 7-Continued

```
WRITE(1,*)  
WRITE(6,*)  
GOTO 350  
1000 END
```

Table 8. Fortran Program To Determine The Effects Of Data Errors On The Effective Diffusion Coefficient

```

C      PROGRAM TO CALCULATE C/CO VALUES FROM SOLUTION TO 1-
C      DIMENSIONAL DIFFUSION EQUATION. AN ERROR SPREAD OF THE
C      NORMAL CURVE AT VARIOUS STANDARD DEV'S IS THEN GIVEN
C      FOR EACH C/Co CALCULATED ABOVE; THE DIFFUSION
C      COEFFICIENT IS THEN RECALCULATED USING PROBIT
C      ANALYSIS. THIS PROGRAM WAS WRITTEN BY CRAIG G. RIEGER,
C      MONTANA STATE UNIVERSITY, BOZEMAN, MT 59715
C*****
C      THE ERROR FUNCTION IS CALCULATED FROM P.299 OF M.
C      ABRAMOWITZ AND I.A. STEGUN, HANDBOOK OF MATHEMATICAL
C      FUNCTIONS. AN ALGORITHM TO CALCULATE THE AXIS VALUES
C      OF THE NORMAL CURVE IS FROM R.E. LUND, MONTANA STATE
C      UNIVERSITY
C*****
      REAL RND,X,XD(120),CONCP(120),CONCPN(120),FX,TC,T,
      *PROBIT(120)
      REAL ZVSAL,SDEV(10),ERR,Z,RJ,SUMX,SUMXY,SUMY,
      *SUMX2,DEE(30)
      REAL DET,B,SUMDEE,SUMDEE2,SUMMD,SUMMD2,
      *SDEVDEE(10),SDEVMD
      REAL MDEE(10),MD,DEEA(10,30),SUMY2,R(10,30),
      *SUMR,MR(10)
      REAL SUMA,A,MA(10)
      INTEGER ISEED
      DO 10 I=1,50
      ISEED=55555
      RND=RAN(ISEED)
10    CONTINUE
      T=1.55E4
      DET=3.32E-6
C*****IMPLIED DO TO GET EXACT C/CO VALUES*****
      X=-3.
      J=1
20    CONTINUE
      IF(X.GE.0.000)THEN
      FX=X/(2.*SQRT(DET*T))
      TC=1/(1.+47047*FX)
      CONCP(J)=.5*(.34802*TC-.09587*TC**2+.74785*TC**3)
      *EXP(-(FX**2))
      ELSE
      FX=-X/(2.*SQRT(DET*T))
      TC=1/(1.+47047*FX)
      CONCP(J)=-.5*(.34802*TC-.09587*TC**2+.74785*TC**3)
      *EXP(-(FX**2))+1.
      ENDIF

```

Table 8-- Continued

```

IF(CONCP(J).GE.1)THEN
  X=X+.10
  GOTO 20
ENDIF
IF(CONCP(J).LE.0.001)GOTO 30
XD(J)=X
J=J+1
X=X+.025
GOTO 20
30 CONTINUE
RJ=REAL(J)
SDEV(1)=.0001
SUMMD=0.
SUMMD2=0.
DO 50 K=1,10
  SUMDEE=0.
  SUMDEE2=0.
  SUMR=0.
  SUMA=0.
  DO 40 L=1,30
    SUMY=0.
    SUMXY=0.
    SUMX=0.
    SUMX2=0.
    SUMY2=0.
    DO 35 M=1,J
      RND=RAN( ISEED)
      ERR=ZVSAL(RND)
      CONCPN(M)=CONCP(M)+ERR*SDEV(K)
      PROBIT(M)=ZVSAL(CONCPN(M))+5.
      SUMY=PROBIT(M)+SUMY
      SUMY2=SUMY2+PROBIT(M)**2
      SUMXY=SUMXY+XD(M)*PROBIT(M)
      SUMX=SUMX+XD(M)
      SUMX2=SUMX2+XD(M)**2
35 CONTINUE
      B=(RJ*SUMXY-SUMX*SUMY)/(RJ*SUMX2-SUMX**2)
      A=SUMY/RJ-B*(SUMX/RJ)
      DEE(L)=1./(2.*(B**2)*T)
      R(K,L)=(RJ*SUMXY-SUMX*SUMY)/SQRT((RJ*SUMX2-SUMX**2)*
      (RJ*SUMY2-SUMY**2))
      DEEA(K,L)=DEE(L)
      SUMDEE=SUMDEE+DEE(L)
      SUMDEE2=SUMDEE2+DEE(L)**2
      SUMR=SUMR+R(K,L)
      SUMA=SUMA+A

```

Table 8--Continued

```

40  CONTINUE
    L=L-1
    RL=REAL(L)
    SDEVDEE(K)=SQRT((RL*SUMDEE2-SUMDEE**2)/((RL-1.)*RL))
    MDEE(K)=SUMDEE/RL
    MR(K)=SUMR/RL
    MA(K)=SUMA/RL
    SDEV(K+1)=SDEV(K)+.005
    SUMMD=SUMMD+MDEE(K)
    SUMMD2=SUMMD2+MDEE(K)**2
50  CONTINUE
    MD=SUMMD/10.
    SDEVM=SQRT((10.*SUMMD2-SUMMD**2)/90.)
    WRITE(6,55)
    WRITE(4,55)
55  FORMAT(' ',10('SD OF NORM',2X))
    WRITE(6,58)(SDEV(K),K=1,10)
    WRITE(4,58)(SDEV(K),K=1,10)
58  FORMAT(' ',10(E10.3,2X))
    WRITE(6,*)' '
    WRITE(4,*)' '
    WRITE(6,60)
    WRITE(4,60) 60  FORMAT(' ', 'DIF CO 1',4X, 'DIF CO
2',4X, 'DIF CO 3',
*4X, 'DIF CO 4',4X, 'DIF CO 5',4X, 'DIF CO 6',4X,
*'DIF CO 7',4X, 'DIF CO 8',4X, 'DIF CO 9',4X, 'DIF CO 10')
    WRITE(6,65)((DEEA(K,L),K=1,10),L=1,30)
    WRITE(4,65)((DEEA(K,L),K=1,10),L=1,30) 65
    FORMAT(10(E10.3,2X))
    WRITE(6,*)' '
    WRITE(4,*)' '
    WRITE(6,68)
    WRITE(4,68)
68  FORMAT(' ',1X, 'COR CO 1',5X, 'COR CO 2',5X, 'COR CO 3',
*5X, 'COR CO 4',5X, 'COR CO 5',5X, 'COR CO 6',5X,
*'COR CO 7',5X, 'COR CO 8',5X, 'COR CO 9',5X, 'COR CO 10')
    WRITE(6,69)((R(K,L),K=1,10),L=1,30)
    WRITE(4,69)((R(K,L),K=1,10),L=1,30) 69  FORMAT(10('
',E10.4,2X))
    WRITE(6,*)' '
    WRITE(4,*)' '
    WRITE(6,70)DET
    WRITE(4,70)DET 70  FORMAT(' ', 'ORIGINAL THEORETICAL
DIFFUSION
*COEFFICIENT=',E10.3)
    WRITE(6,*)' '

```

Table 8--Continued

```

WRITE(4,*)' '
WRITE(6,75)(K,MDEE(K),MR(K),K=1,10)
WRITE(4,75)(K,MDEE(K),MR(K),K=1,10)
75  FORMAT(' ', 'MEAN DIFF COEFF' & ' CORR COEFF' PER SET
*SD OF NORMAL'//,10(' ',I2,' ',E10.3,4X,E10.4/))
WRITE(6,*)' '
WRITE(4,*)' '
WRITE(6,80)(K,SDEVDEE(K),K=1,10)
WRITE(4,80)(K,SDEVDEE(K),K=1,10)
80  FORMAT(' ', 'STAND DEV OF MEANS PER SET SD OF NORMAL'//,
*10(' ',I2,' ',E10.3/))
WRITE(6,*)' '
WRITE(4,*)' '
WRITE(6,85)MD,SDEVMD
WRITE(4,85)MD,SDEVMD
85  FORMAT(' ', 'TOTAL MEAN DIFF COEFF=' ,E10.4/ ,
*' , 'STANDARD DEV IN TOTAL MEAN DIFF COEFF=' ,E10.4)
WRITE(6,*)' '
WRITE(4,*)' '
WRITE(6,90)(MA(K),K=1,10)
WRITE(4,90)(MA(K),K=1,10)
90  FORMAT(' ', 'Y*INTERCEPT'//,10(' ',F5.3/))
END

```

C*****

C*****FUNCTION ZVSAL, BY R.E. LUND, FEB. 1977*****

REAL FUNCTION ZVSAL(P)

C CALCULATES NORMAL DIST QUANTILE ZVSAL GIVEN

P=PROB(Z<ZVSAL).

C PROCEDURE BY WETHERILL, APPLIED STATISTICS (1965),

*14:201-204. C

W=2.*ABS(.5-P)

IF(W.LT.1.)GOTO 7

Y=9.999

GOTO 37

7 IF(W.GT.0.91)GOTO 17

WSQ=W*W

Y=1.2533140*W

W=W*WSQ

Y=Y+.3281170*W

W=W*WSQ

Y=Y+.1083290*W

W=W*WSQ

Y=Y+.3630000*W

W=W*WSQ

Y=Y-.8559000*W

W=W*WSQ

Table 8--Continued

```
Y=Y+1.048000*W
GOTO 37
17 Z=ALOG(1.0-W)
Y=.4017030-.6256000*Z
Z1=Z*Z
Y=Y-.0398110*Z1
Z1=Z1*Z
Y=Y-.0014160*Z1
37 IF(P.LT.0.5)Y=-Y
IF(P.EQ.0.5)Y=0.0
ZVSAL=Y
RETURN
END
```

Table 9 Program To Calculate Multiple Linear Regression Coefficients, Basic

```

1  REM THIS IS A MULTIPLE LINEAR REGRESSION PROGRAM FOR TWO INDEPENDENT
2  REM INDEPENDENT VARIABLES AND ONE INDEPENDENT VARIABLE. THE DATA IS
3  REM INPUT FROM A DATA FILE "DATA.PRN" AND IS SIMPLE TO MAKE UP WITH
4  REM THE LOTUS 123 PACKAGE. THE EQUATIONS ARE BASED ON THE STATISTICAL
5  REM METHODS OUTLINED IN STEEL AND TORRIE. THIS PACKAGE WAS WRITTEN BY
6  REM JOHN RELYEA, (509) 373-1037, 15 AUG 1984.
7  REM
8  LPRINT "INPUT DATA SET FOR MULTIPLE LINEAR REGRESSION ANALYSIS "
9  LPRINT " FOR 1 DEPENDENT AND 2 INDEPENDENT VARIABLES"
10 REM INPUT DATA IS FOUND IN THE FILE "DATA.PRN" FROM LOTUS 123 ON DISK B:
11 OPEN "B:DATA.PRN" FOR INPUT AS #1
12 REM THE NUMBER OF OBSERVATIONS OF THE VALUES FOR CORRESPONDING VARIABLES
13 REM IS INPUT AS "N" FROM THE FIRST LINE OF THE DATA FILE "DATA.PRN"
14 INPUT #1,N
15 REM THE VARIABLE NAMES ARE DIMENSIONED AS STRING VARIABLES AND READ
16 REM FROM THE SECOND LINE OF THE FILE "DATA.PRN"
17 DIM VAR$(3)
18 FOR I = 1 TO 3
19 INPUT #1,VAR$(I)
20 NEXT
21 REM THE VARIABLES ARE DEFINED AS SINGLE PRECISION NUMBERS Y,X1 AND X2 AND
22 REM READ FROM THE NEXT "N" LINES OF THE DATA FILE DATA.PRN
23 DIM X1(N),Y(N),X2(N)
24 FOR I = 1 TO N
25 INPUT #1,Y(I),X1(I),X2(I)
26 NEXT
27 CLOSE #1
28 REM THE HEADING FOR THE DATA OUTPUT IS PRINTED NEXT
29 LPRINT USING "\          \";"";"Y";"X1";"X2"
30 LPRINT USING "\          \";"";VAR$(1);VAR$(2);VAR$(3)
31 REM THE DATA FROM FILE DATA.PRN IS NOT PRINTED FOR CHECKING IF NEEDED
32 FOR I = 1 TO N
33 LPRINT USING "    ##.###^";Y(I);X1(I);X2(I)
34 NEXT
35 REM THE SUMS OF PRODUCTS AND CROSS PRODUCTS,ETC ARE INITIALIZED AT ZERO
36 X1Y = 0:X2Y = 0:X1X2 = 0:X1X1 = 0:X2X2 = 0:SY = 0:YY = 0
37 REM THE SUMS OF PRODUCTS,CROSS PRODUCTS,ETC ARE ACCUMULATED FOR ALL N
38 REM OBSERVATIONS OF THE VARIABLES
39 FOR I = 1 TO N
40 X1Y = X1Y + X1(I)*Y(I)
41 X2Y = X2Y + X2(I)*Y(I)
42 X1X1 = X1X1 + X1(I)*X1(I)
43 X2X2 = X2X2+X2(I)*X2(I)
44 X1X2 = X1X2 + X1(I)*X2(I)
45 SX1 = SX1 + X1(I)
46 SX2 = SX2 + X2(I)
47 SY = SY + Y(I)
48 YY = YY + Y(I)*Y(I)
49 NEXT
50 REM NOW THE ACTUAL SET OF EQUATIONS FOR THE LEAST SQUARES REGRESSION OF
51 REM Y ON X1 AND X2 ARE SOLVED FOR THE REGRESSION COEFFICIENTS
52 M = N
53 A1 = X1X2-SX1*SX2/M
54 A2 = X1X1-SX1*SX1/M
55 A3 = X1Y -SX1*SY/M
56 A4 = X2Y -SX2*SY/M
57 A5 = X2X2-SX2*SX2/M
58 B2 = (A1*A3/A2-A4)/(A1*A1/A2-A5)
59 B1 = (A3-A1*B2)/A2
60 B0 = (SY-B1*SX1-B2*SX2)/M
61 R2 = (B0*SY+B1*X1Y+B2*X2Y-SY*SY/M)/(YY-SY*SY/M)
62 REM THE RESULTS OF THE MULTIPLE LINEAR REGRESSION ARE NOW PRINTED
63 LPRINT CHR$(10); "REGRESSION COEFFICIENTS FOR THE EQUATION"
64 LPRINT "    Y = B0 + B1*X1 + B2*X2";CHR$(10)
65 LPRINT "B0 = ";B0;" INTERCEPT FOR X1=X2=0"
66 LPRINT "B1 = ";B1;" SLOPE FOR Y VS X1"
67 LPRINT "B2 = ";B2;" SLOPE FOR Y VS X2"
68 LPRINT "R = ";R2;" REGRESSION CORRELATION COEFFICIENT"
69 LPRINT "N = ";N;" NUMBER OF POINTS USED FOR THE REGRESSION"
70 LPRINT CHR$(12)
71 END

```

APPENDIX B

RAW DATA FOR TESTS DISPLAYED IN FIGURES

<u>Figure</u>	<u>Chloride-36 Diffusion Test</u>	<u>Page</u>
13.	D-C136-020-002	78
14.	D-C136-020-003	79
15.	D-C136-060-004	80
16.	D-C136-060-005	81
17.	D-C136-060-006	82
18.	D-C136-090-007	83
19.	D-C136-090-008	84
20.	D-C136-090-009	85
21.	D-C136-020-010	86
22.	D-C136-060-011	87
23.	D-C136-020-013	88
24.	D-C136-090-015	89
25.	D-C136-020-016	90
26.	D-C136-060-017	91
27.	D-C136-090-018	92
28.	D-C136-020-019	93
29.	D-C136-020-020	94
30.	D-C136-090-021	95
31.	D-C136-060-022	96

<u>Figure</u>	<u>Carbon-14 Diffusion Test</u>	<u>Page</u>
32.	D-C14-020-002	97
33.	D-C14-060-003	98
34.	D-C14-060-004	99
35.	D-C14-090-005	100
36.	D-C14-090-006	101
37.	D-C14-020-007	102
38.	D-C14-020-008	103
39.	D-C14-060-009	104
40.	D-C14-020-011	105
41.	D-C14-090-012	106
42.	D-C14-020-014	107
43.	D-C14-060-016	108
44.	D-C14-020-020	109
45.	D-C14-020-021	110

Conditions of Tests

Chloride-36 Tests (Diffusion)

Figure	Conditions
13	Temperature: 26 degrees C; Bulk Density: 1.63g/cm ³
14	23 1.64
15	60 1.63
16	60 1.63
17	60 1.63
18	90 1.57
19	90 1.59
20	90 1.57
21	27 1.86
22	60 1.81
23	26 1.81
24	90 1.90
25	25 1.81
26	60 1.71
27	90 1.77
28	25 1.68
29	25 1.59
30	90 1.81
31	60 1.75

Carbon-14 Tests (Diffusion)

Figure	Conditions
32	Temperature: 24 degrees C; Bulk Density: 1.60g/cm ³
33	60 1.64
34	60 1.63
35	90 1.64
36	90 1.57
37	24 1.66
38	24 1.63
39	60 1.63
40	24 1.62
41	90 1.60
42	24 1.66
43	60 1.63
44	20 1.61
45	20 1.62

(Diffusion Coefficient (D) in cm²/s)

Figure 13.

D-CL36-020-002

CHLORIDE-36 C/Co

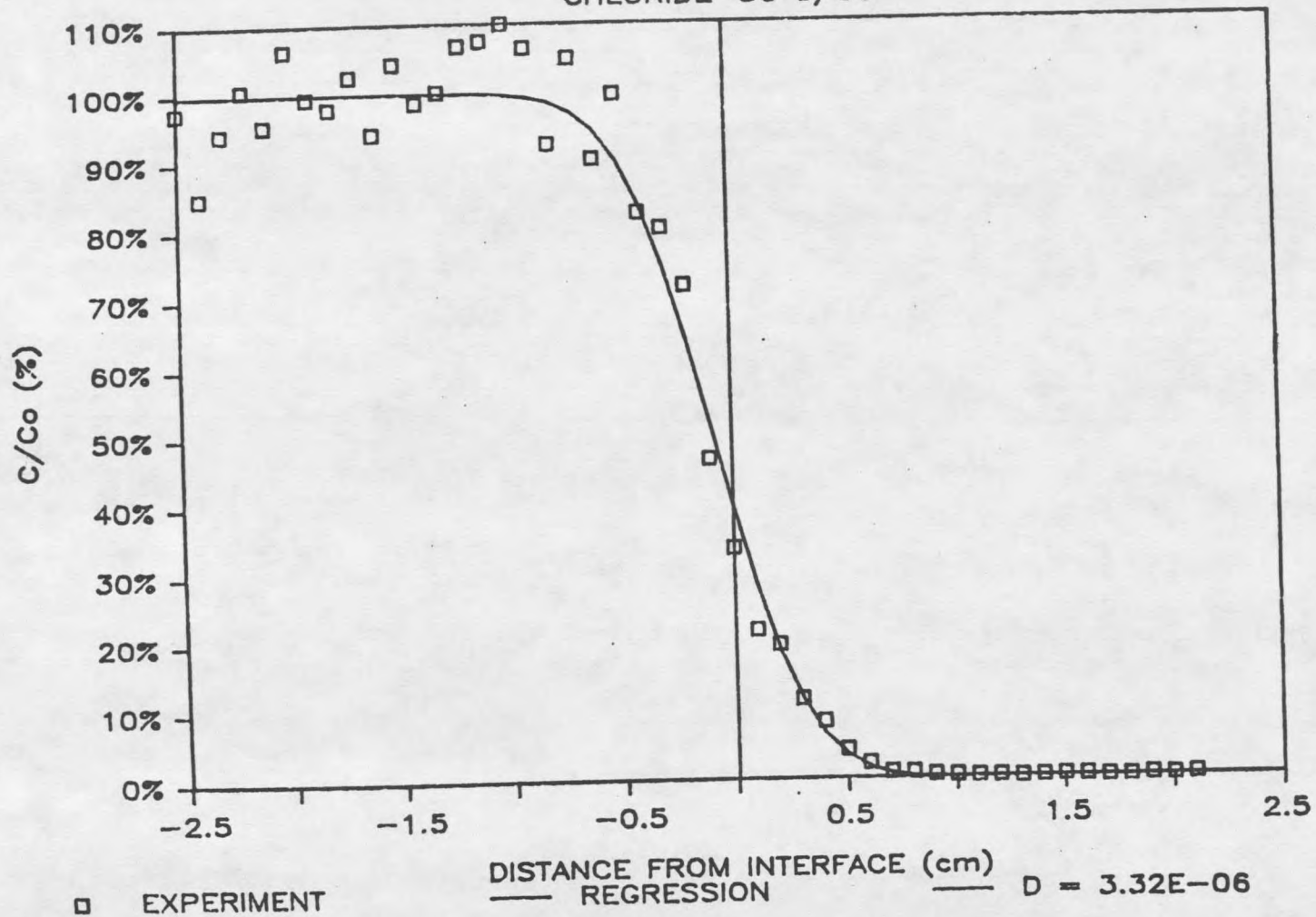


Figure 14.

D-CL36-020-003

CHLORIDE-36 C/Co

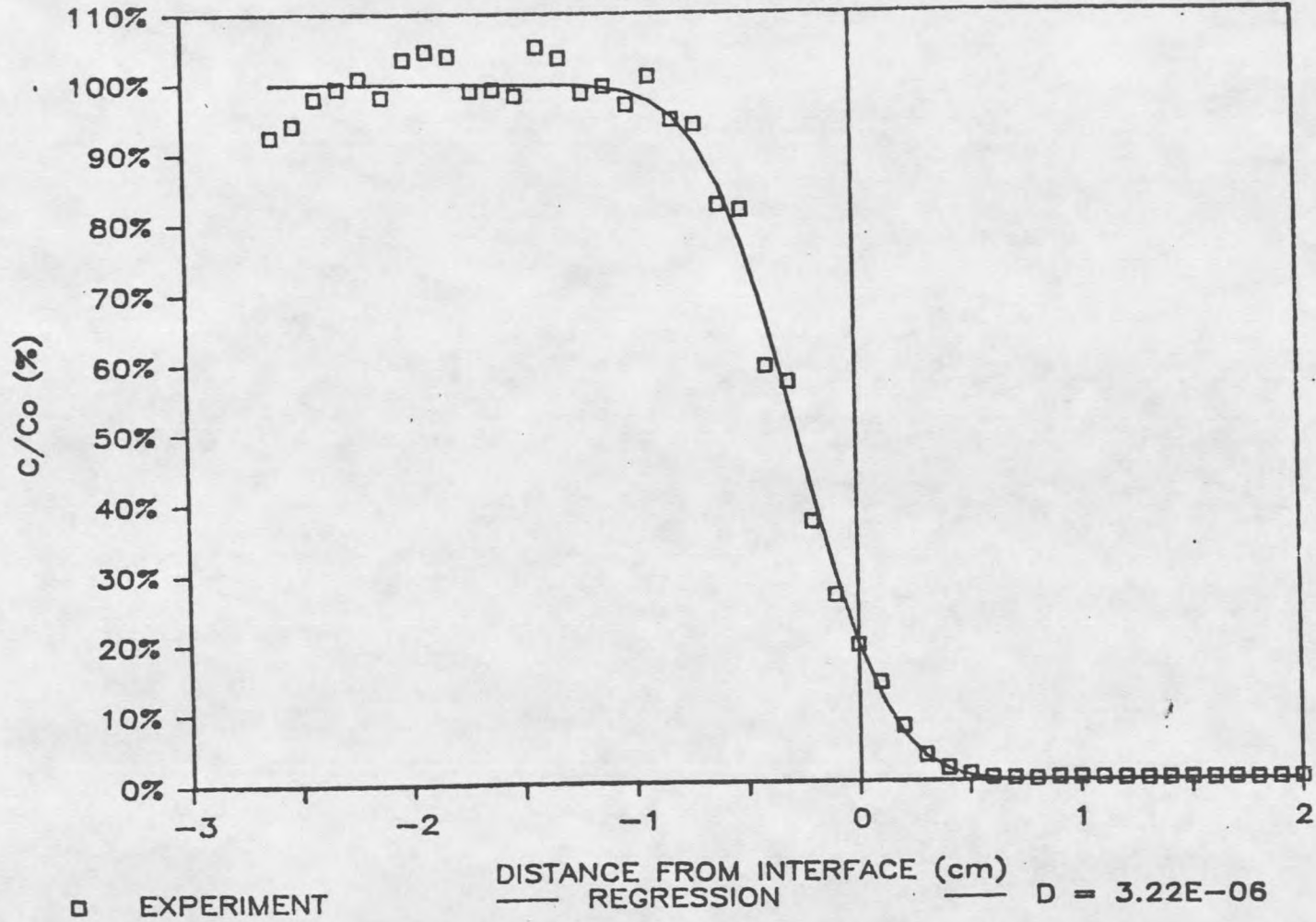


Figure 15.

D-CL36-060-004

CHLORIDE-36 C/Co

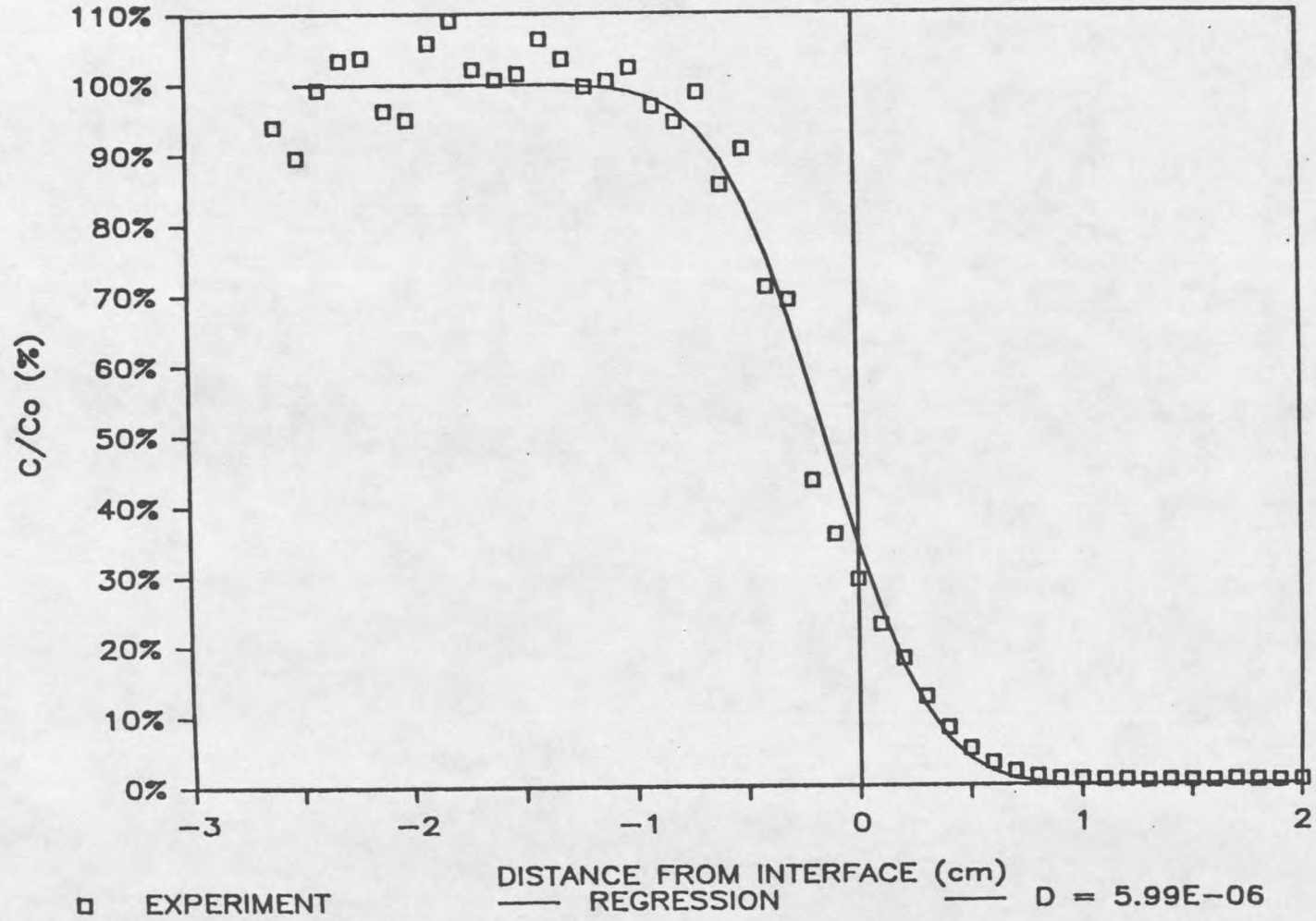


Figure 16.

D-CL36-060-005

CHLORIDE-36 C/Co

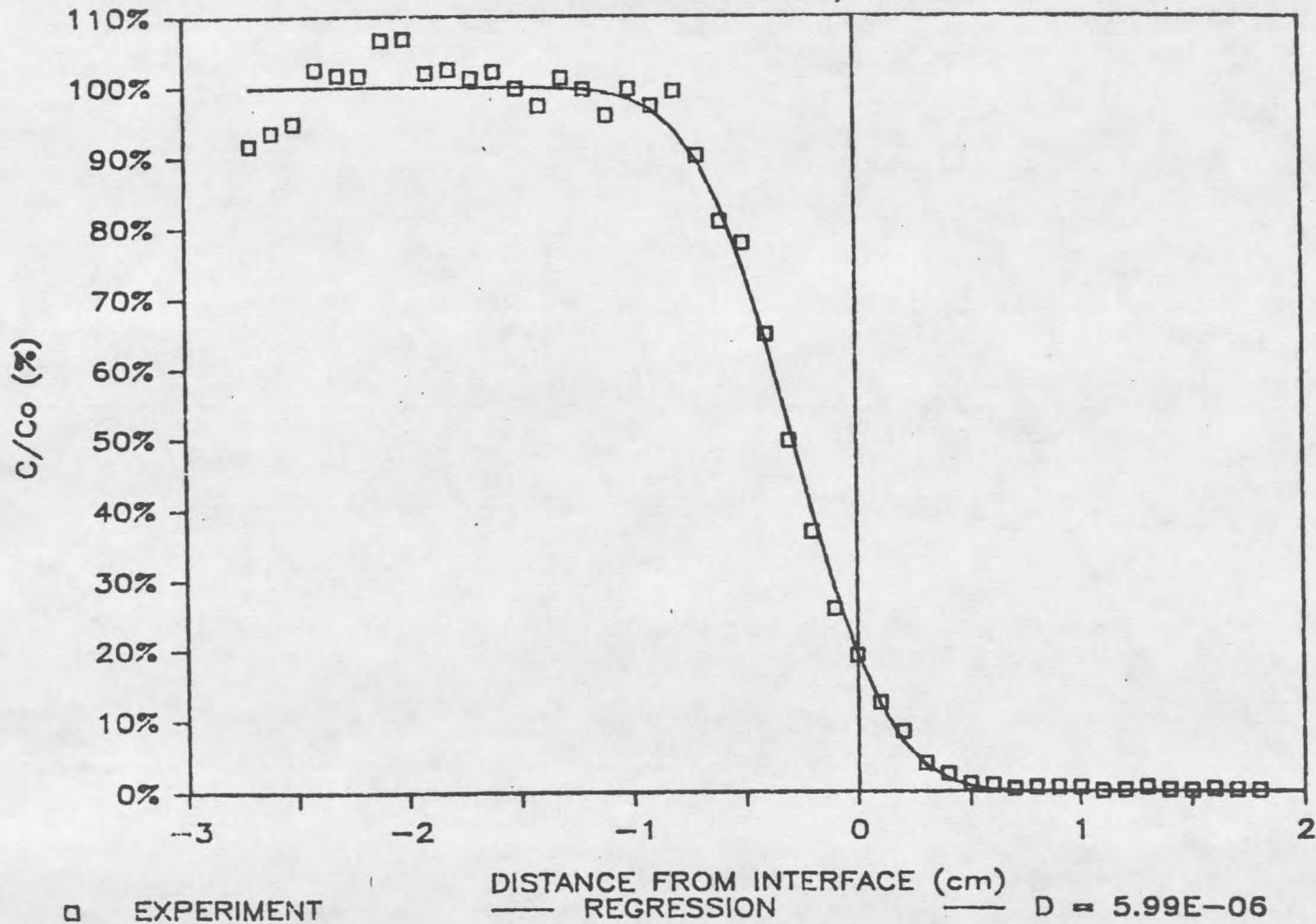


Figure 17.

D-CL36-060-006

CHLORIDE-36 C/Co

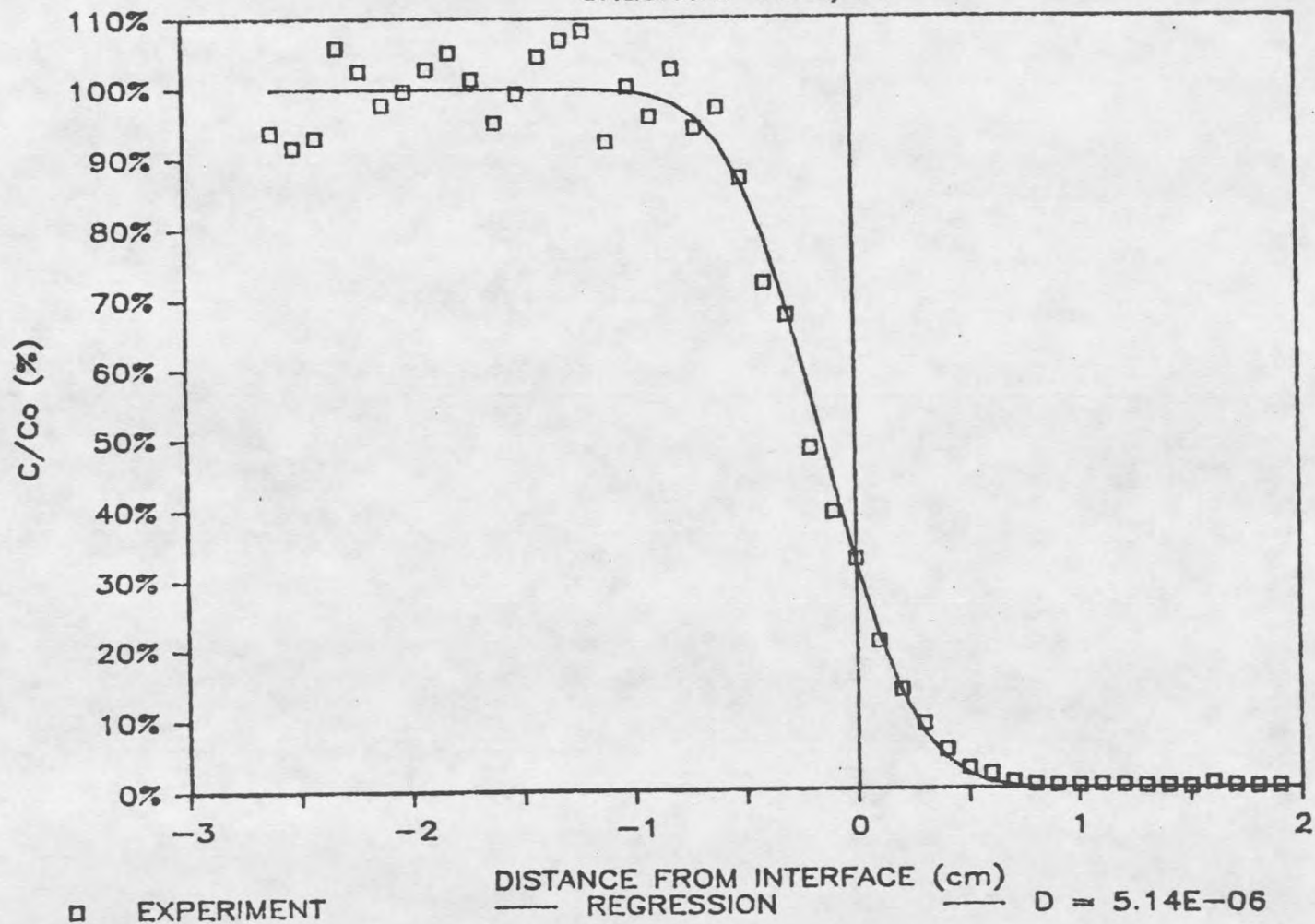


Figure 18.

D-CL36-090-007

CHLORIDE-36 C/Co

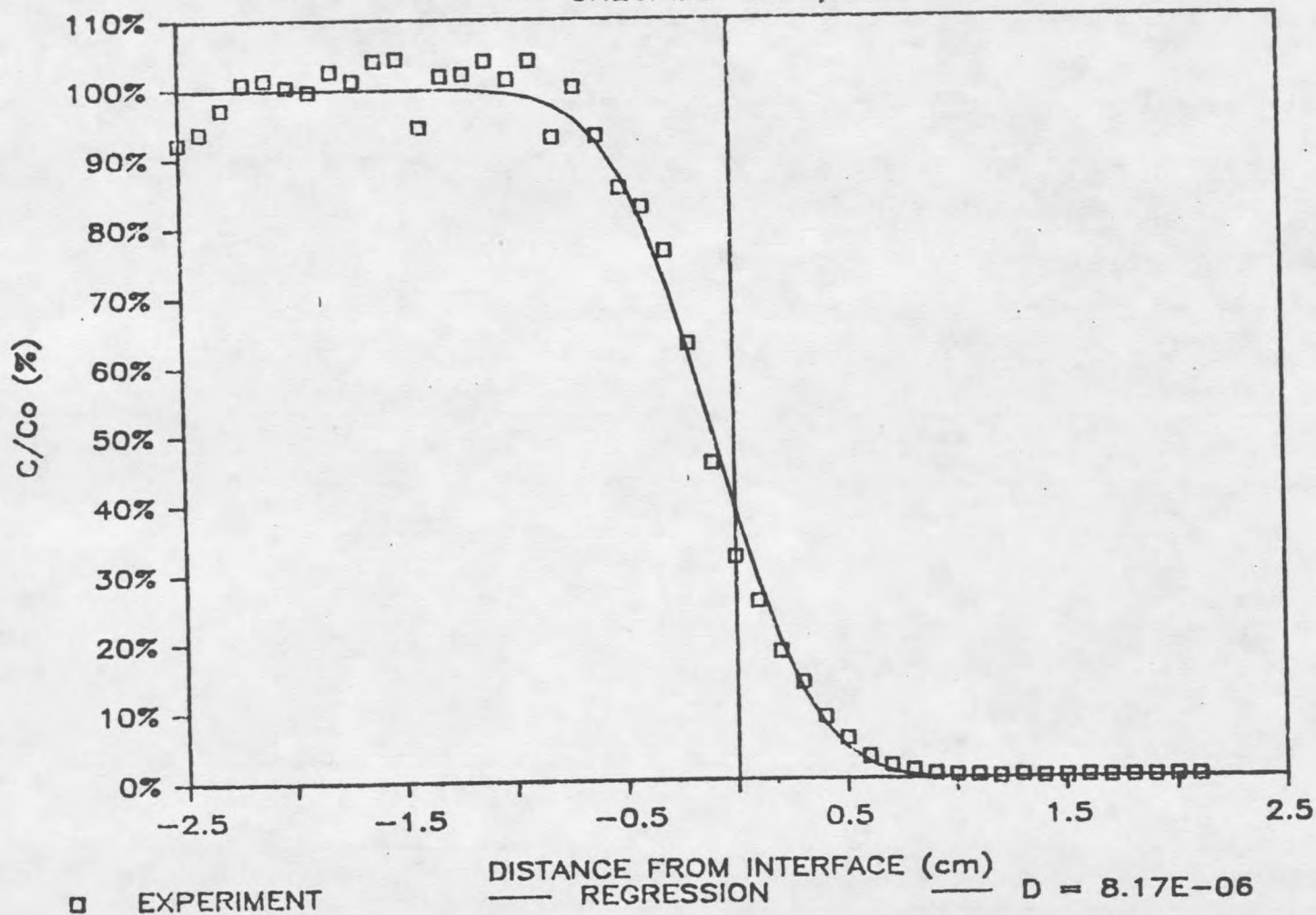


Figure 19.

D-CL36-090-008

CHLORIDE-36 C/Co

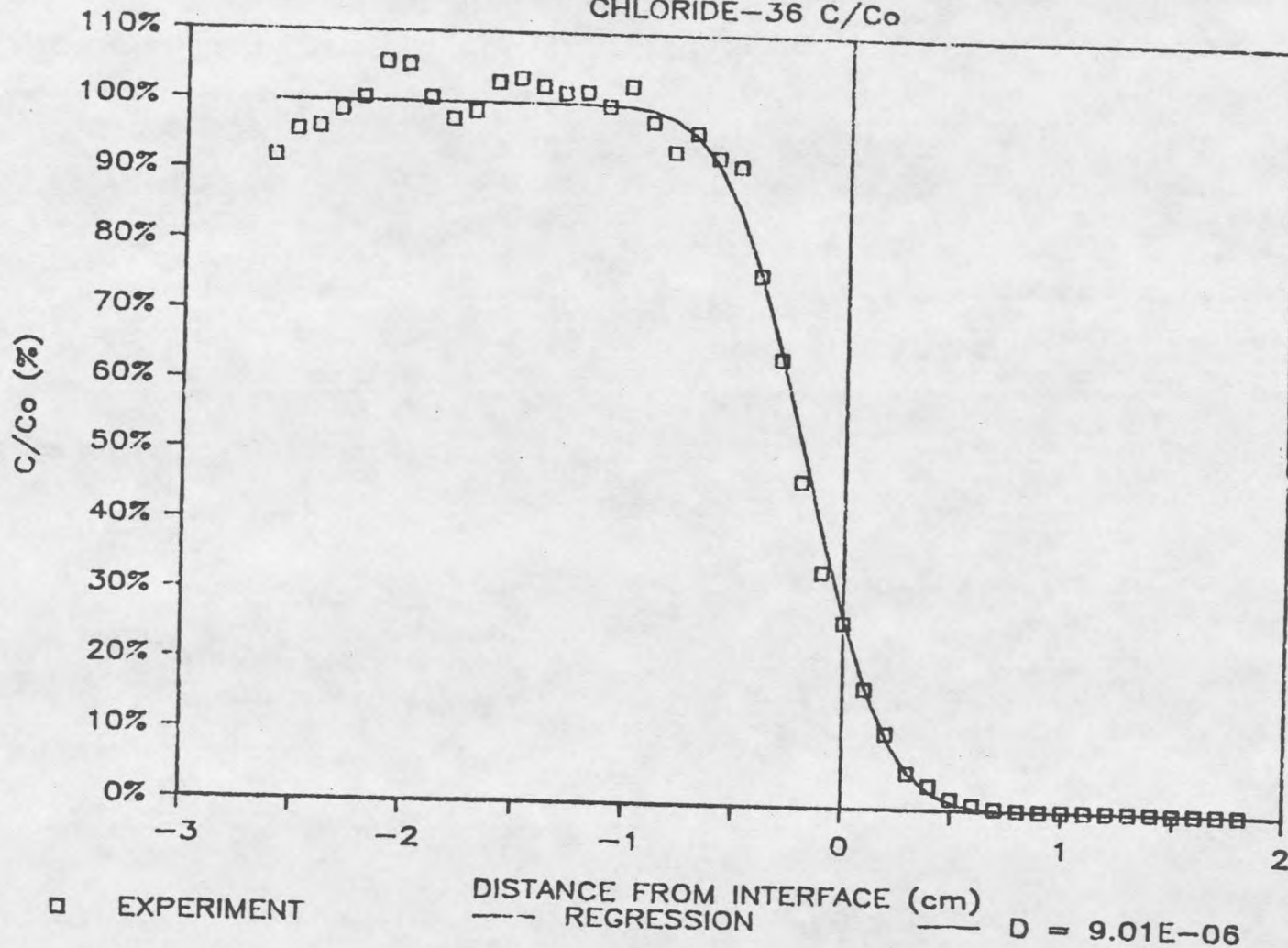


Figure 20.

D-CL36-090-009

CHLORIDE-36 C/Co

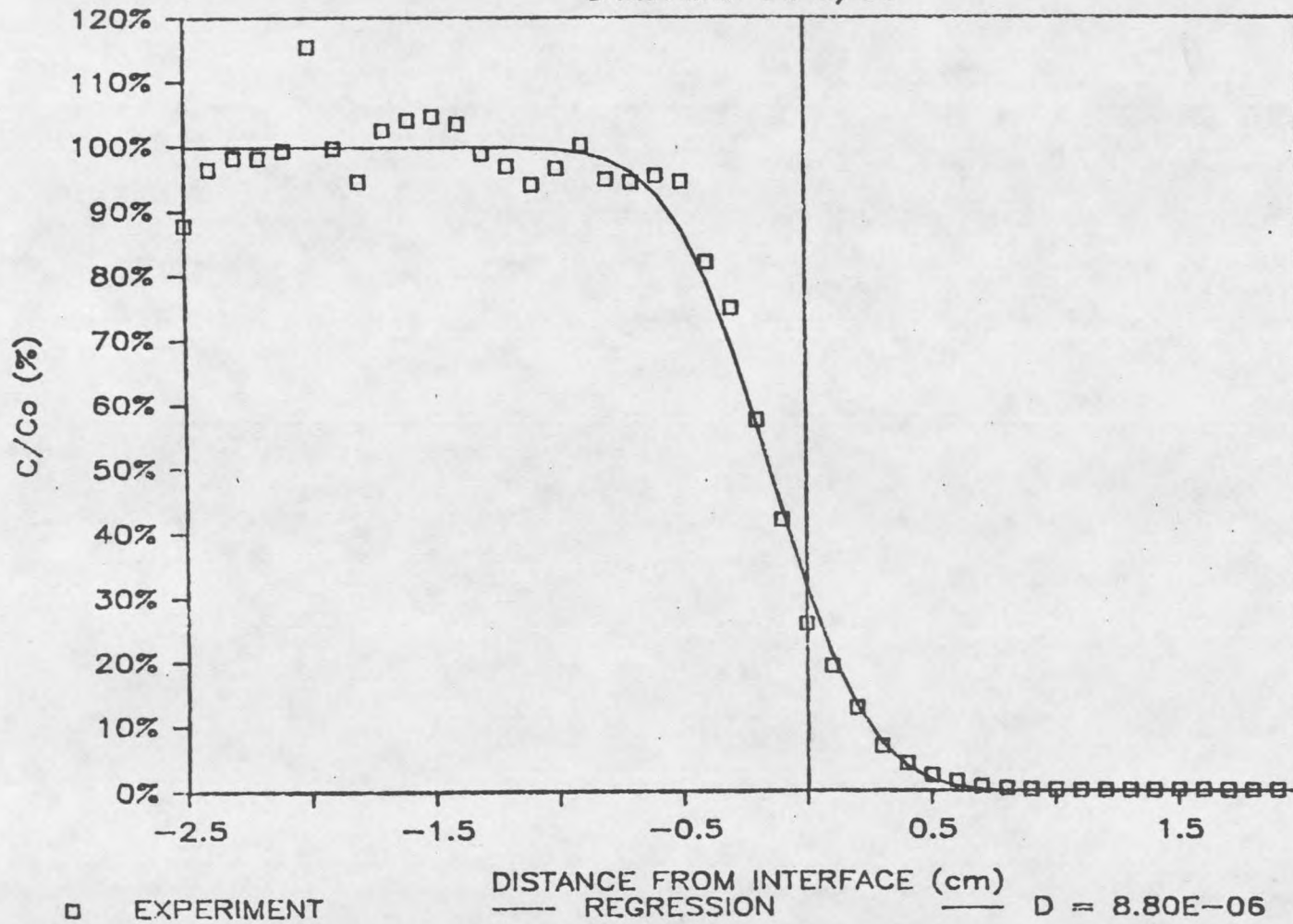


Figure 21.

D-CL36-020-010

CHLORIDE-36 C/Co

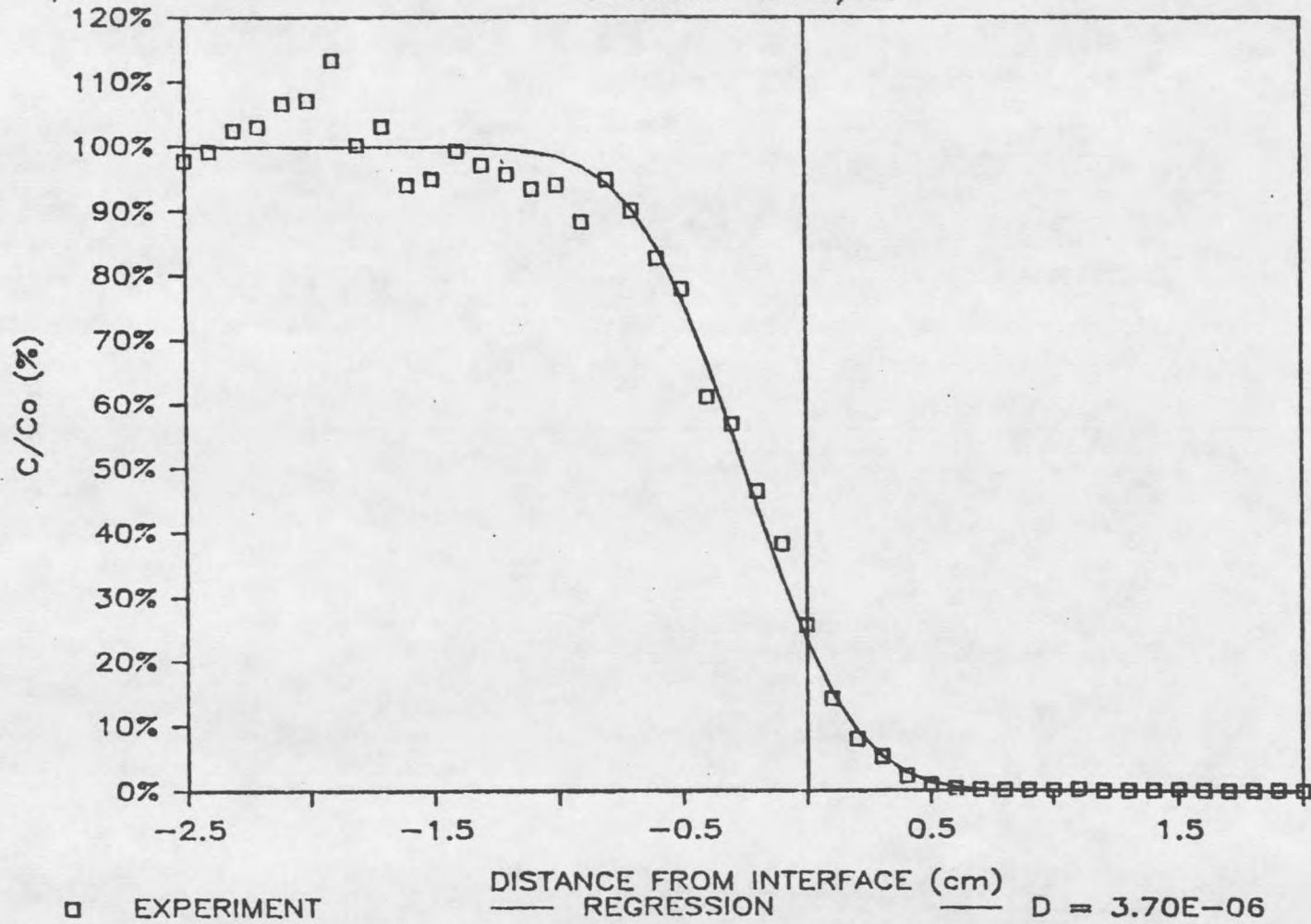


Figure 22.

D-CL36-060-011

CHLORIDE-36 C/Co

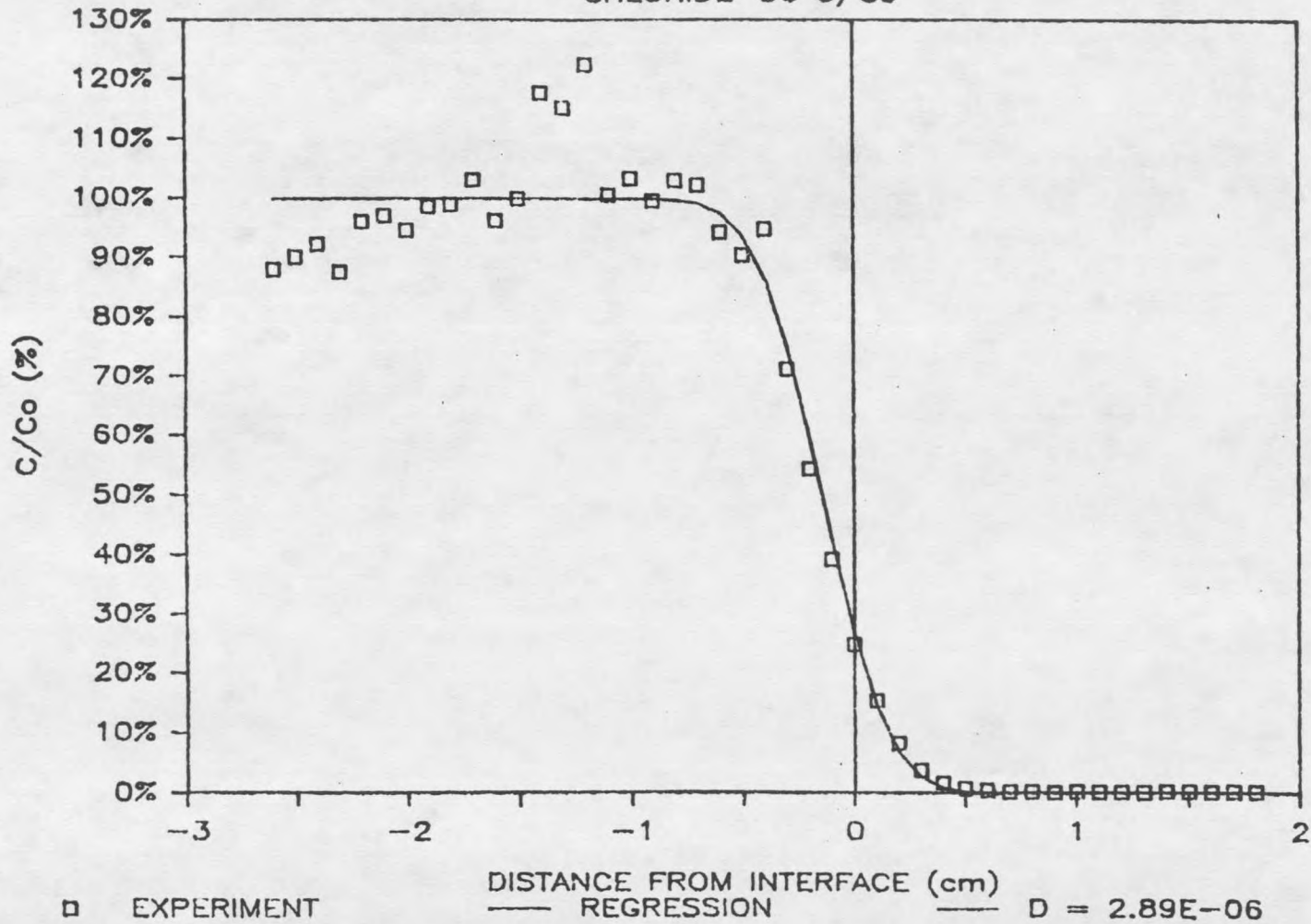


Figure 23.

D-CL36-020-013

CHLORIDE-36 C/Co

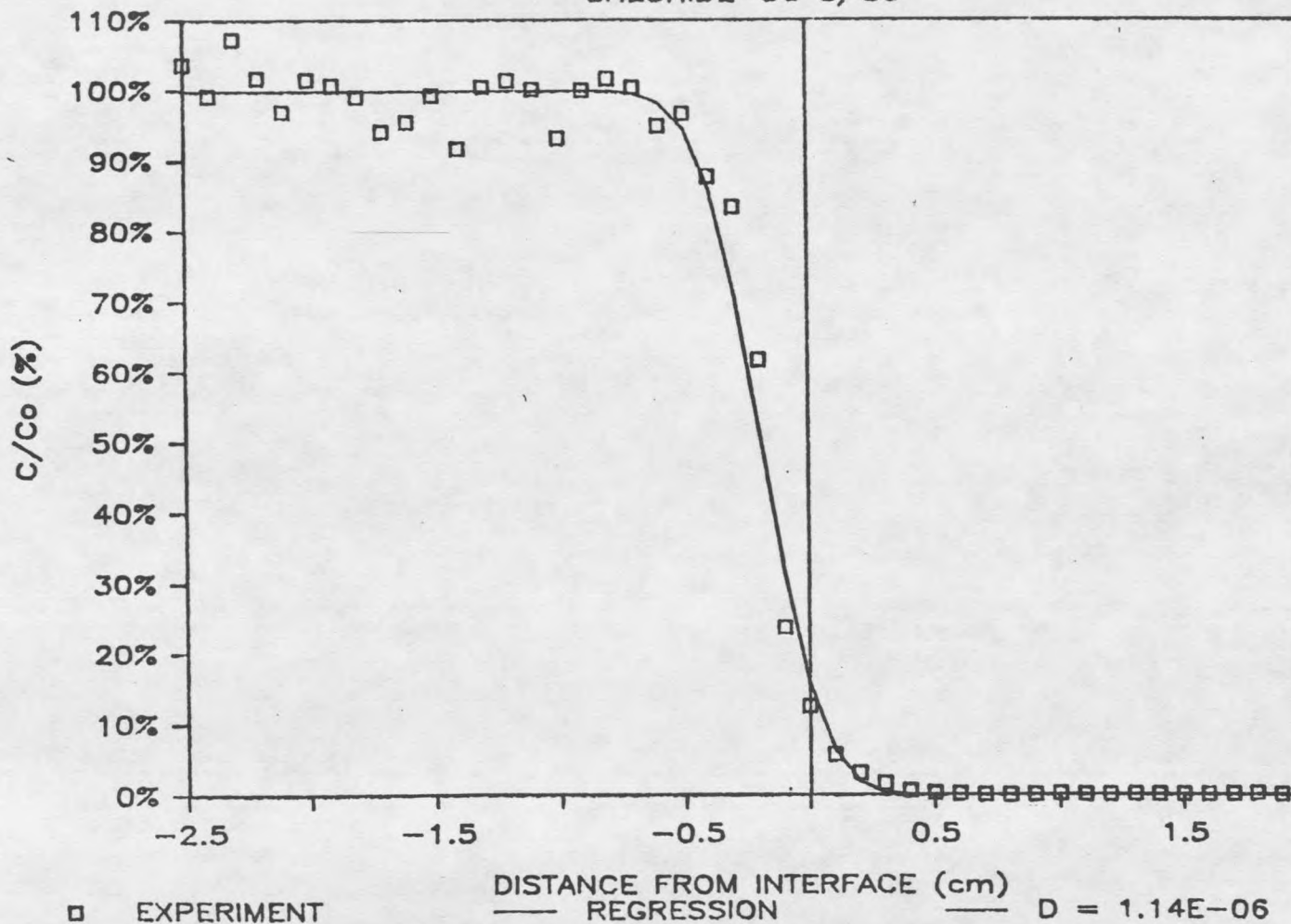


Figure 24.

D-CL36-090-015

CHLORIDE-36 C/Co

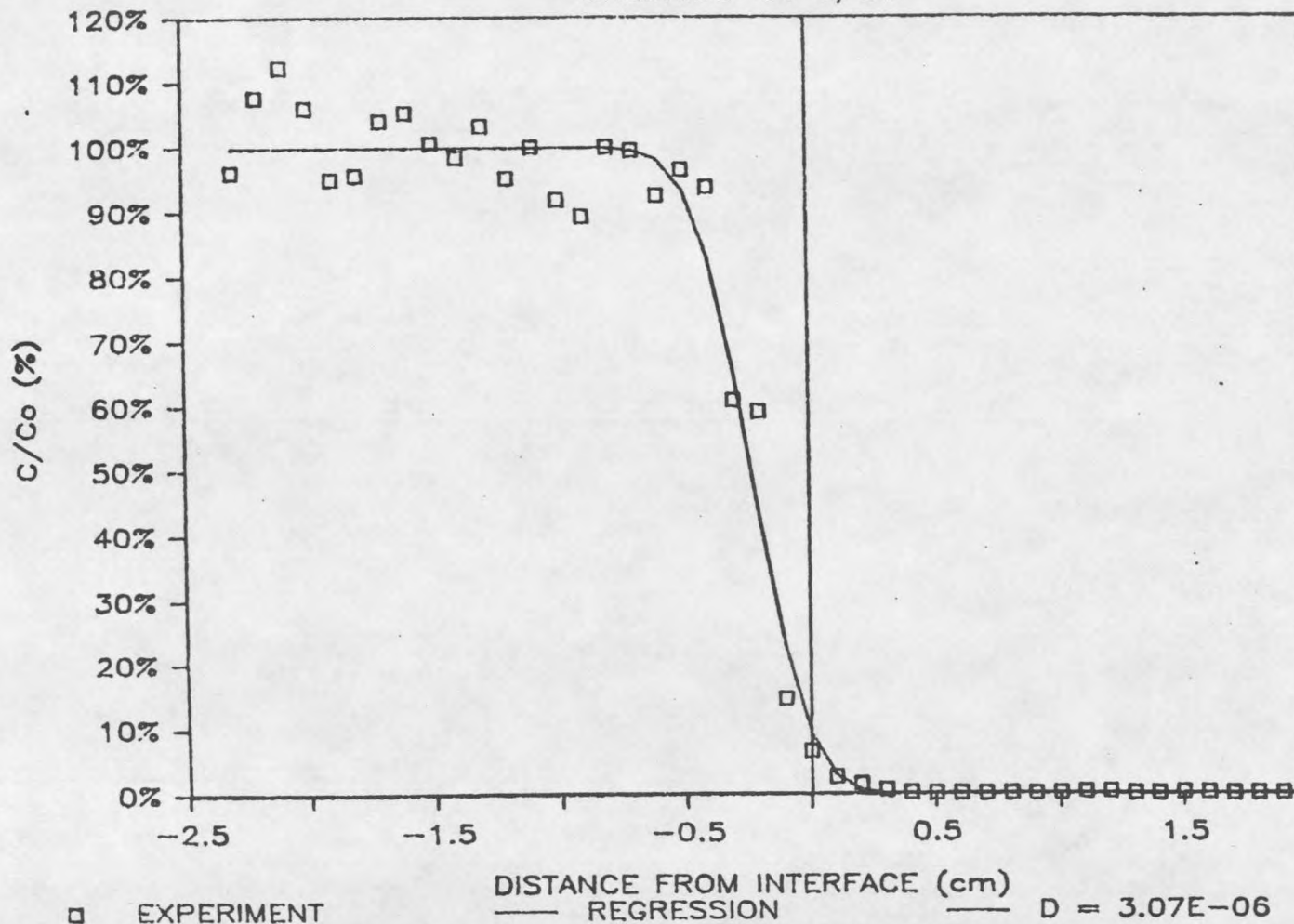


Figure 25.

D-CL36-020-016

CHLORIDE-36 C/Co

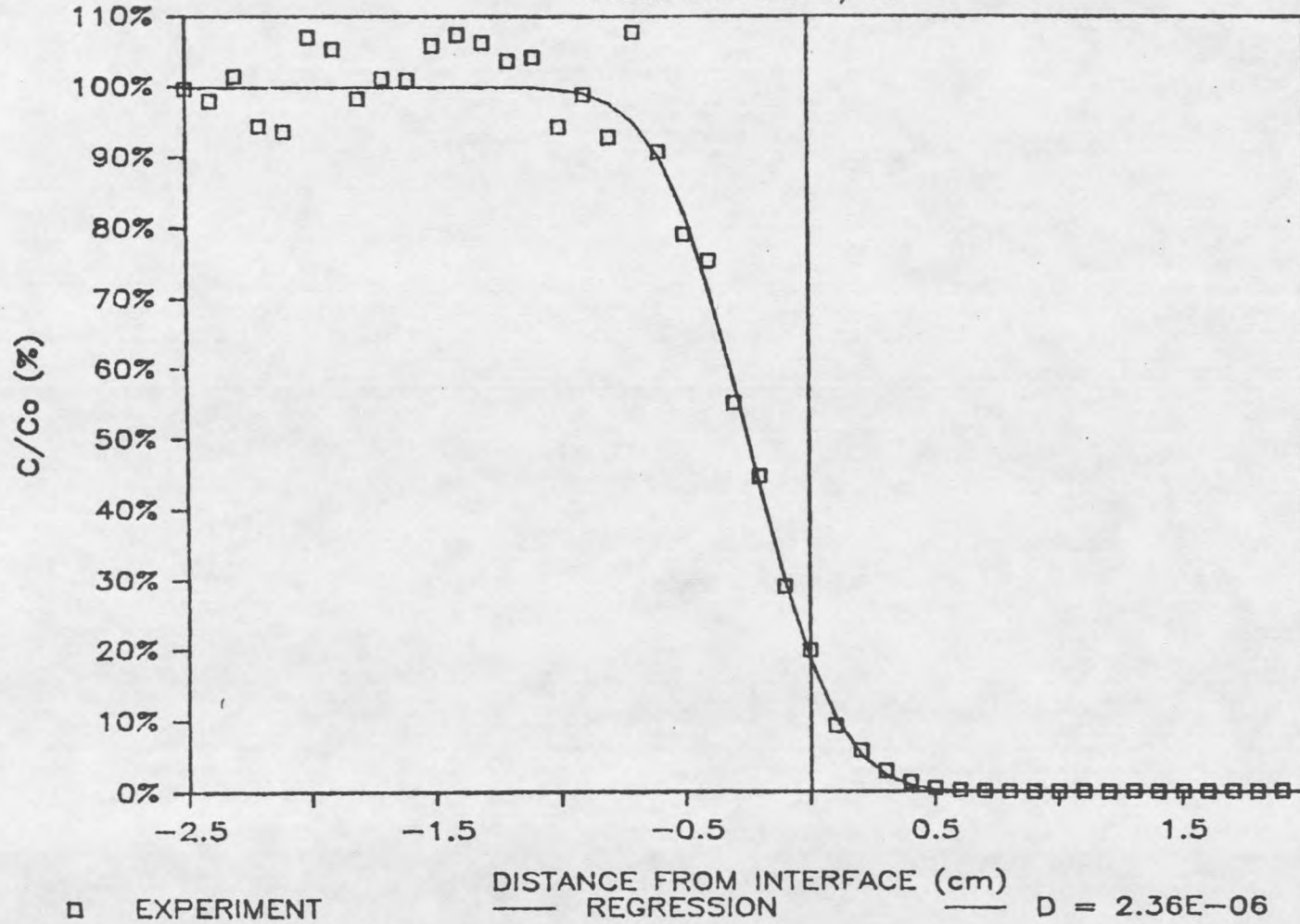


Figure 26.

D-CL36-060-017

CHLORIDE-36 C/Co

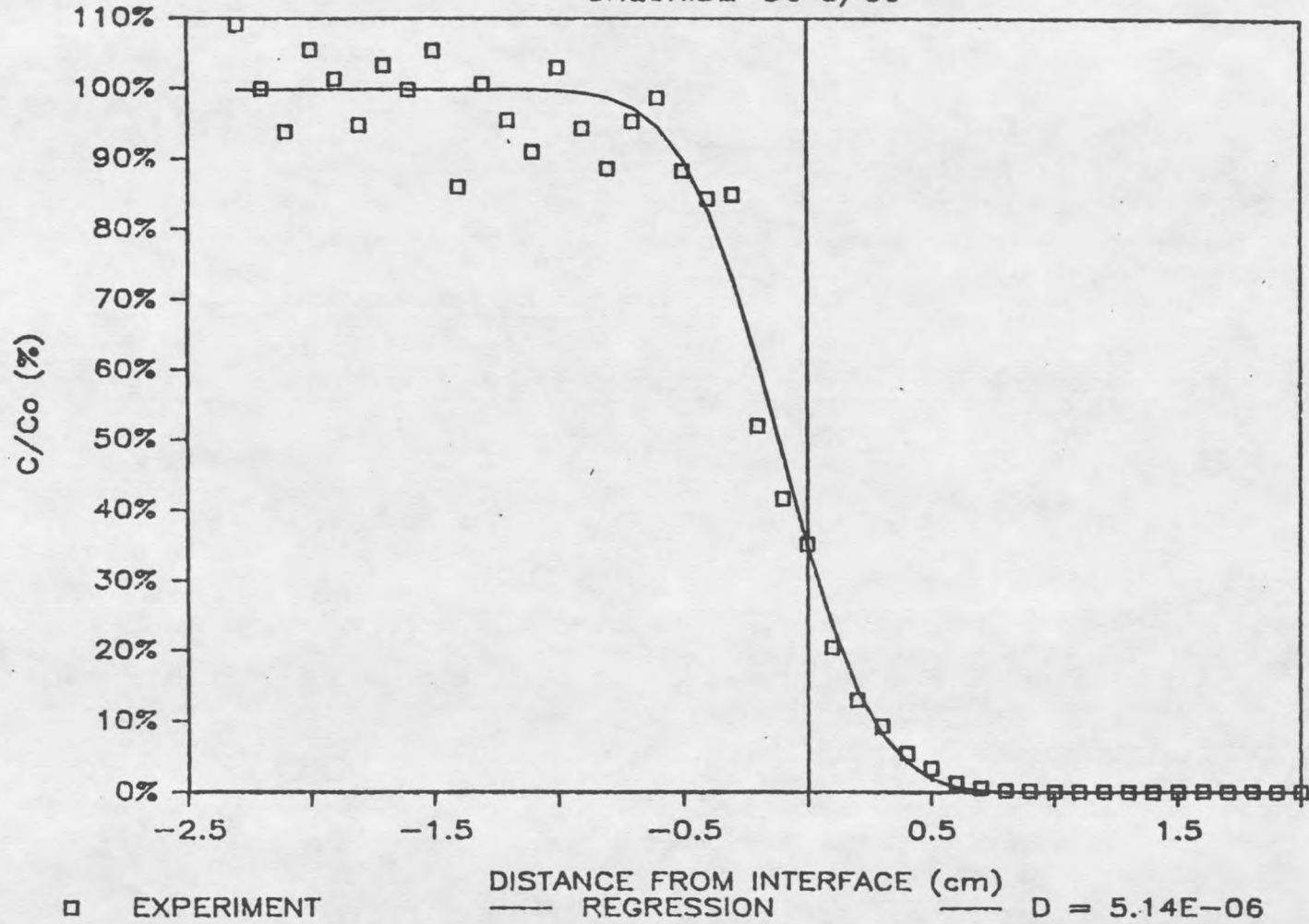


Figure 27.

D-CL36-090-018

CHLORIDE-36 C/Co

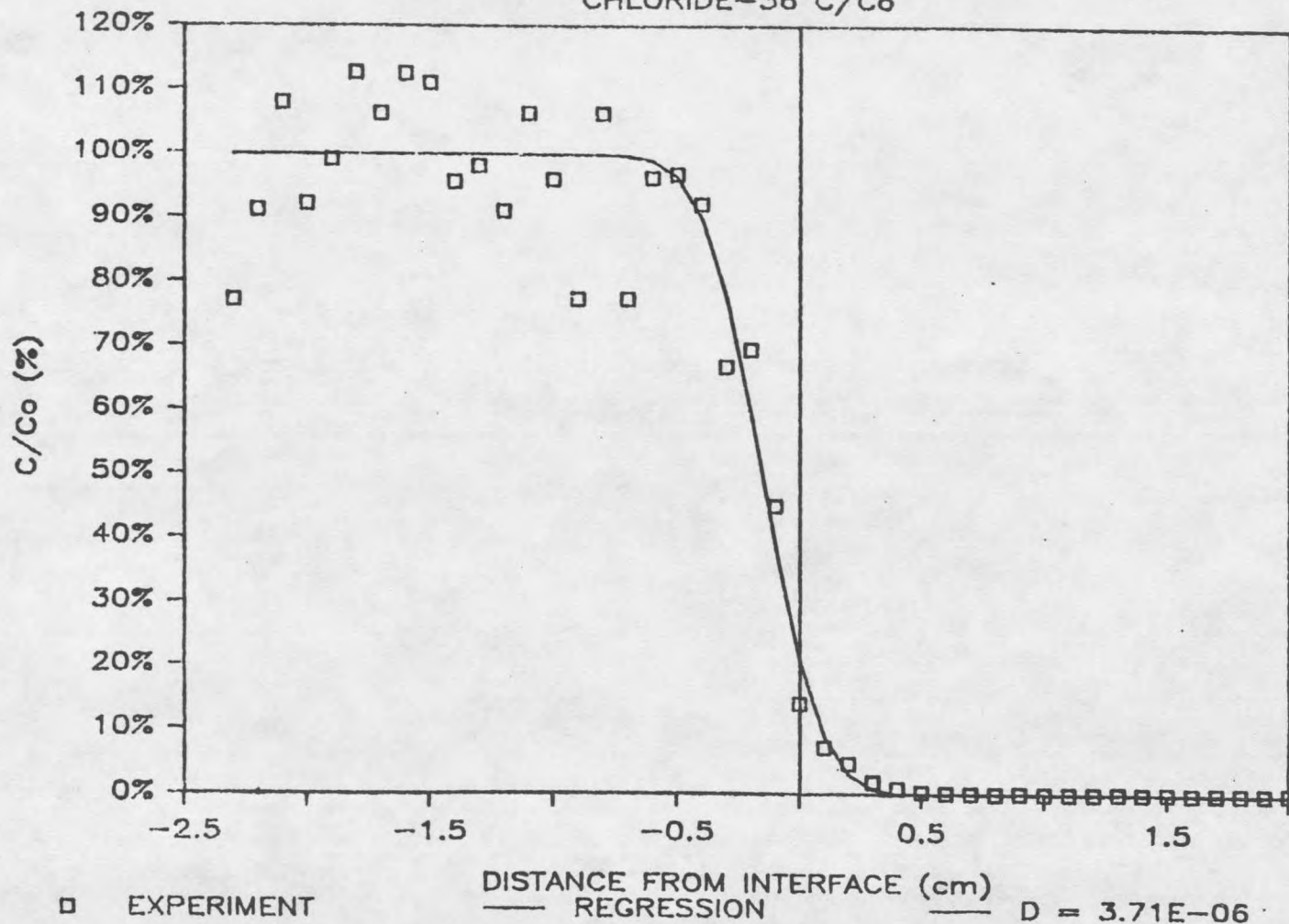


Figure 28.

D-CL36-020-019

CHLORIDE-36 C/Co

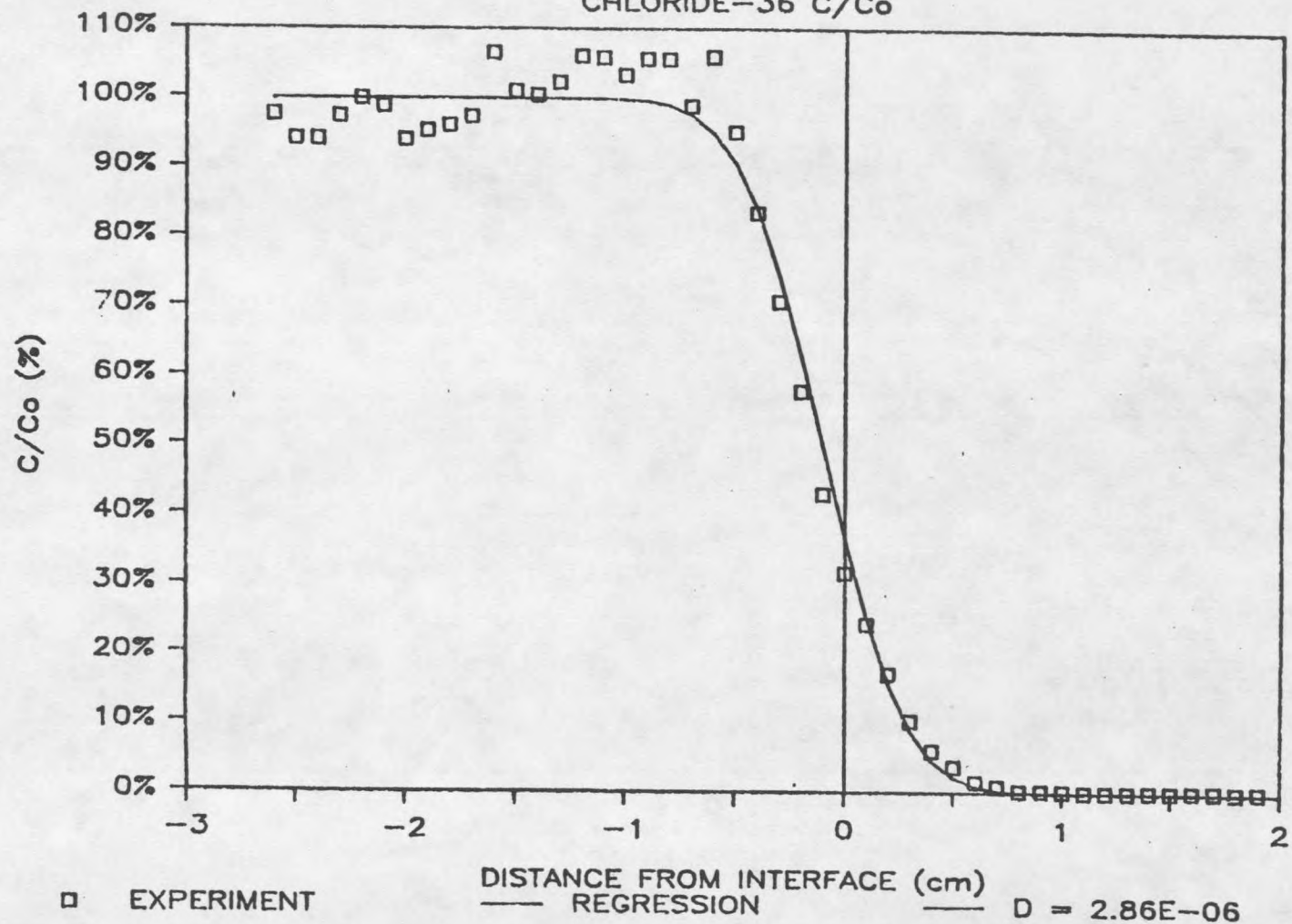


Figure 29.

D-CL36-020-020

CHLORIDE-36 C/Co

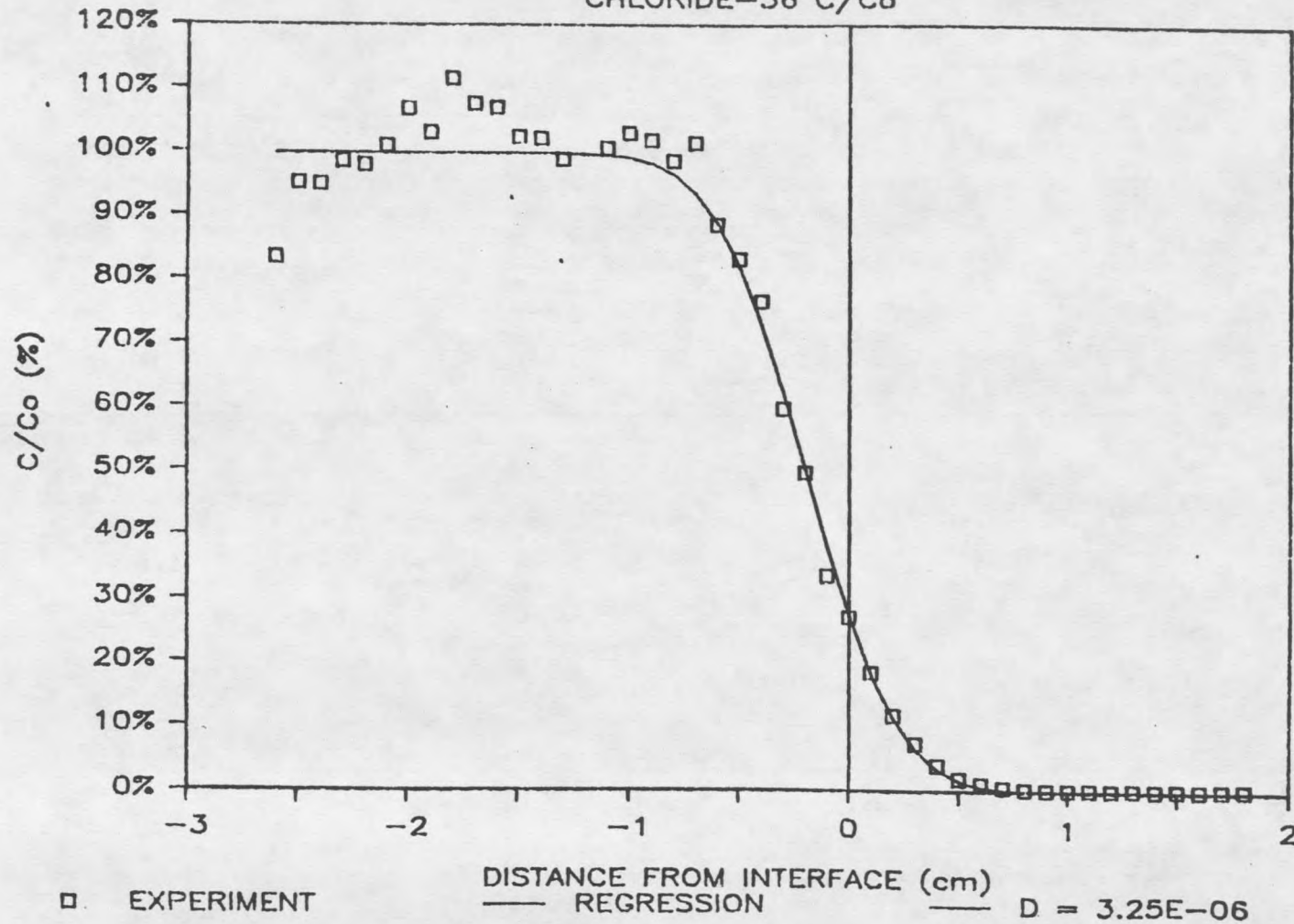


Figure 30.

D-CL36-090-021

CHLORIDE-36 C/Co

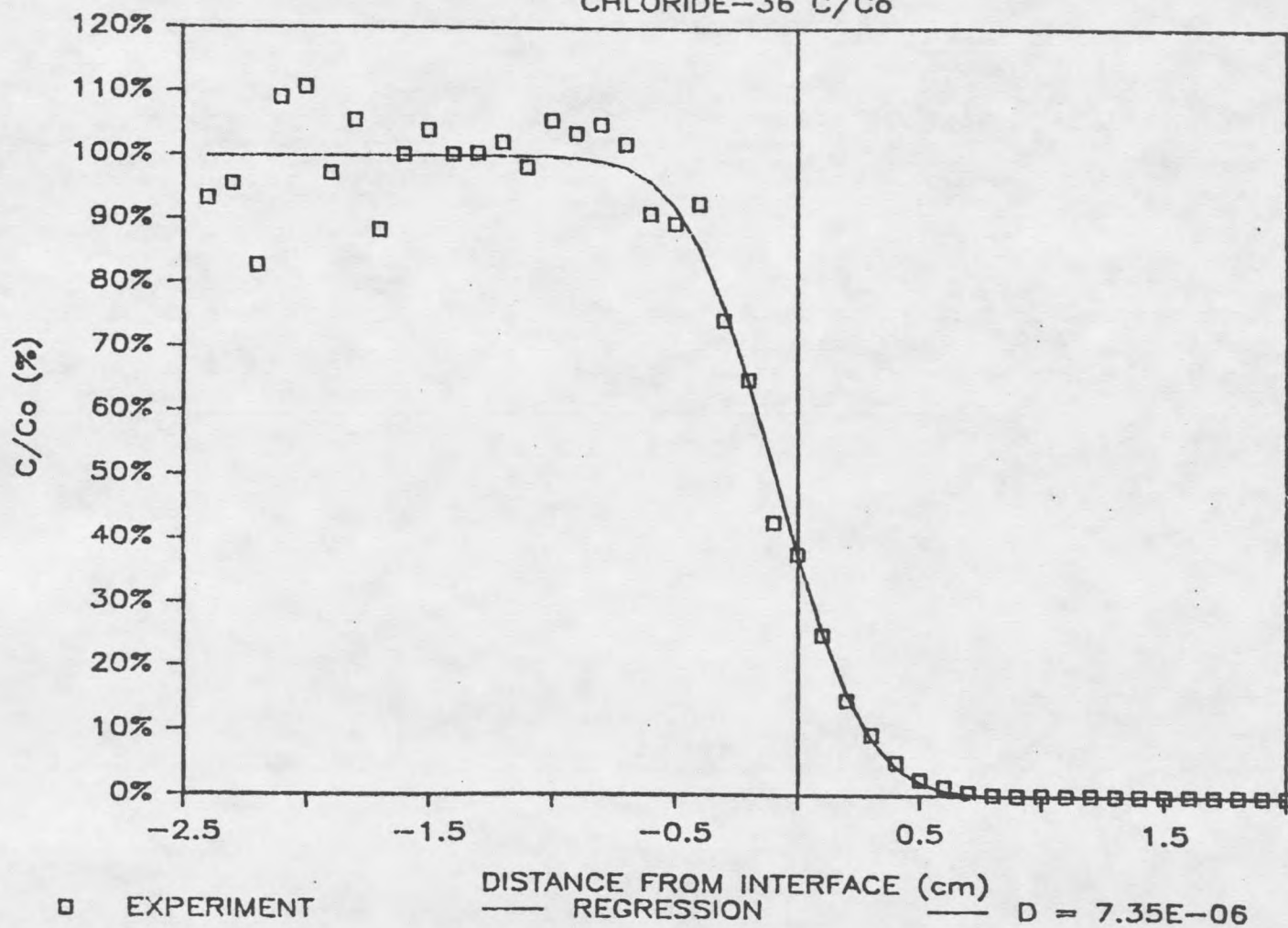


Figure 31.

D-CL36-060-022

CHLORIDE-36 C/Co

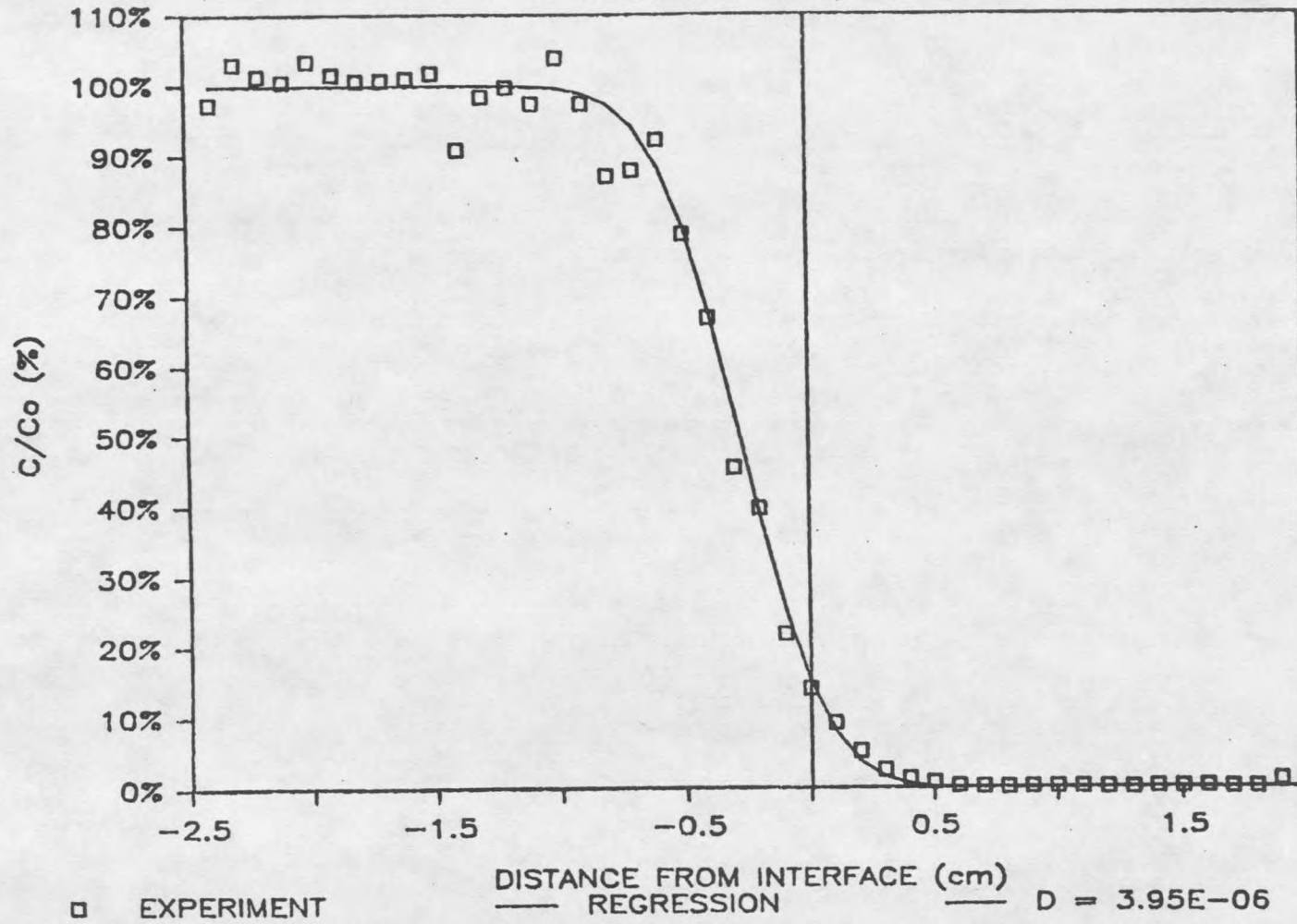


Figure 32.

D-C14-020-002

CARBON-14 C/Co

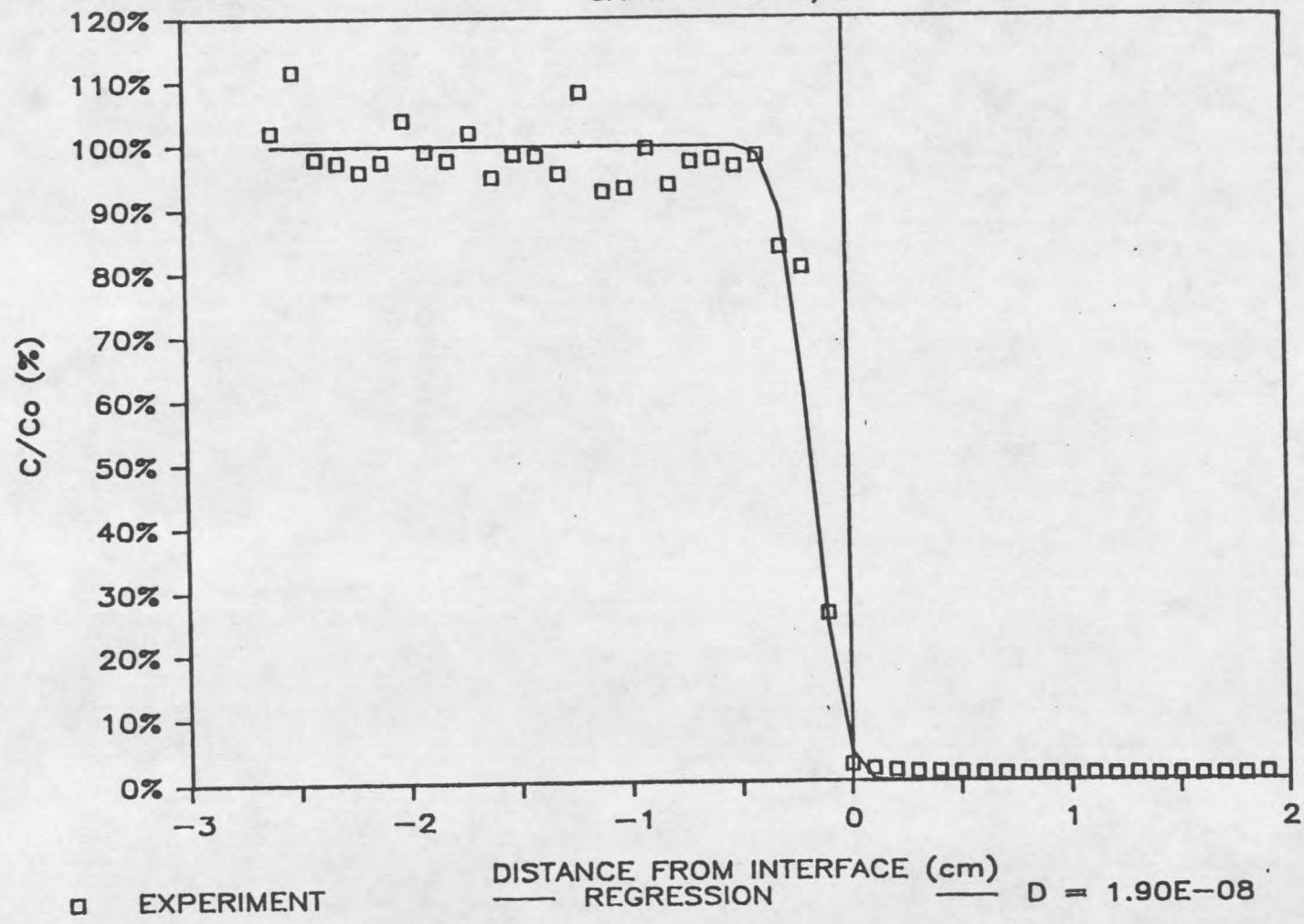


Figure 33.

D-C14-060-003

CARBON-14 C/Co

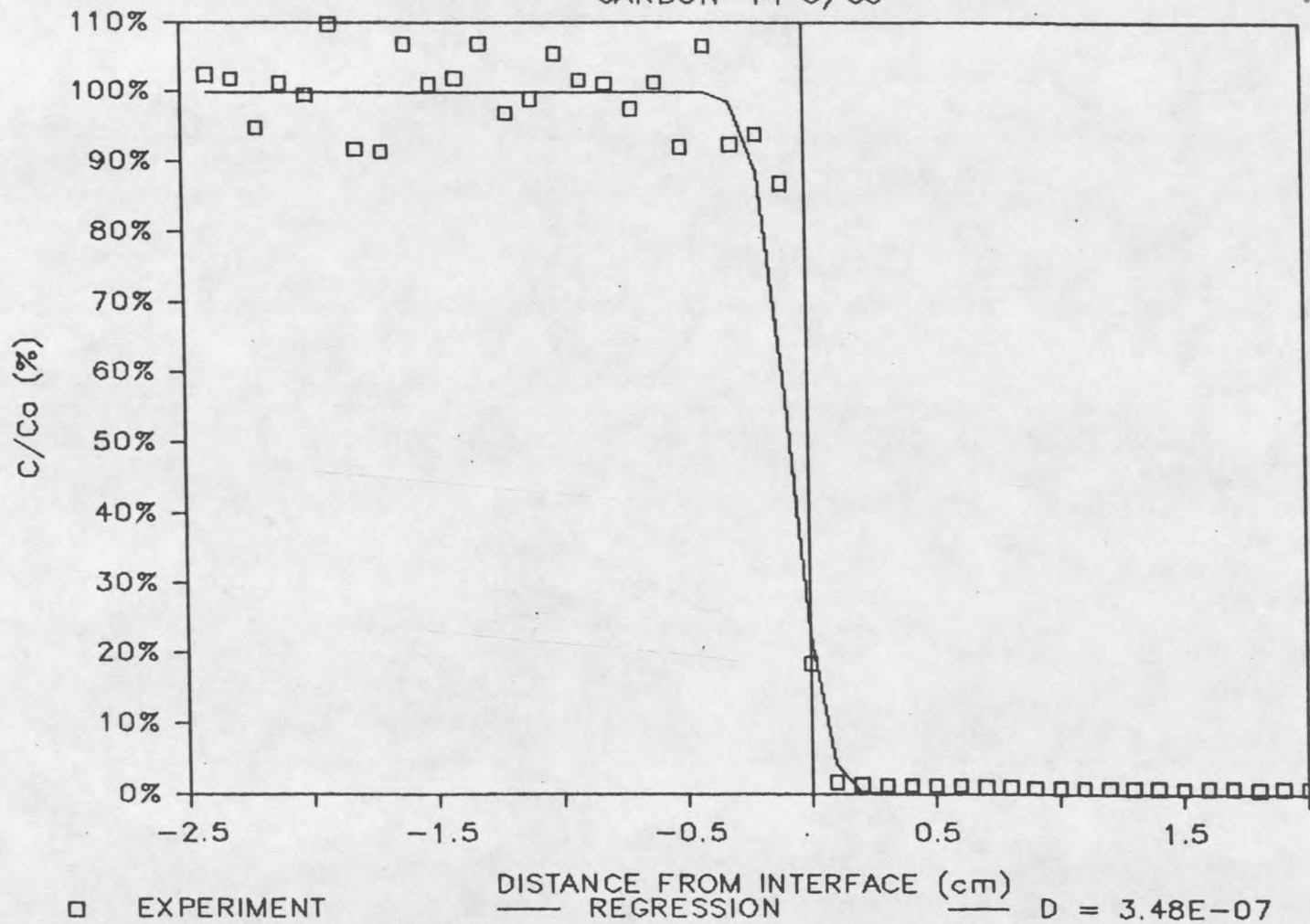


Figure 34.

D-C14-060-004

CARBON-14 C/Co

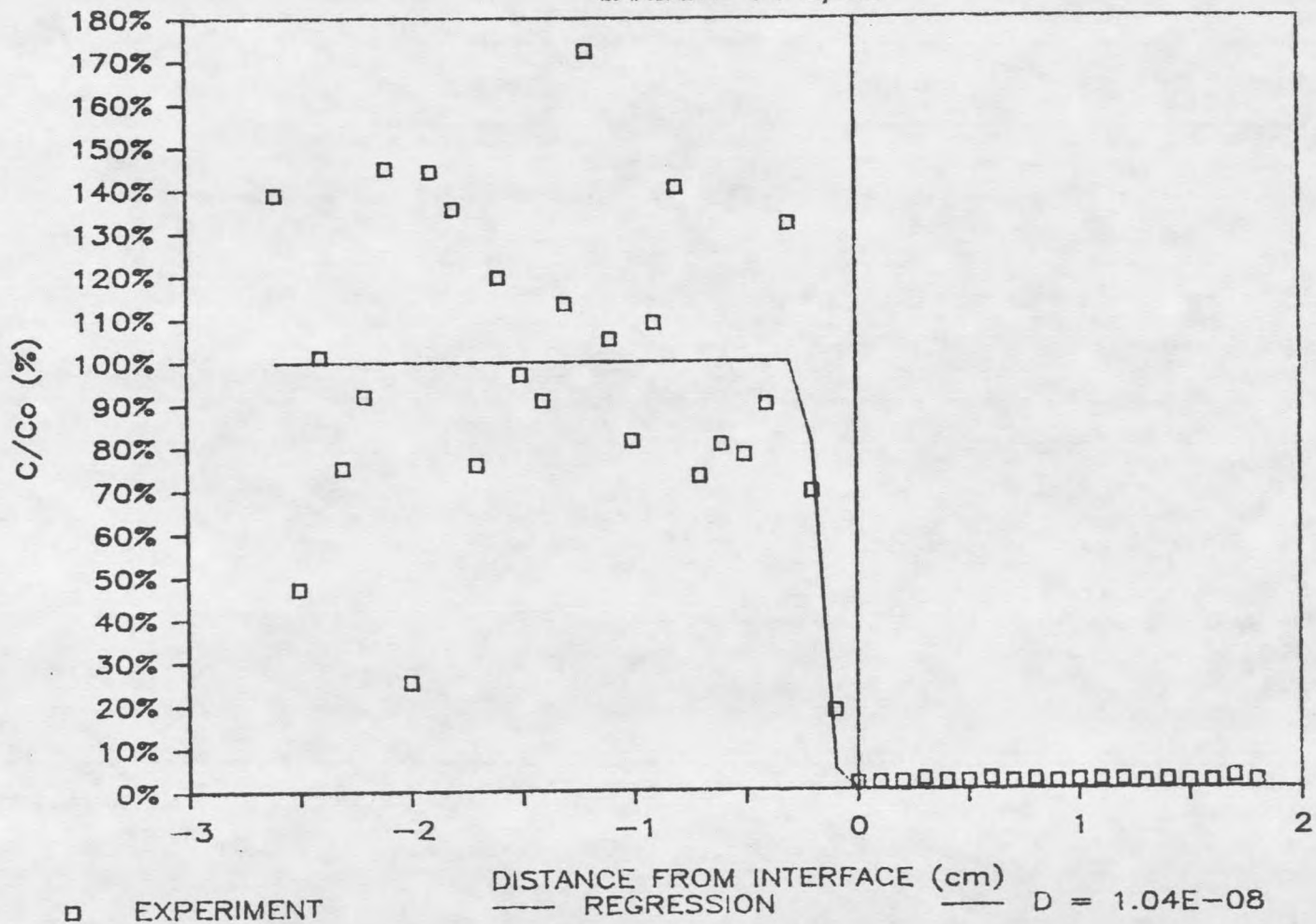


Figure 35.

D-C14-090-005

CARBON-14 C/Co

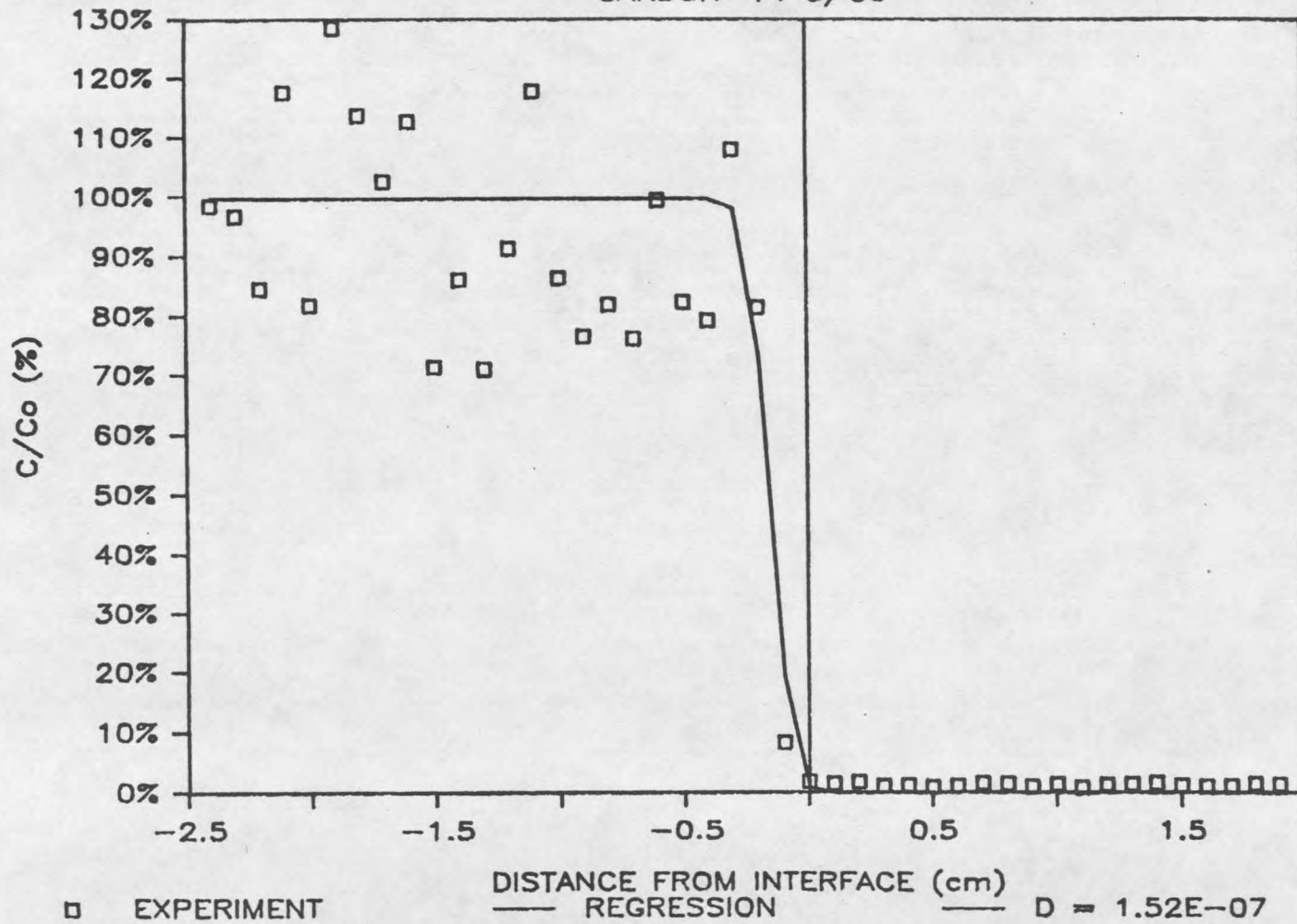


Figure 36.

D-C14-090-006

CARBON-14 C/Co

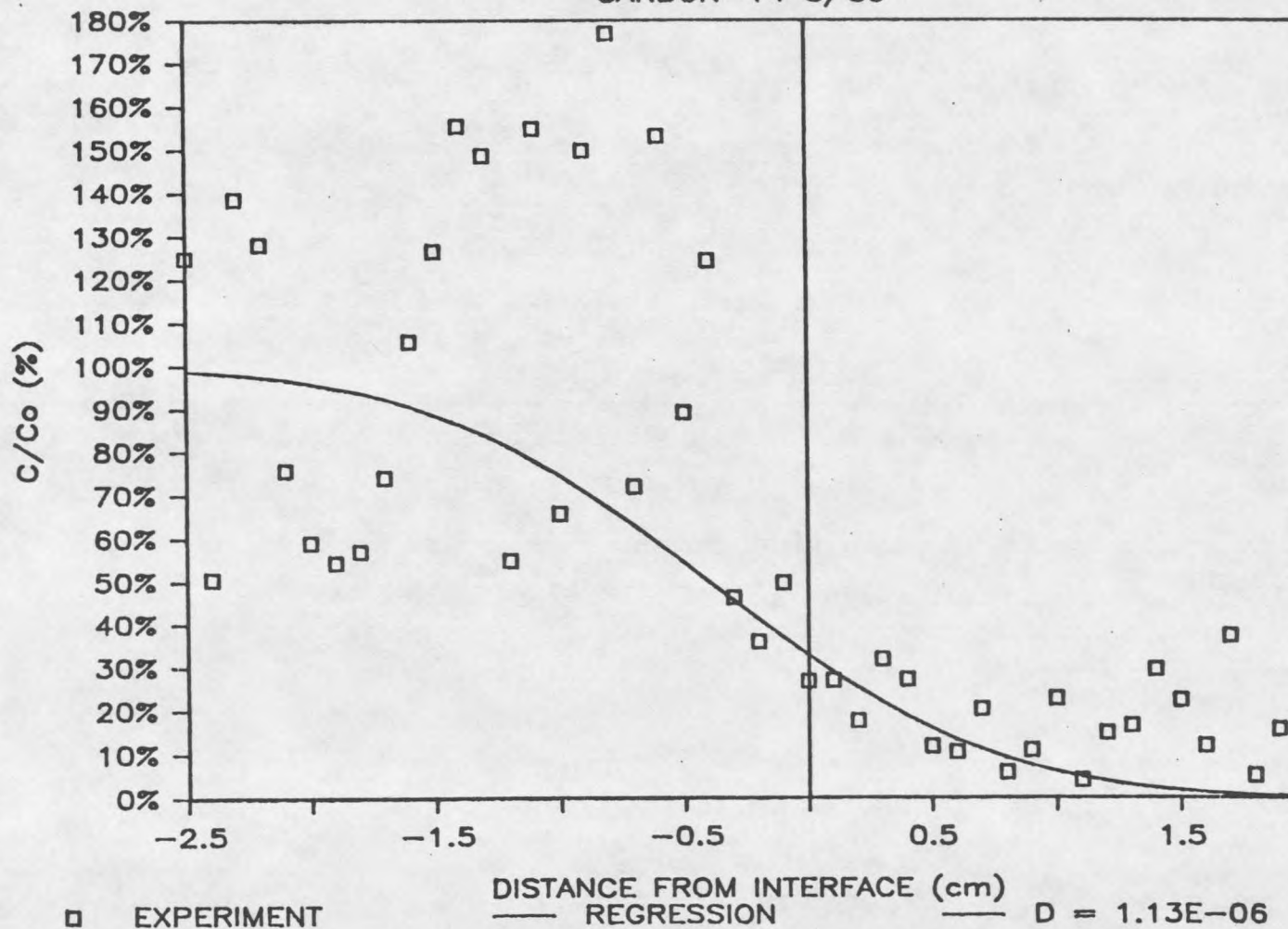


Figure 37.

D-C14-020-007

CARBON-14 C/Co

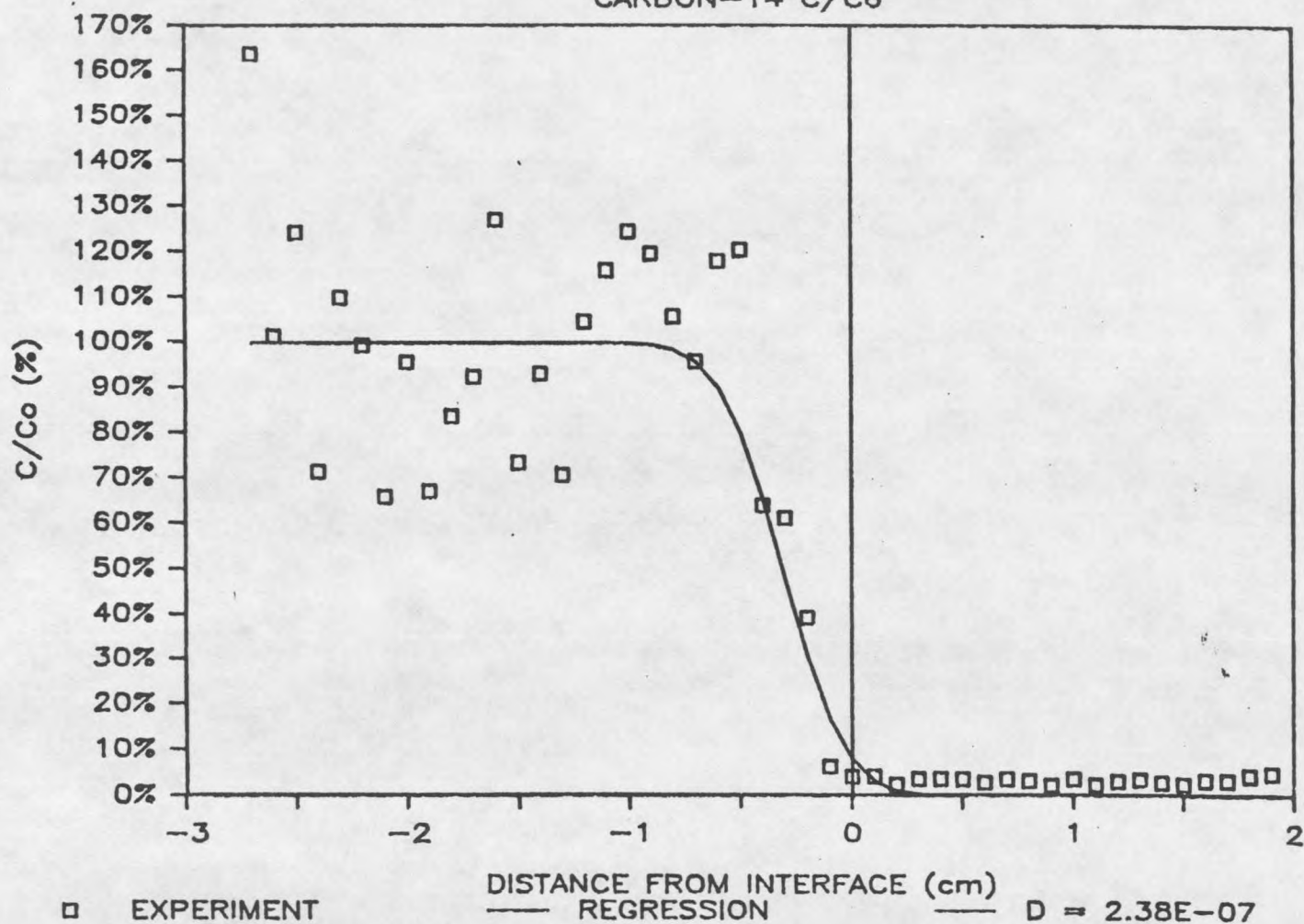


Figure 38.

D-C14-020-008

CARBON-14 C/Co

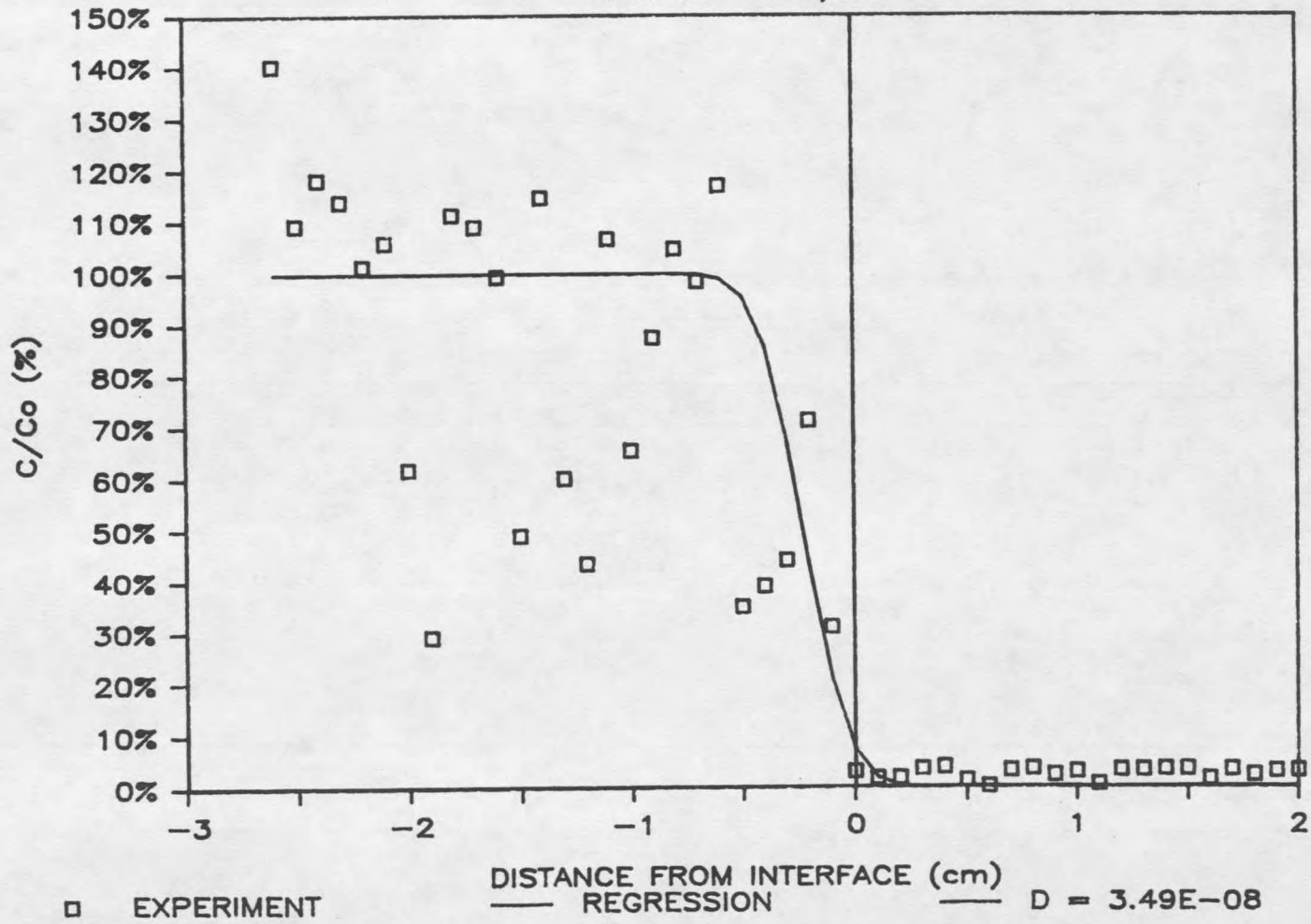


Figure 39.

D-C14-060-009

CARBON-14 C/Co

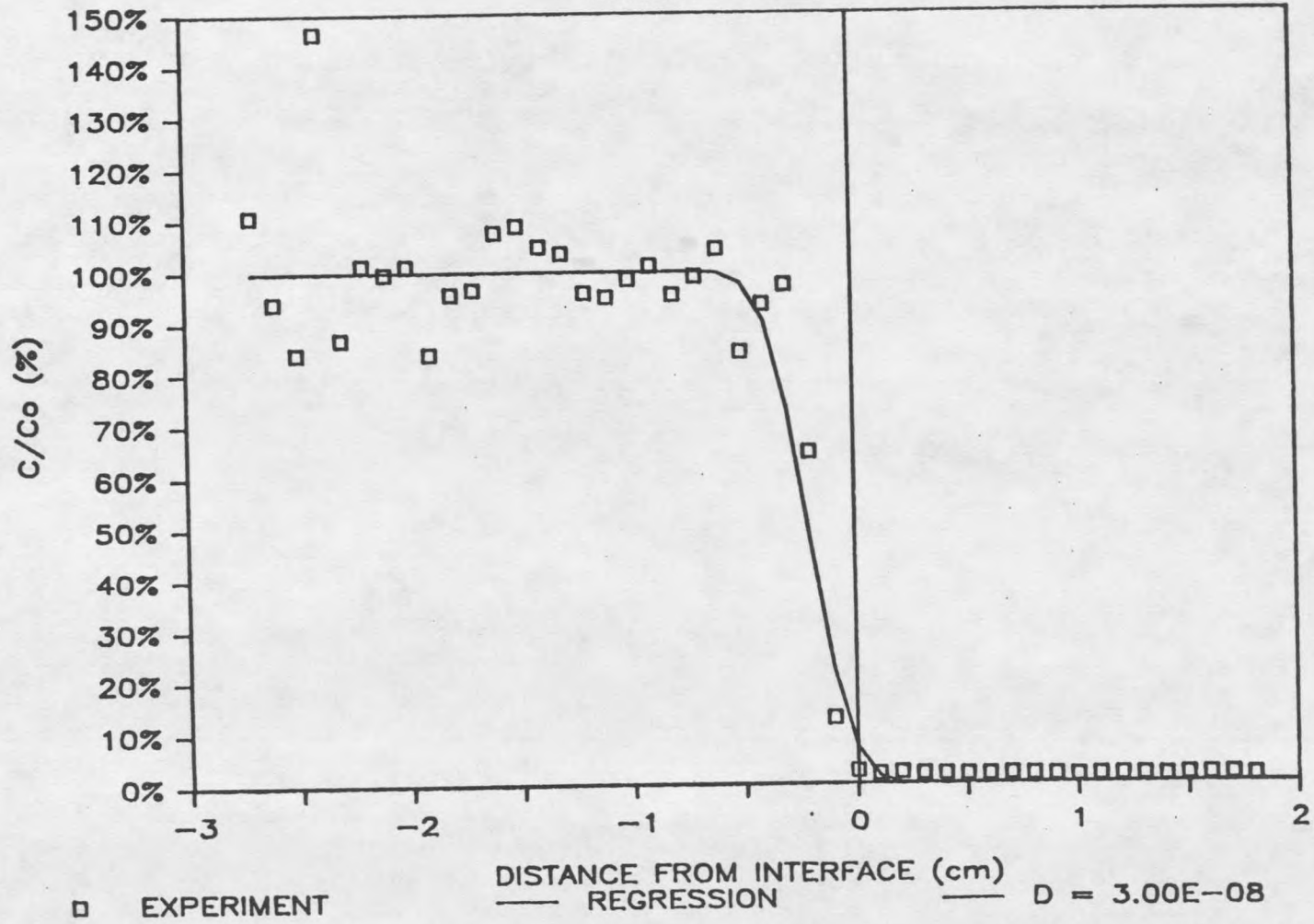


Figure 40.

D-C14-020-011

CARBON-14 C/Co

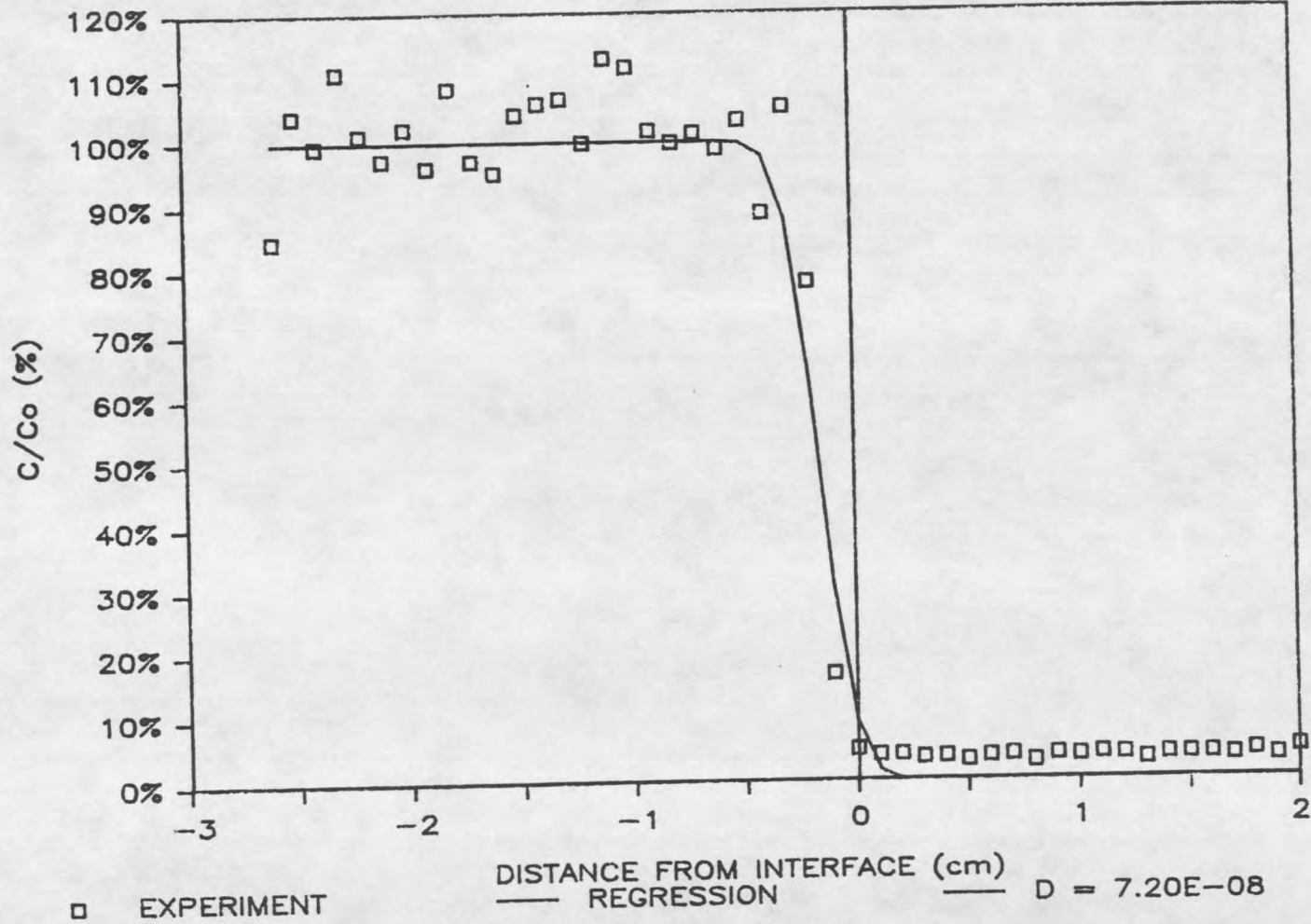


Figure 41.

D-C14-090-012

CARBON-14 C/Co

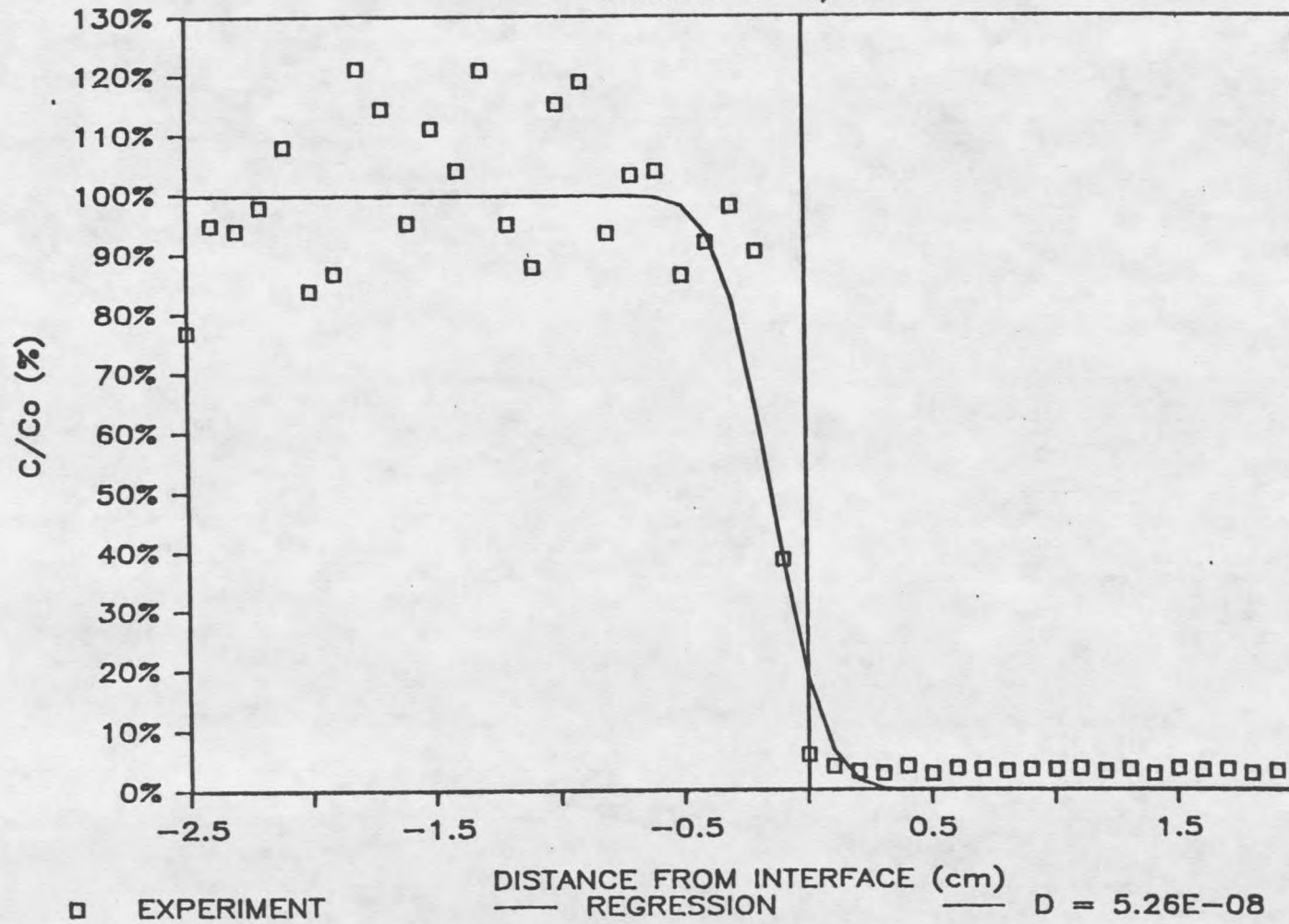


Figure 42.

D-C14-020-014

CARBON-14 C/Co

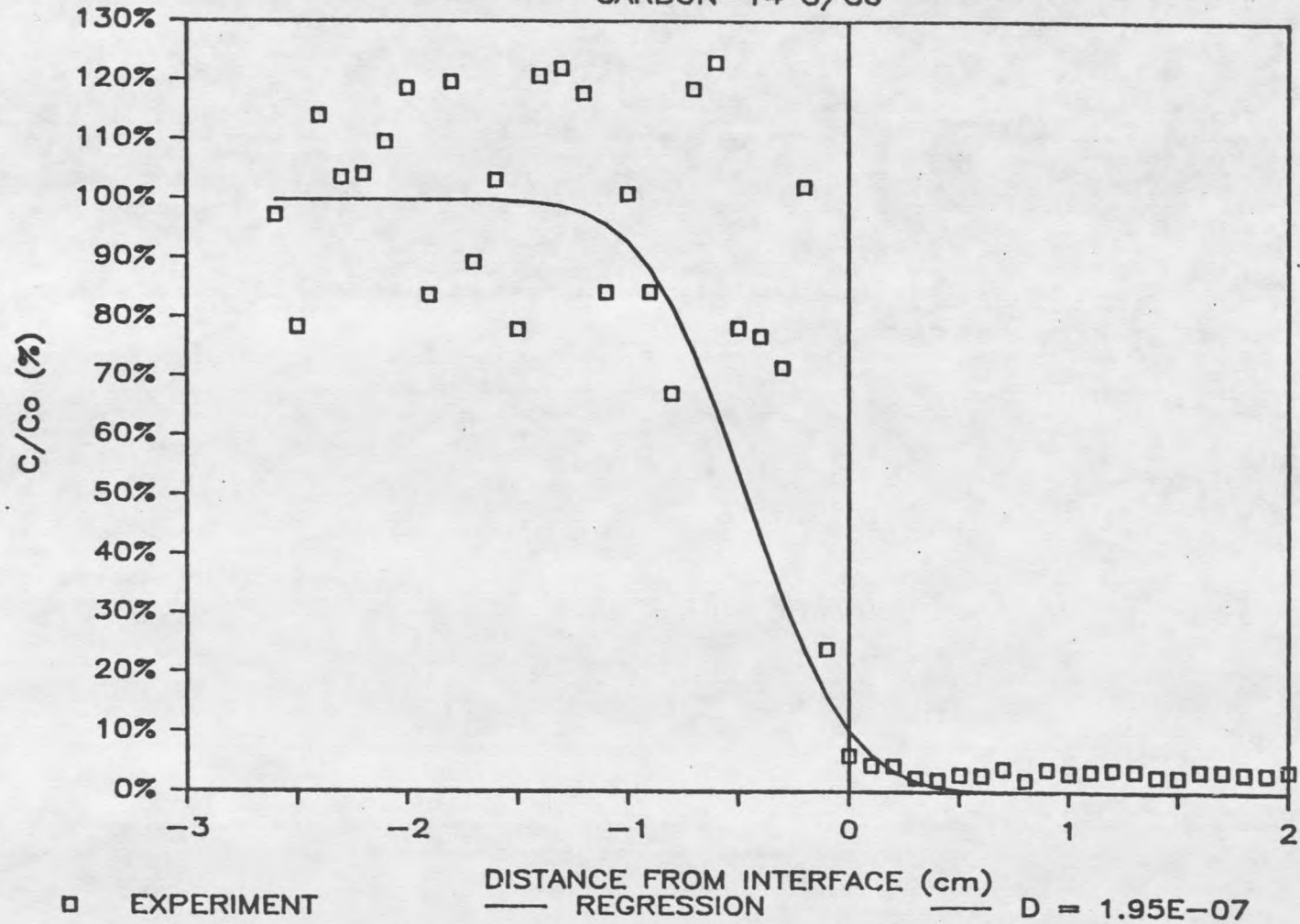


Figure 43.

D-C14-060-016

CARBON-14 C/Co

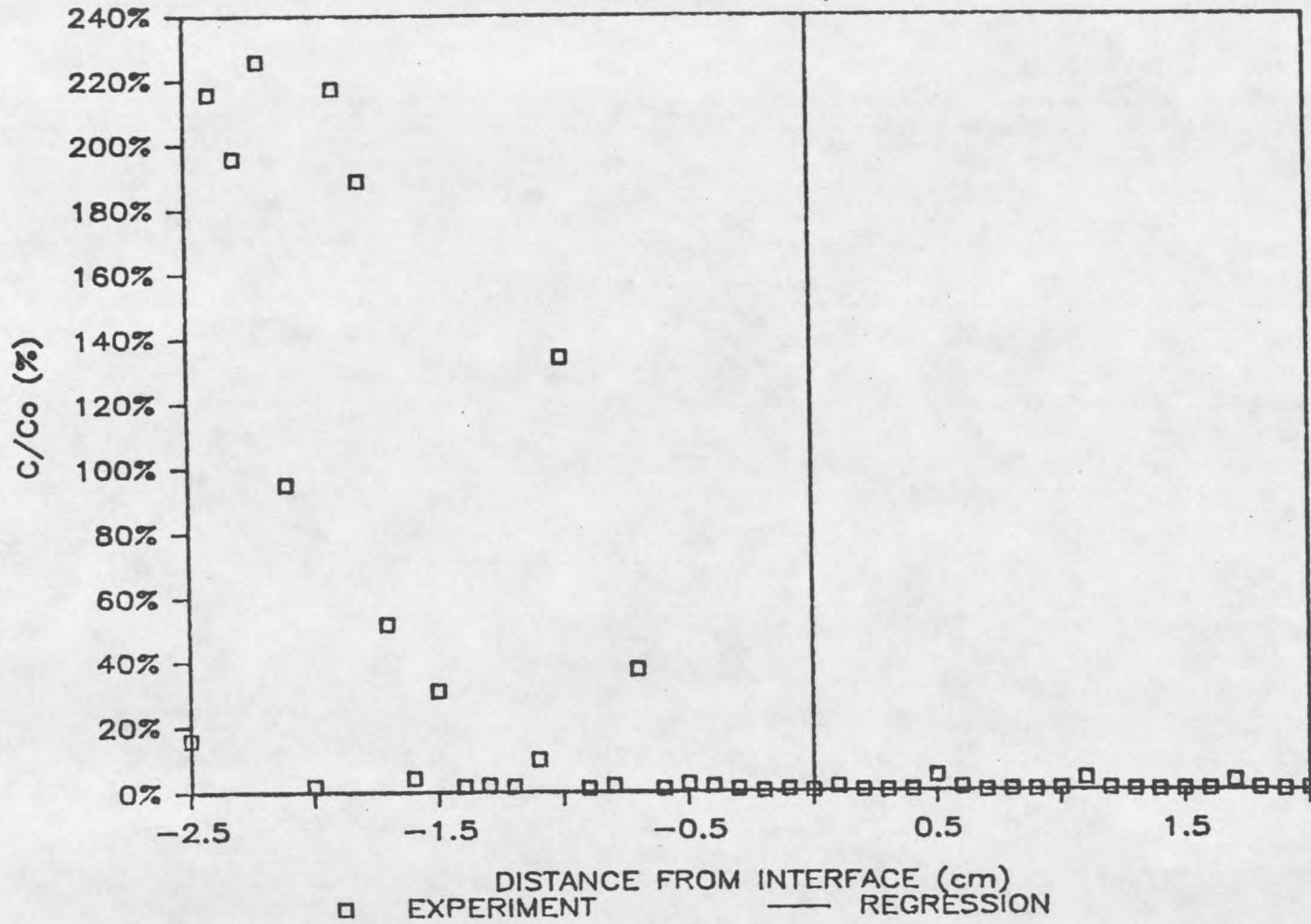


Figure 44.

D-C14-020-020

CARBON-14 C/Co

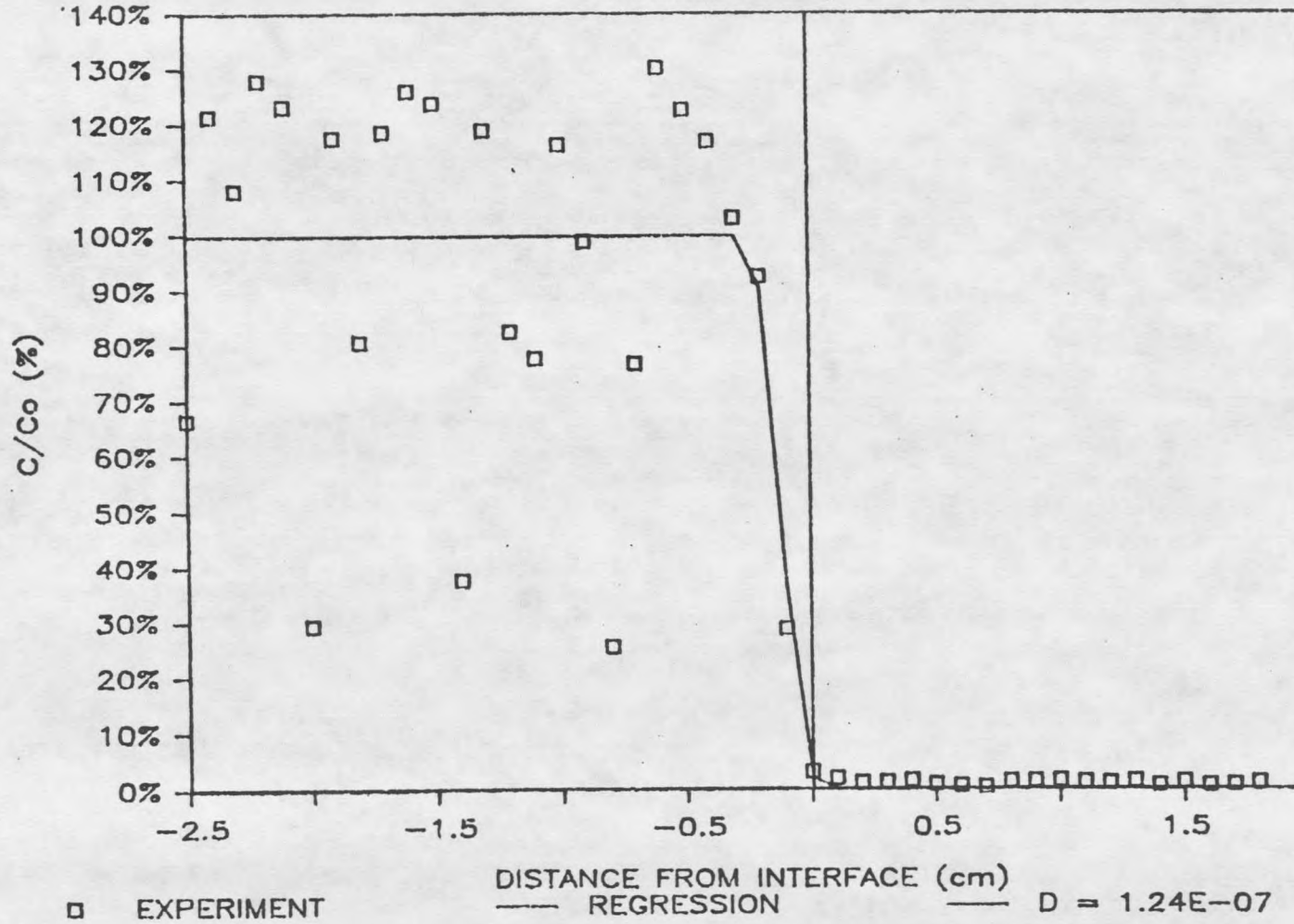
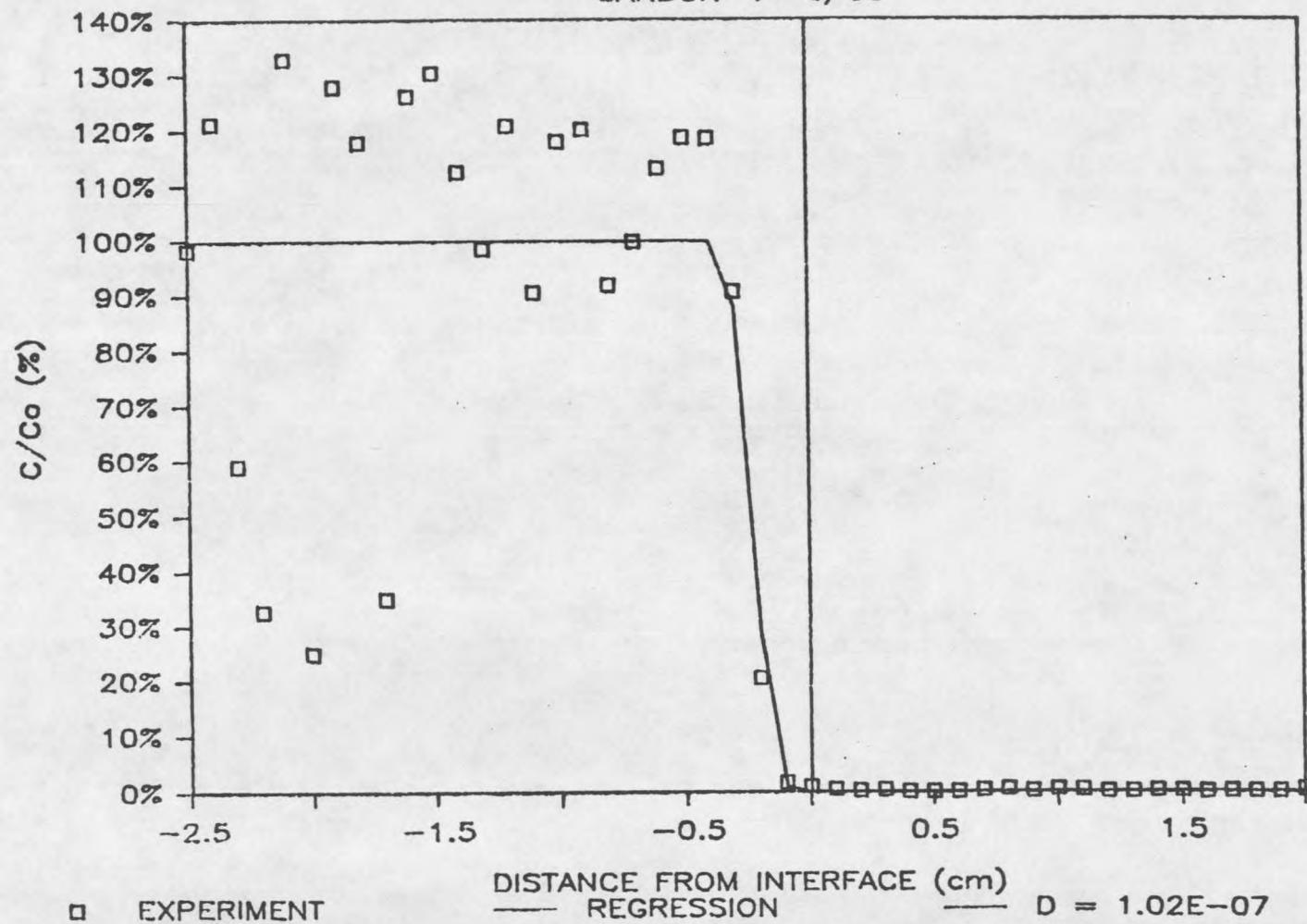


Figure 45.

D-C14-020-021

CARBON-14 C/Co



APPENDIX C

SPECIFIED CONCENTRATION OF IONS IN
SYNTHETIC GROUNDWATER

Table 10. Specified Concentration of Ions in Synthetic
Groundwater

Component	(mg/L)	Component	(mg/L)
Na	363	F	33.4
K	3.43	Cl	310
Ca	2.75	SO ₄	173
Mg	0.032	Inorganic	
Si	35.6	Carbon:	
		HCO ₃ + CO ₃	9.03E-4 M

APPENDIX D

NOMENCLATURE

NOMENCLATURE

a.....	y-intercept of linear regression line
A.....	Arrhenius frequency factor
b.....	slope of linear regression line
B, B ₁ , B ₂	constants in multiple linear regression eqn.
BD.....	bulk density of diffusive medium
C.....	anion concentration
C ₀	initial anion concentration
D ^o	effective diffusion coefficient
E.....	macroscopic average activation energy
F ^a	weight fraction of basalt in backfill
F ₁	weight fraction of bentonite in backfill
F ₂	weight fraction of bentonite in backfill
K _d	distribution coefficient
M _d	water mass in saturated backfill
M _w	solid mass in saturated backfill
N _s	number of data points (statistics)
Q.....	volumetric moisture content of sat'd soil paste
PD ^y	grain density of basalt in backfill
PD ₁	grain density of basalt in backfill
PD ₂	grain density of bentonite in backfill
PW ₂	density of water
P _t	total porosity of saturated backfill
r _t	statistical correlation coefficient
r ²	statistical coefficient of determination
R.....	gas constant
R ₀	retardation factor
S ₀	amount of anion sorbed by soil
SDEV(x).....	standard deviation in independent variable
SDEV(y).....	standard deviation in dependent variable
SDEV(b).....	standard deviation in slope
t.....	diffusion time
T.....	absolute temperature
x.....	axial distance in diffusion cells
x ₁ , x ₂	independent variables in multi-linear regression
X ₁	amount of air-dried backfill
V.....	water volume of saturated backfill
V ^w	solid volume of saturated backfill
V ^s	volume of halfcell
V ^h	total water and solid volumes of sat'd backfill
W.....	moisture content of backfill
Y.....	probit value of concentration percentage (C/C ₀)
Y _w	amount of water needed with air-dry backfill to get a specified bulk density

